Master's thesis

NTNU
Norwegian University of Science and Technology
Faculty of Natural Sciences
Department of Biotechnology and Food Science

Stinus Reklev Øverbø

The Effect of Oxygen Limitation on Growth Characteristics and The Redox State of *Escherichia coli* BL21 During Recombiant Protein Production

Master's thesis in Biotechnology
Supervisor: Per Bruheim
Co-supervisor: Laura García-Calvo
May 2023

NTNU
Norwegian University of
Science and Technology

Stinus Reklev Øverbø

The Effect of Oxygen Limitation on Growth Characteristics and The Redox State of *Escherichia coli* BL21 During Recombiant Protein Production

Master's thesis in Biotechnology
Supervisor: Per Bruheim
Co-supervisor: Laura García-Calvo
May 2023

Norwegian University of Science and Technology
Faculty of Natural Sciences
Department of Biotechnology and Food Science

NTNU
Norwegian University of
Science and Technology

Abstract

The market of recombinant protein production has grown drastically in the last years and is set to grow even bigger in the future. One of the preferred expression hosts is *Escherichia coli*, with its well-known genome and wide range of expression systems. The industry of recombinant protein production faces some challenges, with non-homogenous aeration being one of them. The effect this has on *Escherichia coli* has been little researched.

In this thesis, *Escherichia coli* BL21 strains with or without a pVB expression vector were used. The expression vector was based on the RK2 plasmid, with a native XylS/*Pm* regulator/promotor system and a plasmid copy number of 20, expressing mCherry as the reporter protein. These strains were used to investigate the effect of oxygen limitation on growth characteristics, overflow metabolism, redox state and recombinant protein production. The growth characteristics were investigated by batch cultivations in 1 L bench-top bioreactors. The overflow metabolism was investigated by analysing the extracellular organic acids using High Performance Liquid Chromatography, while the redox state was investigated by quantifying pyridine nucleotides by Zwitterionic Hydrophilic Interaction Liquid Chromatography Tandem Mass Spectrometry. Additionally, samples to investigate the central carbon metabolism were taken for quantification by the use of Ion Chromatography Tandem Mass Spectrometry. Due to time-limitations, these samples were not quantified. The concentration of produced mCherry was quantified by western blot.

It was found that limiting the availability of an external electron acceptor led to a reduction in growth rate of both strains and increased overflow metabolism. Additionally, an increased production of the recombinant protein was observed when oxygen was limited. This came at a lower cost of substrate. However, the specific production rate did not differ between the two conditions. Lastly, a time-delay between the onset of oxygen limitation and the effect it imposed on the redox state of the cells was found.

Samandrag

Markedet tilknytt produksjon av rekombinante protein har vekst kraftig dei siste åra, og det er forventa at det skal vekse seg endå større i framtida. Ein av dei føretrekte ekspresjonsvertane er *Escherichia coli*, med sitt godt kjente genom og breie arsenal av ekspresjonssystem. Industrien rundt rekombinant proteinproduksjon har nokre utfordringar, der inhomogen oksygenering er eit av desse. Effekten dette har på *E. coli* er lite forska på.

I denne oppgåve vart *E. coli* BL21 stammer med og utan ein pVB ekpresjonsvektor brukt. Ekspresjonsvektoren var basert på RK2 plasmidet, med eit XylS/*Pm* regulator/promoter system og eit plasmidkopinummer på 20, som utrykk mCherry som reporterproteinet. Desse stammene vart brukt til å undersøke effekten av oksygenlimitering på veksteigenskapane, overflodsmetabolismen, redokstilstanden og den rekombinante proteinproduksjonen. Veksteigenskapane vart undersøkt ved batchdyrking i 1 L benketoppsbioreaktorar. Overflodsmetabolismen vart undersøkt ved analyser av ekstracellulære organiske syrer med bruk av High Performance Liquid Chromatography, medan redokstilstanden vart undersøkt ved å kvantifiserer pyridinnukleotid gjennom Zwitterionic Hydrophilic Interaction Liquid Chromatography Tandem Mass Spectrometry. Prøver vart tatt til å kvantifisere den sentrale karbonmetabolsimen ved bruk av Ion Chromatography Tandem Mass Spectometry, men på grunn av tidsbegrensingar vart ikkje dette gjennomført. Konsentrasjonen av mengda produsert mCherryv vart kvantifisert gjennom bruke western blot.

Det vart funne at limitering av ein ekstern elektronakseptor førte til ein reduksjon i vekstrate av begge stammane. Det første også til ein auke i overflodsmetabolismen. Det vart også funne ein auke i produksjon av det rekombinante proteinet når oksygen vart limitert. Likevel gjekk dette på ei høgare kostand av substrat og den spesifikke produksjonsraten var ikkje ulik mellom dei to vilkåra. Det vart også funne ei tidsforsinking frå oksygenlimitering vart sett i gong og effekten det medførte på redokstilstanden til cellene.

Acknowledgments

This thesis was conducted at the Department of Biotechnology and Food Science (IBT) at the Norwegian University of Science and Technology (NTNU).

I would like to express my gratitude to my supervisor, Prof. Per Bruheim, for letting me be a part of the MetaboProt team for the last year and supervising me through the work. The feedback has been invaluable in the work relating to the thesis. Many thanks to my co-supervisor Dr. Laura García Calvo for the invaluable time, lessons and feedback in the lab. I also want to thank Divyata Vilas Rane for being a part of the team, performing the mass spectrometry analyses and help with interpreting the data. Thank you, all three, for always being available. A big gratitude to Åse Refsnes for being a great lab partner, all the gossip and shittalk in the lab.

Lastly, I want to thank my friends and family for supporting me, and my mum for not letting me start at the cookery school at VGS. I would not be where I am today without you guys!

Table of Contents

List of Abbreviations

Abbreviations	Explanation
5’-UTR	5’-untranslated region
ACN	Acetonitrile
AMP	Adenosine monophosphate
Asp	Aspartate
ATP	Adenosine triphosphate
CDW	Cell dry weight
dH_2O	Distilled water
DI-H_2O	Deionized water
DO	Dissolved oxygen
ESI	Electrospray ionization
ESTD	External standard
FAD(H_2)	Flavin adenine dinucleotide
GFP	Green fluorescent protein
HCl	Hydrochloric acid
HILIC-MS/MS	Hydrophilic Interaction Liquid Chromatography MS/MS
HPLC	High Performance Liquid Chromatography
IC-MS/MS	Ion Chromatography MS/MS
LB	Lysogeny broth
LN_2	Liquid nitrogen
MeOH	Methanol
mQ-H_2O	Milli-Q water
MS/MS	Tandem Mass Spectrometry
NA	Nicotinic acid
NAD(H)	Nicotinamide adenosine dinucleotide
NADP(H)	Nicotinamide adenosine dinucleotide phosphate
NAM	Nicotinamide
NaMN	Nicotinic acid mononucleotide
NaOH	Sodium hydroxide
NMN	Nicotinamide mononucleotide
NR	Nicotinamide riboside
OD_{600}	Optical density at 600 nm
PCA	Principal component analysis
PCN	Plasmid copy number
(p)ppGpp	Guanosine tetra/pentaphosphate
PPP	Pentose phosphate pathway
RFP	Red fluorescent protein
RP	Recombinant protein
RPP	Recombinant protein production
RI	Refractive index
TCA	Tricarboxylic acid
WT	Wild type

1. Introduction

1.1. Recombinant protein production (RPP)

Recombinant proteins (RPs) are proteins which have had their expression, mRNA encoding sequence or expression host modified. They have been termed recombinant because the protein is produced using recombinant DNA technology ("Recombinant Protein," 2006). One way this is done is by engineering a DNA sequence encoding the protein of interest from DNA sequences of different sources. To produce RPs, the gene encoding the protein of interest must be isolated from its origin. Thereafter, the gene is cloned into a suitable expression vector (Rosano et al., 2019; Waegeman & Soetaert, 2011). Thus, an expression host is able to produce the RP and it can be used of after isolation and purification (Rosano et al., 2019).

1.1.1. Industrial impact of RPP

Prior to the rise of RPP, proteins of interest were obtained from plants and animals. This could often result in low yields and, consequently, high prices, due to high demand (Waegeman & Soetaert, 2011). The use of microbial expression hosts, such as *Escherichia coli* (*E. coli*), has made it easier to produce RPs at higher yields, compared to the old method of isolating proteins from their natural source (Waegeman & Soetaert, 2011).

The first reported case of the production of a functional RP was in 1977, when Itakura et al. (1977) produced the mammalian hormone somatostatin in *E. coli*. In 1978 the first case of the production of human insulin, based on the method of Itakura et al., was reported (Goeddel et al., 1979). Recombinant insulin produced from a recombinant source was in 1982 the first RP to be approved by the drug regulatory agencies in the UK, the Netherlands, West Germany and the US (Johnson, 1983). This technology developed by Itakura et al. and continued by Goeddel et al. revolutionized the industrial enzyme and biopharmaceutical industry (Waegeman & Soetaert, 2011).

The industry of RPs encompasses a vast range of proteins. Industrial grade RPs include many different types of enzymes e.g. amylases, proteases, and lipases, with a wide range of applications, including production of fuel ethanol and biodiesel, food and beverages, animal feed, cleaning material, waste management and components in clothing and cosmetics (Kirk et al., 2002; Puetz & Wurm, 2019). RPP is also used to produce biopharmaceutical grade RPs, such as antibodies, growth factors and hormones (Walsh, 2018). As of 2018, there were 316 individual biopharmaceutical products on the market with active licenses (Walsh, 2018). In a report from MarketsandMarkets from 2023, the net global market value of RPs was estimated to be $1.4 billion in 2022 and it is expected to reach $2.4 billion by 2027 (MarketsandMarkets, 2023).

1.1.2. Challenges related to RPP at industrial levels

There are several challenges affecting RPP at industry level, some of which have been solved, while others persist (Rudge & Ladisch, 2020). When producing recombinant therapeutics, high purity is essential. This is due to some expression hosts giving rise to toxic by-products, such as endotoxin from *E. coli* (Rudge & Ladisch, 2020). Another

challenge is the need for a high cell density to acquire a larger output of the recombinant product. When the production is finished, it is necessary to separate the protein of interest from the expression host without compromising the quality and quantity of the product. Thereafter, the product must be purified (Rudge & Ladisch, 2020). All of these requirements can be laborious and expensive (Rudge & Ladisch, 2020).

Oxygen transfer is also a major challenge in the use of industrial-scale bioreactors for the production of RPs (O'Beirne & Hamer, 2000b). In industrial-scale bioreactors, oxygen is not homogenously distributed, which could give zones with low oxygen levels, potentially leading to oxygen limitation. Lowering the oxygen availability has shown to decrease the growth rate of *E. coli* (Losen et al., 2004; O'Beirne & Hamer, 2000b). It is also evident that a fluctuating availability of oxygen confers a dynamic response in *E. coli*. Under such conditions, the metabolism of the bacteria is constantly shifting to adapt to the available electron acceptors (O'Beirne & Hamer, 2000a).

1.2. Expression host

When producing RPs, a wide range of expression hosts can be used, with different advantages and disadvantages. It is possible to use prokaryotic hosts, such as bacteria (Terpe, 2006), or eukaryotic hosts, such as yeast (Mattanovich et al., 2012), filamentous fungi (Ward, 2012), transgenic plants (Kusnadi et al., 1997), and animal cells such as mammalian or insect cells (Kost et al., 2005; Wurm, 2004). One of the clearest differences between eukaryotic and prokaryotic expression systems is that eukaryotic expression systems can modify the protein after translation, while prokaryotic expression systems cannot (Overton, 2014). Bacterial expression systems, *E. coli* being most common, are one of the preferred systems due to their low cost of cultivation, well mapped genome, and wide range of promoter systems (Chen, 2012; Terpe, 2006).

In this project, *E. coli* was the used as the expression host. Therefore, only this type of host will be described in detail.

1.2.1. *Escherichia coli* as an expression host

E. coli is a Gram-negative facultative anaerobe bacterium, meaning it has the capacity to live in both oxygen-rich and oxygen-poor environments (Tenaillon et al., 2010). *E. coli* uses organic sugars, preferably glucose due to carbon catabolic repression (Magasanik, 1961), as its main carbon and energy source. In the presence of an electron acceptor, such as O_2, glucose is converted to pyruvate, which further goes into the tricarboxylic acid (TCA) cycle (Clark, 1989). This produces protonated nicotinamide adenine dinucletide (NADH), which in turn is reoxidized into NAD^+ by oxidative phosphorylation to regenerate adenosine triphosphate (ATP) from adenosine diphosphate (ADP) (Clark, 1989; Jensen & Michelsen, 1992). In anaerobic conditions, when an external electron acceptor, such as nitrate, is not present, oxidative phosphorylation is not possible. Instead *E. coli* regenerates ATP from ADP by substrate level phosphorylation in a fermentation process, which also reoxidizes NADH into NAD^+ (Clark, 1989). Another important pathway in *E. coli* is the pentose phosphate pathway (PPP). This pathway is important for the production of precursors of nucleotides, lipopolysaccharides, vitamins and amino acids, as well as providing reducing power in the form of protonated nicotinamide adenosine dinucleotide phosphate (NADPH) (Kanehisa, 2019; Kanehisa et al., 2023; Kanehisa & Goto, 2000; Ow et al., 2006).

E. coli is preferred as an expression host for RPs due to many factors, one being its growth rate. In rich media, some strains of *E. coli* have shown to have a doubling time of roughly 20 minutes (Rosano et al., 2019) and methods have been developed to cultivate *E. coli* at concentrations of up to 190 grams cell dry weight (CDW) per litre (Lee, 1996; Shiloach & Fass, 2005). In minimal media, the B line of *E. coli* strains, such as BL21, have shown to grow faster than the clonal strain K-12 (Yoon et al., 2009). Another advantage of *E. coli* is its well-known genome and the myriad of tools and techniques to genetically engineer the bacterium (Overton, 2014; Waegeman & Soetaert, 2011).

Conversely, *E. coli* also has some shortcomings as an expression host. A major problem is the accumulation of acetate in high cell densities, which inhibits growth and the production of RPs (Eiteman & Altman, 2006). However, this is negligible in the BL21 stain, commonly explained by the heightened activity of the glyoxylate shunt, the main pathway for the utilization of acetate (Yoon et al., 2009). Another shortcoming of *E. coli* is its poor ability to secrete proteins (Ni & Chen, 2009). However, BL21 has been shown to have a higher level of secreted proteins compared to other *E. coli* strains, although at a low level (Yoon et al., 2012). Other disadvantages of *E. coli* are its inability to perform post-translational modifications, codon bias, plasmid instability, and formation of endotoxins (Overton, 2014; Waegeman & Soetaert, 2011).

1.3. Expression vector

The expression vector used is this project is based on the RK2 plasmid. Therefore, this plasmid will be described.

1.3.1. RK2 plasmid

Plasmids are extrachromosomal DNA, naturally found in prokaryotes and some eukaryotes, that are capable of self-replication. When using a prokaryotic expression host, plasmid-based systems of RPP are the most common choice (Palomares et al., 2004). Plasmid-based systems confer different advantages over expression systems integrated into the host genome, as they are easier to transfer and manipulate and can give a higher gene dose, due to the plasmid copy number (PCN) (Palomares et al., 2004). The RK2 plasmid is an antibiotic-resistant plasmid, belonging to the P-1 incompatibility group (Inc P-1), which is capable of self-transmission (Figurski & Helinski, 1979). The replication of RK2 is initiated at the origin of replication, *oriV*, which is under control of TrfA, a protein encoded by the *trfA* gene (Durland et al., 1990).

The RK2 plasmid has been shown to replicate at a defined PCN (Toukdarian & Helinski, 1998), reported to be at four to seven copies per cell (Thomas et al., 1984). The replication is controlled by a mechanism called handcuffing, in which TrfA binds to *oriV* when there is as many plasmids as its copy number. This forms a handcuffed complex which prevents DNA replication (Toukdarian & Helinski, 1998). To increase the PCN, specific point mutations in the *trfA* gene can be introduced, which have shown up to a 24-fold increase in the PCN compared to the wildtype *trfA* gene (Blatny et al., 1997).

1.3.2. The XylS/*Pm* expression system

The usage of the XylS/*Pm* expression system enables the regulation of expression of recombinant genes in *E. coli*. This regulator/promoter system originates from the TOL plasmid pWW0 of *Pseudomonas putida* (Gawin et al., 2017). The system contains a *Pm*

promoter sequence, a 5'-untranslated region (5'-UTR) of the *Pm*-derived transcript, and the XylS encoding sequence (Gawin et al., 2017). The expression system is initiated when the positive regulatory transcription factor XylS is activated by a benzoate-derived inducer, such as m-toluate (Winther-Larsen et al., 2000). Once activated, XylS dimerizes, binds to its operator sites, and induces transcription from *Pm* (Gawin et al., 2017).

Advantages of the XylS/*Pm* expression system includes its capability to express proteins at industrial levels in high cell density cultivations (Sletta et al., 2004; Sletta et al., 2007) and having a cheap inducer (Balzer et al., 2013). It is also possible to greatly increase the expression of the native XylS/*Pm* expression system by introducing mutations in the *xylS* gene (Vee Aune et al., 2010), the *Pm* promoter sequence (Bakke et al., 2009), or the 5'-UTR (Berg et al., 2009).

1.3.3. Selection marker

To ensure the cultivation of only bacteria containing the expression vector, a selection marker must be used (Wang et al., 2009). At a laboratory scale, the usage of antibiotic resistance as a selection marker is the most common method (Rosano et al., 2019). One such antibiotic is ampicillin, the most commonly used selection marker (Feizollahzadeh et al., 2017). Ampicillin is a β-lactam, which kill bacteria by inhibiting the bacterial transpeptidase, ultimately preventing the formation of the bacterial cell wall (Wilke et al., 2005). Introducing the *bla* gene confers ampicillin-resistance by encoding a β-lactamase. These enzymes hydrolyse β-lactam rings, thereby inactivating the antibiotic (Brinas et al., 2002).

1.3.4. Reporter protein

Reporter genes produce a phenotype which is easy to measure upon expression and thus provide a method for more rapid and conventiant analysis of genetic activity (Wood, 1995). In comparison to selection markers, they do not convey a selective advantage. Rather, they produce a way to differentiate transformed and non-transformed organism (Miki & McHugh, 2004). One such reporter gene, *gfp*, express green fluorescent protein (GFP) (Ghim et al., 2010). After the discovery of the wildtype-GFP, focus has been on producing fluorescent proteins that are brighter, cover a broad spectral range, show enhanced photostability, reduced oligomerization, pH insensitivity, and faster maturation rates (Shaner et al., 2007). Of the fluorescent proteins, those that absorb and emit light in the red region of the spectrum are most desirable, due to the low cellular autofluorescence in this region (Chapagain et al., 2011). One of the most promising variants of red fluorescent proteins (RFP) is mCherry, which has excitation peaks at 587 nm and emission peaks at 610 nm and is far more photostable than other RFPs (Lambert, 2019; Shaner et al., 2007). However, a drawback of fluorescent proteins is that their chromophore requires oxygen to mature (Chapagain et al., 2011). On the other hand, it has also been shown that the photostability of RFPs is negatively impacted by the presence of oxygen (Shaner et al., 2008).

1.4. Consequences of the metabolic burden inflicted by the presence of recombinant plasmids

Cells harbouring plasmids have an additional burden imposed on them, in comparison to cells without plasmids. This is due to the maintenance of the plasmid and the expression

of the proteins encoded by the plasmid. Both of these processes drain the cell of resources, a phenomenon termed "metabolic burden" (Diaz Ricci & Hernandez, 2000; Glick, 1995). Some of the resources that would need to be shared between biomass accumulation and RPP are ATP, NADPH, and amino acids (Overton, 2014). This could lead to adverse effects such as loss of the expression vector (Palomares et al., 2004), adjustments to the metabolic flux (Wang et al., 2006), different type of stress responses (Silva et al., 2012), and inhibition of growth (Ow et al., 2006; Valenzuela et al., 1996).

1.4.1.Loss of expression vector

The metabolic burden imposed by expression vectors could lead to cells that lose their plasmid, thereby alleviating said metabolic burden (Waegeman & Soetaert, 2011). This could lead to a culture where the plasmid-free bacteria are able to outcompete the plasmid-containing bacteria. The plasmid-free bacteria are most likely a product of segregational instability of the plasmid, but could also be a product of structural instability (Summers, 1991). Segregational instability arise from the failure to separate the plasmids to both daughter cells. If the plasmids are randomly distributed, a high copy number will lead to an increased segregational instability (Summers, 1998). Different strategies have been implemented to prevent plasmid-free cultures from arising. One such method is the usage of active partitioning of the plasmids, where the *par* sequence is introduced into the plasmid (Palomares et al., 2004), thereby preventing the formation of plasmid-free cells all together. Another method is by giving the plasmid-containing cells an advantage over the plasmid-free ones. This could be by using a selection marker, such as antibiotics resistance (Palomares et al., 2004).

1.4.2.Metabolic flux adjustment

It has been shown that cells harbouring plasmids have an altered metabolic flux compared to cells of the same type without the given plasmids (Wang et al., 2006). To meet the high energy demand needed for the production of RPs and plasmid-induced metabolic stress, the bacteria need to shift its metabolism towards energy producing pathways, such as glycolysis and the TCA cycle. A shift from anabolic pathways to catabolic pathways is required to meet the high energy demand of protein production and plasmid-induced metabolic responses (Özkan et al., 2005). This shift is shown to lead to a marked reduction in biomass (Andersson et al., 1996).

Different studies have shown different alterations of the metabolic flux for recombinant *E. coli*, depending upon the strain, type of plasmid, and cultivation media. Some studies found a down-regulation of the TCA cycle genes (Harcum & Haddadin, 2006), which could indicate a reduced flux in the TCA cycle. Others have indicated an increase in the TCA cycle fluxes (Ow et al., 2006; Özkan et al., 2005). The flux through glycolysis has been shown to both increase and decrease at different steps in the pathway (Harcum & Haddadin, 2006; Ow et al., 2006; Özkan et al., 2005). Regarding the PPP, a study by Ow et al. (2006) found no drastic change in the expression of PPP genes, while Wang et al. (2006)pointed at significant down-regulation of PPP genes in plasmid-harbouring cells. This down-regulation of PPP genes can indicate a shift from anabolic pathways to catabolic pathways.

1.4.3.Stress response

It has been shown that stress induced by plasmids is often related to the plasmid copy number (Seo & Bailey, 1985). This is not only due to the higher number of plasmids being replicated, but also the expression of plasmid-encoded proteins and selection marker protein (Bentley et al., 1990; Rozkov et al., 2004). Some of the plasmid-induced stress responses are heat shock, stringent and SOS response (Lin et al., 2004; Silva et al., 2012).

1.4.3.1. Heat shock response

The heat shock response is a response mechanism which allows cells to adapt to environmental and metabolic changes (Arsene et al., 2000). The response is induced by a variety of stress conditions, such as physiochemical factors. These factors include an upshift in temperature, harmful metabolic substances, and complex metabolic processes (Arsene et al., 2000). Additionally, RPP has been shown to induce the heat shock response (Hoffmann & Rinas, 2001).

The heat shock response in *E. coli* is positively regulated by σ^{32} (Arsene et al., 2000). When no heat shock is present, the level of σ^{32} is kept low by three different mechanisms. The first mechanism is at the translational level, where inefficient initiation of *rpoH* mRNA translation, the mRNA translated into σ^{32}, is due to base pairing within the Shine-Dalgarno sequence (Schumann, 2016). The second mechanism is at the inhibitory level, where σ^{32} is bound to either of the chaperone systems DnaK/DnaJ/GrpE and GroEL/GroES (Schumann, 2016). The third mechanism is at the degradational level, where free σ^{32} is guided towards FtsH metalloprotease or ClpXP protease for degradation by SRP and ThiS, respectively (Lim et al., 2013; Xu et al., 2015). When a heat shock occurs, the *rpoH* mRNA strands separate, allowing for high levels of σ^{32} translation (Schumann, 2016). This results in elevated levels of heat shock proteins, such as chaperons, promoting protein folding, and proteases, degrading unfolded and damaged proteins (Arsene et al., 2000). The heat shock response returns the cell to homeostasis and increases its thermotolerance, albeit at a different steady state with decreased growth rate and protein production, modification of ratio between lipids and proteins in the membrane, ribosome destructions and DNA relaxation (Valdez-Cruz et al., 2011).

1.4.3.2. Stringent response

In environments where nutrients are limited, the cell must alter its gene expression and metabolism from one that supports cell growth to one that supports a prolonged survival with minimal growth (Traxler et al., 2008). This adjustment of cellular state is called the stringent response and is mediated by the alarmones guanosine tetra- and pentaphosphate ((p)ppGpp) (Traxler et al., 2008). As stated above, RPP drains the cell of resources, especially amino acids, which could lead to a stringent-like stress response (Kumar et al., 2020).

Under amino acid starvation, the amount of deacetylated tRNAs increase, enabling them to bind to ribosomes and inhibiting ribosome function (Wendrich et al., 2002; Wilson & Nierhaus, 2007). The stringent factor RelA then binds to the inhibited ribosome and initiates the synthesis of the alarmone (p)ppGpp from ATP and GTP/GDP (Kumar et al., 2020). Another enzyme responsible for the synthesis of (p)ppGpp is SpoT, but with a weaker synthase activity than RelA (Traxler et al., 2008). SpoT is active in response to carbon, iron, and fatty acid starvation (Traxler et al., 2008). Once (p)ppGpp is produced,

it acts synergistically with DksA to modulate the activity of RNA polymerase. Together they inhibit the transcription of rRNA and tRNA genes, and stimulate the expression of amino acid biosynthetic and transporter genes (Perederina et al., 2004).

1.4.3.3. SOS response

The SOS response is a stress response mediated by massively damaged DNA (Majchrzak et al., 2006). The SOS response can also occur under specific physiological stress, such as changes in the pH, starvation, and transition from exponential to stationary growth (Majchrzak et al., 2006). The SOS response is regulated by the proteins LexA and RecA (Majchrzak et al., 2006). Under normal conditions, the SOS genes are repressed in varying degrees by LexA. If the cell senses increased levels of DNA damage, RecA induces the autocleavage of LexA, leading to the SOS response (Michel, 2005). The SOS response leads to a complex cascade of expression of SOS genes, whose products promote the repair of damaged DNA. However, DNA synthesis is prone to errors due to the usage of the mutagenic DNA Pol IV and V (Goodman, 2000; Michel, 2005). A study done by Gill et al. (2000) showed that under RPP the expression of genes related to the SOS response was induced.

1.4.4. Growth inhibition

One of the major and most notable consequences of the plasmid-induced metabolic burden is the growth inhibition it confers (Diaz Ricci & Hernandez, 2000). It is clear that the need to maintain a plasmid negatively affect the growth rate and cell density. Ow et al. (2006) found that *E. coli* DH5α carrying a NS3 plasmid had a lower growth rate than the plasmid-free *E. coli* DH5α, 0.64 h^{-1} compared to 0.87 h^{-1}. It becomes evident from the consequences explained above why this happens. Cells harbouring a plasmid have an altered metabolic flux as compared to plasmid-free cells (Wang et al., 2006). A metabolic flux prioritizing catabolic pathways, as compared to anabolic pathways, will give a lower growth rate due to the fact that more energy is required for the maintenance of plasmids and the expression of the RP (Özkan et al., 2005). The production of structural proteins, membrane lipids, and other macromolecules necessary for growth is not prioritized. As stated above, the overproduction of RPs induces the stringent response, which makes the cells enter the stationary growth phase (Kumar et al., 2020; Traxler et al., 2008), yielding a lower cell density.

1.5. Pyridine nucleotide metabolism of *E. coli*

Pyridine nucleotides are important coenzymes that have vital roles in energy transduction and in cellular defence systems (Pollak et al., 2007). The most widely described and known role of pyridine nucleotides is their participation as electron carriers (Nakamura et al., 2012). Pyridine nucleotides consist of adenosine monophosphate (AMP) and nicotinamide mononucleotide (NMN). In *E. coli*, NAD^+ and $NADP^+$ can either be synthesized *de novo* or by salvage pathways (Osterman, 2009). In the *de novo* synthesis of pyridine nucleotides, aspartate (Asp) is converted to nicotinic acid mononucleotide (NaMN) in a three step pathway (Osterman, 2009). NaMN is further converted into NAD^+. In the salvage pathway, both NAD^+ and $NADP^+$ can be broken down into nicotinamide (NAM). Then, NAM can either be converted to nicotinic acid (NA) or nicotinamide riboside (NR) and further converted to NMN. Both NA and NMN can be converted to NaMN, which is further converted to NAD^+.

NMN can also be directly converted to NAD^+ (Osterman, 2009). The different pathways are shown in Figure 1.1.

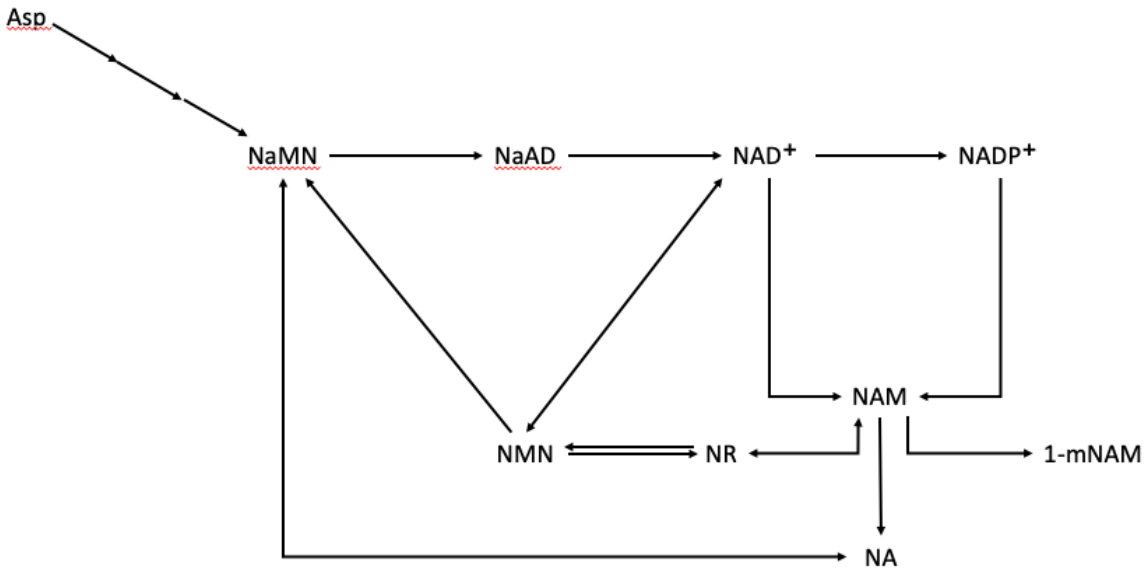

Figure 1.1: Biosynthesis of pyridine nucleotides in *Escherichia coli*. Abbreviations: Asp: aspartate; NAM: nicotinamide; NA: nicotinic acid; 1-mNAM: 1-methylnicotinamide; NR: nicotinamide riboside: NMN: nicotinamide mononucleotide; NaMN: nicotinic acid mononucleotide; NaAD: nicotinic acid adenine dinucleotide; NAD^+: nicotinamide adenine dinucleotide; $NADP^+$: nicotinamide adenine dinucleotide phosphate. One-headed arrow indicates irreversible reaction. Two-headed arrow indicates reversible reaction. Modified from (Kanehisa, 2019; Kanehisa et al., 2023; Kanehisa & Goto, 2000), highlighting metabolites in biosynthesis of pyridine nucleotides being investigated.

1.6. Aim of study

The aim of this study is to investigate the effect of oxygen limitation on the metabolism and the RPP of *E. coli* BL21 and the mCherry-producing strain A2mCh.

E. coli is, to this day, the most widely used expression host for RPP, despite its drawbacks leading to reduced yields of desirable proteins. Many factors play into this, for instance PCN and expression cassette strength. There is a lack in knowledge about how the metabolic burden imposed by the presence of an expression vector affects the metabolism of *E. coli*. Additionally, in industrial-scale bioreactors, non-homogenous aeration occurs and how this affects the metabolism of *E. coli* is not widely investigated.

The work in this thesis is done in coordination with the MetaboProt project, whose aim is to investigate the metabolic burden inflicted by RPP. Based on the work done by previous master students (Everson, 2022; Humlebrekk, 2022; Mæhlum, 2021; Mathiassen, 2022), a promising expression system has been chosen to investigate the effect of oxygen limitation on the metabolism and RPP. The growth and biomass accumulation were investigated, in addition to the overflow metabolism. Furthermore, potential bottlenecks that could be used as targets for improved productivity were attempted to identify.

2. Materials and Methods

2.1. Bacterial strains

The bacterial strain studied in this thesis is *E. coli* BL21, a strain widely used for RPP (Selas Castineiras et al., 2018). The strain was acquired from New England BioLabs (Irving, MA, USA) with the genotype *fhuA2 [lon] ompT gal [dcm] ΔhsdS*. Throughout this thesis, this strain will be referred to as the wildtype (WT). In addition to the wildtype strain, a recombinant strain was used, referred to as A2mCh, which contains a recombinant plasmid. The recombinant plasmid is a pVB expression vector, based on the genetically modified RK2 plasmid. The A2mCh plasmid contains the native XylS/*Pm* regulator/promotor system. The PCN of the A2mCh plasmid is 20, compared to a RK@ plsmid PCN of 5, achieved by a mutation in the *trfA* gene (271A mutant). Furthermore, the plasmid contains the *bla* gene, giving the recombinant cells resistance to ampicillin. The use of only the recombinant strain A2mCh is based on the research done by previous master students in the MetaboProt project (Everson, 2022; Humlebrekk, 2022; Mæhlum, 2021; Mathiassen, 2022) and by García-Calvo et al. (2023).

2.1.1. Glycerol stocks of *E. coli* cultures

To preserve and store the bacterial strains, glycerol stocks (16 %) of *E. coli* BL21 WT and A2mCh were prepared. 50 mL of lysogeny broth (LB) medium (Table 2.3) in a 250 mL baffled flask were inoculated with *E. coli*. Baffled flasks with recombinant strains contained 100 µg/mL ampicillin. The flasks were incubated overnight (16±1 hrs, 37 °C, 200 rpm). The cultures were transferred to sterile 50 mL Falcon tubes and centrifuged (4000 rcf, 5 min). The supernatant was removed to reach a volume of 16 mL before the cell pellets were resuspended in the remaining supernatant. 4 mL sterile glycerol (80 %, VWR, 24387.292) was added and mixed by inverting the tube. Glycerol cell suspensions were aliquoted into sterile labelled cryotubes, 1 mL per tube, before being snap-frozen in liquid nitrogen (LN_2) and stored at -80 °C.

2.2. Media and stock solution

2.2.1. Stock solutions

2.2.1.1. Ampicillin (1000x) stock solution

As the selective marker, ampicillin stock solution was made by dissolving ampicillin sodium salt (BioChemica, A0839) in Milli-Q water (mQ-H_2O) to a concentration of 100 mg/mL. The solution was filter sterilized with syringe filters (0.2 µm Supor Membrane, 32 mm, Acrodisc, 4652) and aliquoted into sterile Eppendorf tubes, either 0.5 or 1.0 mL per tube. The stock solution was stored at -20 °C.

2.2.1.2. m-Toluate (500x) stock solution

As the inducer for mCherry production, m-toluate stock solution was made by dissolving m-toluate (Sigma-Aldrich, T36609) in absolute ethanol (VWR, 2081.310) to a

concentration of 500 mg/mL. The stock solution was filter sterilized with syringe filters (0.2 µm Supor Membrane, 32mm, Acrodisc, 4652) and aliquoted into sterile Eppendorf tubes, 2 mL per tube, and stored at -20 °C.

2.2.1.3. Cobalt stock solution

The cobalt stock solution was prepared by dissolving $CoCl_2 \bullet 6H_2O$ (Sigma-Aldrich, C8661) in mQ-H_2O to a concentration of 0.05 g/L. The solution was filter sterilized with syringe filters (0.2 µm Supor Membrane, 32 mm, Acrodisc, 4652) into sterile containers and stored at 4 °C .

2.2.1.4. Magnesium sulphate stock solution

The magnesium sulphate stock solution was prepared by dissolving $MgSO_4 \bullet 7H_2O$ (VWR, 25165.292) in mQ-H_2O to a concentration of 246.5 g/L. The solution was filter sterilized with syringe filters (0.2 µm Supor Membrane, 32 mm, Acrodisc, 4652) into sterile containers and stored at room temperature.

2.2.1.5. Trace mineral stock solution 1

The trace mineral stock solution 1 was prepared by dissolving the different components in 5 M hydrochloric acid (HCl) to the concentrations listed in Table 2.1. The stock solution was stored in 50 mL falcon tubes at 4 °C.

Table 2.1: The concentration [g/L], supplier and product number of the components of the trace mineral stock solution 1. The components were dissolved in 5 M HCl and stored in 50 mL falcon tubes at 4°C.

Component	Concentration [g/L]	Supplier	Product number
$ZnSO_4 \bullet 7H_2O$	2.25	Sigma-Aldrich	Z0251
$FeSO_4 \bullet 7H_2O$	50	Sigma-Aldrich	F8633
$CuSO_4 \bullet 5H_2O$	1	Sigma-Aldrich	C8027
$MnCl_2 \bullet 4H_2O$	0.375	Sigma-Aldrich	M5005
$(NH_4)_6Mo_7O_{24} \bullet 4H_2O$	0.1	ACROS	20585100

2.2.1.6. Trace mineral stock solution 2

The trace mineral stock solution 2 was prepared by dissolving the different components in 50 mL 5 M HCl to the concentrations listed in Table 2.2. The stock solution was stored in 50 mL falcon tubes at 4 °C.

Table 2.2: The concentration [g/L], supplier and product number of the components of the trace mineral stock solution 2. The components were dissolved in 5 M HCl and stored in 50 mL falcon tubes at 4 °C.

Component	Concentration [g/L]	Supplier	Product number
$ZnSo_4 \bullet 7H_2O$	2.25	Sigma-Aldrich	Z0251
$FeSO_4 \bullet 7H_2O$	10	Sigma-Aldrich	F8633
$CuSO_4 \bullet 5H_2O$	1	Sigma-Aldrich	C8027
$MnCl_2 \bullet 4H_2O$	0.375	Sigma-Aldrich	M5005
$(NH_4)_6Mo_7O_{24} \bullet 4H_2O$	0.1	ACROS	20585100
$CaCl_2 \bullet 2H_2O$	2	Sigma-Aldrich	23506

H_3BO_3	0.14	Sigma-Aldrich	B6768

2.2.1.7. Glucose (50%) stock solution

Glucose (50 %) stock solution was prepared by dissolving D(+)-Glucose anhydrous (VWR, 101176K) in mQ-H_2O to a concentration of 500 g/L. The solution was sterilized by vacuum filtration into 500 mL SteriCups (0.2µm PES membrane, 75mm diameter, Thermo Scientific, 566-0020) through a bottletop filter unit (0.45 µm hydrophilic PTFE membrane, Merck Millipore, SJLHM4710) and stored at room temperature.

2.2.1.8. Sodium hydroxide

4 M sodium hydroxide (NaOH) was prepared by dissolving 160 g NaOH (VWR, 28244.295) in 1 L mQ-H_2O.

2.2.2.Cultivation media

2.2.2.1. LB medium

LB medium is a complex medium and was used to cultivate the primary preculture for all experiments. LB medium was prepared by dissolving the components in mQ-H_2O according to Table 2.3. The medium was autoclaved (121 °C, 20 min) and stored at room temperature.

Table 2.3: The concentration [g/L], supplier and product number of the components of the LB medium. The components were dissolved in mQ-H_2O before being autoclaved (121 °C, 20 min) and stored at room temperature.

Component	Concentration [g/L]	Supplier	Product number
Tryptone	10.00	Sigma-Aldrich	T9410
Yeast extract	5.00	Sigma-Aldrich	92144
NaCl	5.00	VWR	27810.295

2.2.2.2. M9-PC-MtPr media

M9-Pc-MtPr medium is a chemically defined, minimal medium, which was used to cultivate the secondary preculture. Two different recipes were used. Both media were prepared in two steps to avoid precipitation. The basis medium for both was made by dissolving the components in mQ-H_2O, according to Table 2.4. The basis medium was autoclaved (121 °C, 20 min) and stored at room temperature. After autoclaving, the final M9-Pc-MtPr medium 1 was made according to Table 2.5, while the final M9Pc-MtPr medium 2 was made according to Table 2.6, both using sterile technique.

Table 2.4: The concentration [g/L], supplier and product number of the components of the M9-PC-MtPr basis medium. The components were dissolved in mQ-H_2O in containers before being autoclaved (121 °C, 20 min) and stored at room temperature.

Component	Concentration [g/L]	Supplier	Product number
NH_4Cl	10.000	Sigma-Aldrich	A9434
$Na_2HPO_4 \bullet 7H_2O$	112.000	Sigma-Aldrich	S9390
K_2HPO_4	30.000	Sigma-Aldrich	P5655
NaCl	5.000	VWR	27810.295

Table 2.5: The volume [mL/250 mL] added of the different stock solutions to a final volume of 900 mL and the final concentration [g/L] of the components in the M9-PC-MtPr medium. The components were mixed using sterile technique.

Component	Amount added [mL/250 mL]	Concentration [g/L]
M9-PC-MtPr basis medium	25.000	-
NH_4Cl	-	1.000
$Na_2HPO_4•7H_2O$	-	11.200
K_2HPO_4	-	3.000
NaCl	-	0.500
$MgSO_4$ stock solution	0.250	0.246
Trace mineral stock solution 1	0.500	-
$ZnSo_4•7H_2O$	-	0.005
$FeSO_4•7H_2O$	-	0.100
$CuSO_4•5H_2O$	-	0.002
$MnCl_2•4H_2O$	-	0.0008
$(NH_4)_6Mo_7O_{24}•4H_2O$	-	0.0002
Cobalt stock solution	0.500	0.0001
Glucose (50%) stock solution	5.000	10.000
mQ-H_2O	218.750	-

Table 2.6: The volume [mL/250 mL] added of the different stock solutions to a final volume of 250 mL and the final concentration [g/L] of the components in the M9-PC-MtPr medium 2. The components were mixed using sterile technique.

Component	Amount added [mL/250 mL]	Concentration [g/L]
M9-MtPr basis medium 2	25.000	-
NH_4Cl	-	1.000
$Na_2HPO_4•7H_2O$	-	11.200
K_2HPO_4	-	3.000
NaCl	-	0.500
$MgSO_4$ stock solution	0.250	0.246
Trace mineral stock solution 2	0.500	-
$ZnSo_4•7H_2O$	-	0.0045
$FeSO_4•7H_2O$	-	0.0200
$CuSO_4•5H_2O$	-	0.0020
$MnCl_2•4H_2O$	-	0.0008
$(NH_4)_6Mo_7O_{24}•4H_2O$	-	0.0002
$CaCl_2•2H_2O$	-	0.0040
H_3BO_3	-	0.0003
Cobalt stock solution	0.500	0.0001
Glucose (50%) stock solution	5.000	10.000
mQ-H_2O	218.750	-

2.2.2.3. M9-MtPr media

M9-MtPr medium is a chemically defined, minimal medium, which was used to cultivate bacteria in the bioreactor. Two different recipes were used. Both media were prepared in two steps to avoid precipitation. M9-MtPr basis medium 1 was prepared by dissolving the

components in mQ-H_2O according to Table 2.7. The medium was autoclaved (121 °C, 20 min). After autoclaving, the final M9-MtPr medium 1 was made according to

Table 2.8 using sterile technique.

Table 2.7: The concentration [g/L], supplier and product number of the components of the M9-MtPr basis medium 1. The components were dissolved in mQ-H_2O and autoclaved at 121 °C for 20 minutes.

Component	Concentration [g/L]	Supplier	Product number
NH_4Cl	15.0	Sigma-Aldrich	213330
K_2HPO_4	4.00	Sigma-Aldrich	P5655
NaCl	0.50	VWR	27810.295

Table 2.8: The volume [mL/900 mL] added of the different stock solutions to a final volume of 900mL and the final concentration [g/L] of the components in the M9-MtPr medium 1. The components were mixed using sterile technique.

Component	Amount added [mL/900 mL]	Concentration [g/L]
M9-MtPr basis medium 1	700	-
NH_4Cl	-	15.000
K_2HPO_4	-	4.0000
NaCl	-	0.5000
$MgSO_4$ stock solution	5.400	1.479
Trace mineral stock solution 1	1.800	-
$ZnSo_4 \bullet 7H_2O$	-	0.0090
$FeSO_4 \bullet 7H_2O$	-	0.1000
$CuSO_4 \bullet 5H_2O$	-	0.0040
$MnCl_2 \bullet 4H_2O$	-	0.0015
$(NH_4)_6Mo_7O_{24} \bullet 4H_2O$	-	0.0004
Cobalt stock solution	1.800	0.0002
Glucose (50%) stock solution	90.000	50.00
mQ-H_2O	71.000	-
Cell inoculation and mQ-H_2O	30.000	-

M9-MtPr basis medium 2 was prepared by dissolving the components in mQ-H_2O according to Table 2.9. The medium was autoclaved (121 °C, 20 min). After autoclaving, the final M9-MtPr medium 2 was made according to

Table 2.10 using sterile technique.

Table 2.9: The concentration [g/L], supplier and product number of the components of the M9-MtPr basis medium 2. The components were dissolved in mQ-H_2O and autoclaved at 121 °C for 20 minutes.

Component	Concentration [g/L]	Supplier	Product number
NH_4Cl	5.0	Sigma-Aldrich	213330
K_2HPO_4	2.00	Sigma-Aldrich	P5655
NaCl	0.50	VWR	27810.295

Table 2.10: The volume [mL/900 mL] added of the different stock solutions to a final volume of 900mL and the final concentration [g/L] of the components in the M9-MtPr medium 2. The components were mixed using sterile technique.

Component	Amount added [mL/900 mL]	Concentration [g/L]
M9-MtPr basis medium 2	700	-
NH_4Cl	-	5.000
K_2HPO_4	-	2.000
NaCl	-	0.500
$MgSO_4$ stock solution	2.700	0.739
Trace mineral stock solution 2	1.800	-
$ZnSo_4 \bullet 7H_2O$	-	0.0045
$FeSO_4 \bullet 7H_2O$	-	0.0200
$CuSO_4 \bullet 5H_2O$	-	0.0020
$MnCl_2 \bullet 4H_2O$	-	0.0008
$(NH_4)_6Mo_7O_{24} \bullet 4H_2O$	-	0.0002
$CaCl_2 \bullet 2H_2O$	-	0.0040
H_3BO_3	-	0.0003
Cobalt stock solution	1.800	0.0001
Glucose (50%) stock solution	36.000	20.000
mQ-H_2O	127.700	-
Cell inoculation and mQ-H_2O	30.00	-

2.3. Batch cultivation protocol

Batch cultivation in 1 L bench-top bioreactors was performed, compared to shake flask cultivation, to obtain higher cultivation volume. This enabled sampling for metabolite analysis. Moreover, the use of the bioreactors allowed precise control of the cultivations. The reactors were managed through the Applikon Biotechnology myControl system. Batch cultivation was performed on the WT and A2mCh *E. coli* strains.

2.3.1. Precultures

Primary precultures were prepared in 250 mL baffled flasks by inoculating 75 µL glycerol stock in 50 mL LB medium (Table 2.3). For recombinant strains, Amp (1000 x, 100 mg/mL) was added to a concentration of 100 µg/mL. The primary precultures were incubated (8-9 hrs, 30 °C, 200 rpm).

Secondary precultures were prepared in two 500 mL baffled flasks by inoculating 75 µL and 200 µL of primary preculture, respectively, in 100 mL M9-PC-MtPr medium (subsection 2.2.2.2). For the recombinant strains, ampicillin (1000 x, 100 mg/mL) was added to a concentration of 100 µg/mL. The secondary precultures were incubated (13-14 hrs, 37 °C (WT) or 30 °C (A2mCh), 200 rpm) until a measured OD_{600} of 3-3.5.

2.3.2. Bioreactor preparation

The reactor vessel and reactor components were triple-washed with tap water, distilled water (dH_2O), and mQ-H_2O before the M9-MtPr basis medium (Table 2.7 and Table 2.9) was added to the reactor vessel. Thereafter, the DO- and pH-electrodes were calibrated. The DO-electrode was calibrated to 0 % dissolved oxygen (DO) with nitrogen gas, through

a one-point calibration. The pH-electrode was calibrated in a two-point calibration with standard buffers of pH 7.00 and pH 4.01. After calibration, the electrodes were connected to the reactor and filters (0.2 µm, PTFE Membrane, Acro 50, Pall Corporation, 4250) were connected to the air inlet and exhaust outlet, and the bioreactor was autoclaved (121 °C, 20 min). Before starting the cultivation, the preparation of M9-MtPr medium (Table 2.8 and Table 2.10) was completed in a sterile bench.

Afterwards, the bioreactor system was set up according to the instruction manual, the temperature was set to 37 °C (WT) or 30 °C (A2mCh), and the condenser and cooling valves were opened. An autoclaved graduated cylinder containing sodium hydroxide (4 M NaOH) was connected to the bioreactor and the tubing was primed. Furthermore, the pH in the bioreactor system was set to 7.00. The system was sealed and checked for leaks, using a flowmeter (Aalborg® GFM Flowmeter, 0-5 L/min, Supelco). The air flow was set to 600 mL/min. When the system reached the set temperature, the DO-electrode was calibrated to 100 % DO after setting the agitation to 800 rpm for 10 min. Afterwards, an agitation cascade (200-800 rpm) was initiated to keep the DO above 40 %.

To log the pH, agitation, temperature and DO, the software BioXpert V2 was used. To monitor off-gases, a Thermo Scientific™ Prima BT Bench Top Process Mass Spectrometer was used, logging the recorded data using the Thermo Scientific™ GasWorks Software.

2.3.3. Cultivation and sampling

The cultivation was initiated by inoculating the bioreactor with the secondary preculture to obtain an OD_{600} of 0.1. In addition, 200 µL of antifoam (Adeka, NOL LG-109, 10% w/w) was added to prevent foaming. For the recombinant strain, ampicillin (1000 x, 100 mg/mL) was added to a concentration of 100 µg/mL, and the production of mCherry was induced at OD_{600} ~ 0.5 by adding m-toluate (500 x, 500 mg/mL) to a concentration of 1 mg/mL. When the OD_{600} was measured to ~2.0, oxygen limitation was induced for both the WT and A2mCh, by turning off the agitation cascade and setting the agitation to a fixed value of 400 rpm. As mentioned above, the pH, agitation, temperature, DO, and off-gases were logged.

The optical density of the bioreactor was measured regularly, as described in subsection 2.4.1. For the WT, three samples prior to and three samples after oxygen limitation were taken. These were done at OD_{600} ~0.5, ~1.0, ~2.0, ~3.0, ~4.0, and ~5.0. For the A2mCh, one sample prior to and three samples after oxygen limitation were taken. These were done at OD_{600} ~2.0, ~3.0, ~4.0, and ~6.0. Samples were collected as described in subsection 2.4. The samples were taken to analyse extracellular glucose and organic acids, as well as pyridine nucleotide metabolites, according to subsections 2.4.3 and 2.4.4, respectively. A2mCh was also sampled for intracellular protein analyses and central carbon metabolites, according to subsections 2.4.5 and 2.4.6, respectively.

2.4. Sampling and analysis

A number of samples were taken at varying time points during cultivation. When smaller samples were taken, the sampling port available in the bioreactors was used. Prior to sampling, 4 mL were discarded from the port to prevent contamination of the sample. When larger samples were extracted, the antifoam port was used. The port was sterilized prior to opening and closing, using a Flame Boy. The samples were extracted using sterile pipettes.

2.4.1.Optical density

The optical density (OD_{600}) was measured to follow the bacterial growth, both in tandem with exometabolite and NAD sampling, and by itself. When measuring OD_{600} by itself, the samples were extracted from the sampling port after discarding 4 mL. The samples were analysed at 600 nm on a spectrophotometer (V-1200 Spectrophotometer, VWR) diluted in mQ-H_2O to give a measurement inside of the linearity range of the instrument (0.2 – 0.6). The spectrophotometer was blanked with M9-PC-MtPr in the same dilution as the sample. The OD_{600} measurements were translated into CDW using the calibration curve corresponding to the given strain.

2.4.2.Cell dry weight calibration curve

Calibration curves to determine CDW from OD_{600} were made for *E. coli* BL21 WT and A2mCh. Precultures were made by inoculating 50 mL LB (Table 2.3) with 75 µL glycerol stocks (subsection 2.1.1) in 250 mL baffled flasks. For the recombinant strains, ampicillin (1000 x, 100 mg/mL) was added to a concentration of 100 µg/mL. The precultures were incubated (8 hrs, 37 °C (WT) or 30 °C (A2mCh), 200 rpm). Thereafter, cultures were grown in biological quadruplicates by inoculating 100 mL M9-PC-MtPr (Table 2.6) with 100 µL of preculture in 500 mL baffled flasks. For the recombinant strains, ampicillin (1000 x, 100 mg/mL) was added to a concentration of 100 µg/mL. The cultures were incubated (10-14 hrs, 37 °C (WT) or 30 °C (A2mCh), 200 rpm), until they reached an OD_{600} of ~2.5.

Once OD_{600} ~ 2.5 was reached, the cultures were divided into eight sterile 50 mL falcon tubes and centrifuged (4 °C, 4000 rcf, 10 min). Thereafter, supernatants were discarded, and pellets were resuspended in 2 mL M9-PC-MtPr (Table 2.6). The resuspended pellets were pooled together and a dilution series was made from seven dilutions with OD_{600} from 20 to 0.25.

A calibration curve was made by measuring the CDW and the OD_{600} of each dilution simultaneously. The OD_{600} was measured in technical duplicates at 600 nm using a spectrophotometer (V-1200 Spectrophotometer, VWR), as described in subsection 2.4.1. The CDW was measured in technical triplicates, using a fast filtration protocol adapted from Kvitvang and Bruheim (2015). The setup consisted of a filtration manifold (Pall Corporation, 4206), a vacuum pump (ME 4R NT Diaphragm pump, Vacuubrand, 20731100), a vacuum controller (CVC 3000, Vacuubrand), and a waste collector. Filters (0.45 µm, PVDF Membrane, Merck Millipore, HVLP04700) were dried for at least 48 hrs and weighed before use. When sampling for biomass, the filters were positioned onto the filtration manifold and saturated with mQ-H_2O. 1 mL or 5 mL of the samples from the dilution series were transferred to the filter, dependent upon whether the biomass was high or low, respectively. For filtration, the samples were exposed to 800 mbar below the ambient pressure before being washed with 10 mL mQ-H_2O (30 °C). M9-PC-MtPr was filtered as a blank. Thereafter, the filters containing cells were dried for at least 48 hrs before being weighed.

The CDW calibration curve was found by performing linear regression of the average CDW as a function of OD_{600}. The blank value was subtracted from the CDW of all samples. The calibration curves are presented in Appendix A.1.

The CDW was also measured according to the same protocol at given time points for the cultivations with A2mCh.

2.4.3.Exometabolite sampling and analysis

Samples of the cultivation broth were taken during all runs, by the method described in subsection 2.4.3.1. These were collected to analyse the exometabolites acetic acid, citric acid, ethanol, formic acid, fumaric acid, lactic acid, pyruvic acid, and succinic acid, in addition to glucose. The organic acids and glucose were quantified using High Performance Liquid Chromatography (HPLC) (subsection 2.4.3.2).

2.4.3.1. Sampling and sample preparation

For all WT cultivations, six sampling point were selected. Three were before induction of oxygen limitation and three after. Samples were taken at OD_{600} ~0.5, ~1.0, ~2.0, ~3.0, ~4.0 and ~5.0 for the WT cultivations. For the A2mCh cultivations, four sampling points were selected. One was prior to induction of oxygen limitation and three after. Samples were taken at OD_{600} ~2.0, ~3.0, ~4.0 and ~6.0. For the runs where no oxygen limitation was induced, the sampling time was matched with the sampling time of the oxygen limitation runs using the OD_{600} measurements. The sample volume was adjusted based on the biomass concentration to the equivalent of 5 mL of a culture with OD_{600} 1.0. When sampling, four technical replicates were taken from each bioreactor and stored in Eppendorf tubes. During sampling, the samples were kept on ice before being immediately centrifuged (4 °C, 4000 or 10000 rcf[1], 5 min). The supernatant was transferred to a new Eppendorf tube, and both the supernatant and the pellet were snap-frozen in LN_2. The samples were stored at -80 °C until further analysis.

2.4.3.2. Quantification of extracellular organic acids and glucose using HPLC

The concentration of organic acids and glucose in the supernatants was quantified using an Alliance HPLC (Waters) with a Hi-Plex H 300 x 7.7 mm column (Agilent Technologies, PL1170-6830) and detected by a refractive index (RI) and a UV/Vis detector. An external standard (ESTD) mixture was prepared to make a standard curve, making it possible to interpolate the concentration from areas under the chromatographic peaks acquired from the HPLC. The ESTD mixture was prepared from analytical grade standards mixed in mQ-H_2O. The concentration range of each compound in the ESTD series is presented in Table 2.11, together with the supplier and product number.

The samples and standards were analysed in volumes of 200 µL in micro inserts (0.1 mL, VWR, 548-0006) in HPLC vials (1.5 mL, VWR, 548-0030) with caps (VWR, 548-0839). The samples were filtered using syringe filters (0.2 µm PTFE membrane, 13 mm, VWR, 514.0068) and analysed, both diluted (1:10) and undiluted, using two technical replicates for each sampling point. mQ-H_2O was used as blanks and run regularly between samples. The samples were eluted by 0.05 M H_2SO_4 (Merck, 5.43827.0100) as the mobile phase with a 0.6 mL/min flow. The column was set to 45 °C and the RI detector to 35 °C.

[1] Dependent on size of tube, 5-15 mL or 1.5-2 mL tubes, respectively.

Table 2.11: The external standard (ESTD) mix was prepared using the following compounds, with the given product number from the given supplier. The ESTD mix was made in varying concentrations of the compounds where the range of concentration varied between the concentrations given.

Compound	Concentration range [g/L]	Supplier	Product number
Acetate	0.25 – 2.00	Merck (Supelco)	1.00063.1011
Citrate	0.03 – 0.25	Sigma-Aldrich	C7129
Ethanol	0.63 – 5.00	VWR	20821.310
Formate	0.19 – 1.50	VWR	84865.260
Fumarate	0.00063 – 0.0050	Sigma-Aldrich	47910
Lactate	0.25 – 2.00	Sigma-Aldrich	L1500
Pyruvate	0.03 – 0.25	Sigma-Aldrich	P8574
Succinate	0.13 – 1.00	Sigma-Aldrich	S3674
Glucose	0.63 – 5.00	VWR	101176K

2.4.4.Pyridine nucleotides sampling and analysis

During the runs, cell pellets were extracted to analyse pyridine nucleotides by the method described in subsection 2.4.4.1. Pyridine nucleotides were extracted from the cell pellets and quantified using Zwitterionic Hydrophilic Interaction Liquid Chromatography Tandem Mass Spectrometry (HILIC-MS/MS) as described in subsection 2.4.4.2 and 2.4.4.3, respectively.

2.4.4.1. Sampling and sample preparation

Six sampling points were selected for the WT cultivation, three prior to the onset of oxygen limitation and three after. Samples were taken in technical quadruplicates at OD_{600} ~0.5, ~1.0, ~2.0, ~3.0, ~4.0, and ~5.0. For the A2mCh cultivations, four sampling points were selected. One prior to and three after oxygen limitation. These were taken at OD_{600} ~2.0, ~3.0, ~4.0 and ~6.0. For runs with no oxygen limitation, the sampling time was matched with the oxygen limitation runs using the OD_{600} values. The samples were kept on ice before being immediately centrifuged (4 °C, 4000 or 10000 rcf[2], 5 min). The supernatant was transferred to another Eppendorf tube, before the samples were snap frozen in LN_2. The samples were stored at -80 °C until further preparation and analysis.

2.4.4.2. Pyridine nucleotide extraction

As pyridine nucleotides are labile metabolites and show a high degree of unwanted oxidization and reduction under solvent removal (Lu et al., 2018), the extraction protocol was adapted from Rost et al. (2020).

When extracting pyridine nucleotides, 9 or 12 samples were extracted at a time, dependent upon whether the samples were from 5-15 mL tubes or 1.5-2 mL microtubes. Before extracting the samples, ^{13}C pellets were extracted to prepare the internal standards (ISTD). The extraction protocol for samples and ^{13}C pellets were the same, with small differences, as detailed below.

[2] Dependent on size of tube, 5-15 mL or 1.5-2 mL tubes, respectively.

The extraction solution (H_2O (VWR, 83645.320): ammonium acetate (150 mM, Sigma-Aldrich, A2706): methanol (MeOH) (Merck, 1.06035.2500): acetonitrile (ACN) (VWR, 83640.320), 10:10:20:60 v/v), adjusted to pH 9.70 with ammonium hydroxide (25 %, Sigma-Aldrich, 5.33003.0050), was heated to 60 °C on a shaking heat block (VWR, 460-0196). The sample pellets were thawed at room temperature before being centrifuged (4 °C, 4500 or 20817 rcf[3], 2 min). The remaining supernatant was removed and 270 µL extraction solution plus 30 µL ^{13}C extract were added to each pellet (only 300 µL extraction solution was added to the ^{13}C pellets). The pellets were vortexed at an angle to break them up for less than 30 sec or 60 sec[3], before being placed on the heat block at 60 °C. 5-15 mL tubes were shaken at 800 rpm for 3 min, while 1.5-2 mL tubes were shaken at 1500 rpm for 5 min, occasionally vortexing them. The samples were centrifuged (4 °C, 4500 or 8603 rcf[3], 2 min), before the supernatants were transferred to 10 kDa spin filtration tubes (VWR, 82031-350). The samples were centrifuged (4 °C, 20817 rcf, 5 min). Thereafter, the ^{13}C samples were pooled together and stored at 4 °C. As for the experimental samples, 90 µL were spiked with 10 µL extraction solution and transferred to inserts with plastic springs (150 µL, Waters, WAT094171) in individual vials (2 mL, Waters 186000848) with pre-slit caps (Waters, 186000305).

The ^{13}C pellets were prepared from *E. coli* BL21 WT cultivated in shake flasks (30 °C, 200 rpm) in a minimal medium containing glucose labelled with U-^{13}C (99%, Cambridge Isotope Laboratories, CLM-1396-10).

2.4.4.3. Quantification of pyridine nucleotides using Zwitterionic HILIC-MS/MS

The concentration of the pyridine nucleotides in the cells was quantified using zwitterionic HILIC-MS/MS. The HILIC separation was carried out on an AQUITY I-Class UPLC with an AdvanceBio MS Spent Media 2.1x100 mm column (Agilent, 675775-901). Two mobile phases were used. Mobile phase A (ACN (VWR, 83640.320): H_2O (VWR, 83645.320), 1:1 v/v) and mobile phase B ACN (VWR, 83640.320): H_2O (VWR, 83645.320), 4:1 v/v), both with 15 mM ammonium acetate (Sigma-Aldrich, A2706), adjusted to pH 9.70 with ammonium hydroxide (25 %, Sigma-Aldrich, 5.33003.0050), were used, following a gradient. Each sample injection, with injection volume of 0.2 µL, was run for 10 minutes at 0.3 mL/min. For the first 0.5 min, the mobile phase was mixed 1:99 (A:B). Over the next five minutes it was increased to 65:35 (A:B), before being decreased to 1:99 (A:B) over the next 0.5 min and kept constant for the remainder of the runtime. Thereafter, MS/MS was performed using a Waters Xero TQ-XS triple quadrupole mass spectrometer system, which was equipped with an electrospray ionization (ESI) source in positive mode. An ESTD was prepared to make a standard curve, making it possible to interpolate the concentration from the response acquired from the HILIC-MS/MS. The ESTD mix was prepared from analytical grade standards mixed in mQ-H_2O. The range of concentration of each of the compounds in the ESTD is presented in Table 2.12. The response of each sample was acquired using the TargetLynx functionality of MassLynx 4.2 (Waters).

[3] Dependent on size of tube, 5-15 mL or 1.5-2 mL tubes, respectively.

Table 2.12: The external standard (ESTD) mix was made using the following compounds, with the given product number from the given supplier. The ESTD mix was made in varying concentrations of the compounds where the range of concentration varied between the concentrations given.

Metabolite	Concentration range [nM]	Supplier	Product number
NAM	0 – 10000	Sigma-Aldrich	72349
NA	0 – 10000	Sigma-Aldrich	72309
1-mNAM	0 – 10000	Sigma-Aldrich	M4627
NR	0 – 10000	Sigma-Aldrich	SMB00907
NMN	0 – 10000	Sigma-Aldrich	N3501
NaMN	0 – 10000	Sigma-Aldrich	N7764
NAD	0 – 20000	Sigma-Aldrich	N1511
NADH	0 – 20000	Sigma-Aldrich	N8129
NADP	0 – 20000	Sigma-Aldrich	N5755
NADPH	0 – 20000	Sigma-Aldrich	N5130
FAD	0 – 20000	Sigma-Aldrich	F6625
ADPR	0 – 10000	Sigma-Aldrich	A0752

2.4.5.mCherry sampling and analysis

For the A2mCh strain, and in tandem with the sampling for exometabolites, pyridine nucleotides, and central carbon metabolites, sampling for mCherry quantification was performed. Due to the need of oxygen for the maturation of the chromophore in mCherry (Chapagain et al., 2011), two different ways of quantifying the amount of mCherry produced were implemented. One method relied on the fluorescent properties of mCherry, as described by García-Calvo et al. (2023), while the other relied on the ability of specific antibodies to bind to mCherry through a western blot.

2.4.5.1. mCherry sampling and quantification using fluorescence

In the cultivations where oxygen limitation was not induced, the amount of mCherry produced is possible to quantify using the fluorescent properties of mCherry. When sampling for mCherry, three technical replicates of 200 µL were collected and placed into respective wells in a 96-well plate (VWR, 10062-900). Fluorescence was measured using a microplate reader (Tecan Spark®, 20M, Bergman Diagnostika) with bottom reading gain at 66, excitation wavelength at 560 nm, and emission wavelength at 635 nm. The autofluorescence of the media was corrected for by subtracting the fluorescence of the media from the fluorescence of the mCherry samples. The fluorescence of mCherry was translated into the amount of mCherry present interpolating from a calibration curve prepared in triplicates with dilutions of commercial pure mCherry (ABIN412973, antibodies-online GmbH), measured in the Spark 20M Microplate reader with the parameters given above.

2.4.5.2. mCherry sampling and quantification using western blot

In the cultivation where oxygen limitation was induced, the amount of mCherry produced is not possible to quantify using the fluorescent properties of mCherry, since the chromophore will not mature without oxygen present (Chapagain et al., 2011). Therefore, another sampling and quantification method must be used. The method used to quantify the amount of mCherry present was western blotting.

2.4.5.2.1. mCherry sampling

When sampling for mCherry in oxygen limitation, cell pellets were collected the same way as for pyridine nucleotides, in technical quadruplicates. The samples were kept on ice before being centrifuged (4 °C, 4500 or 20817 rcf[4], 5 min). The supernatant was discarded, leaving only the pellet, before the samples were snap frozen in LN_2. The samples were stored at -80 °C until further preparation and analysis.

2.4.5.2.2. mCherry extraction and western blot

Before preparing the western blot, the integrity and concentration of the protein extracts were validated by performing SDS-PAGE. Firstly, the wet weight of the pellets was determined, before they were lysed in 5 µl/mg CellLytic B (2 x, Sigma-Aldrich, B7310), supplemented with 0.4 µL/mL benzonase nuclease (Sigma-Aldrich, E1014). The samples were incubated (room temperature, 100 rpm, 30 min) on a rocking mixer (Heidolph, UNIMAX 1010). Soluble and insoluble fraction were separated by centrifugation (10000 rcf, 5 min) and the insoluble fraction was resuspended in SDS-running buffer (Bio-Rad) with the same volume as the respective pellet was lysed in. The samples were diluted 3:10 in SDS running buffer, then 1:4 in loading dye (4x XT Sample Buffer, Bio-Rad).

Before running the SDS-PAGE, the samples were boiled (95 °C, 5 min). The samples (15 µL) and a protein ladder (Precision Plus Dual Color Standards, Bio-Rad, 5µL) were loaded onto a 26 well SDS-gel (3450119 12 % Criterion™ XT Bis-Tris Protein Gel, Bio-Rad) and ran at 200 V for 30-45 min. Afterwards, the gel was rinsed with RO water before removing it from the cassette and rinsing again. The gels were then stained in Coomassie Brilliant Blue (R-250, Bio-Rad, 1610436) for 1 hr. Afterwards, the gels were washed for 1 h using mQ-H_2O. The gels were imaged using a ChemiDoc™ (ChemiDoc XRS+ system, Bio-Rad, 1708265) with a white-light conversion tray and Software Image Lab 6.0.1.

For the western blot, the gels were prepared the same way as for the SDS-PAGE gels, with two exceptions. When diluting the samples for the SDS-PAGE gel, they were diluted both 500 and 1000 times, and the Coomassie staining step after the gel had run was omitted. When reaching this step, the gels were placed on top of a transfer membrane in between a western blot transfer stack, inside a western blot cassette, and transferred (7 min). The membrane was placed, protein side down, onto an iBind™ Flex Card (Thermo Fischer Scientific) wetted with 10 mL 1 x iBind™ Flex Solution[5] and loaded onto an iBind™ Flex Western Device (Thermo Fischer Scientific). Antibodies and wash solution were then added. 4 mL 1:1000 diluted anti-mCherry antibody (Abcam, ab167453) was added to the first row; 4 mL 1 x iBind™ Flex Solution was added to the second row; 4 mL anti-IgG F(c) Goat Polyclonial Antibody (HRP (Horseradish Peroxidase), ImmunoReagents Inc, IMMRIR2226) was added to the third row and 12 mL 1 x iBind™ Flex Solution was added to the fourth row. The western blot was run (2.5-3 hrs) and washed in RO water (10 min) afterwards. The membrane was revealed using 3,3',5,5'-tetramethyl-benzidine (TMB, Sigma-Aldrich, T0565). After 30 sec, the membrane was removed from the TMB and washed thoroughly using RO water.

[4] Dependent on size of tube, 5-15 mL or 1.5-2 mL tubes, respectively.

[5] 50 mL 1 x iBind™ Flex Solution was made by mixing 500 µL iBind™ Flex 100 x Additive, 10 mL iBind™ Flex 5 x buffer and 39.5 mL RO water.

The gels were imaged using a ChemiDoc™ (ChemiDoc XRS+ system, Bio-Rad, 1708265) with a black tray and Software Image Lab 6.0.1.

2.4.5.3. mCherry calibration curve using fluorescence

To quantify the amount of mCherry using the fluorescence values, a calibration curve was needed. The mCherry calibration curve was made using commercial mCherry (ABIN412973, antibodies-online GmbH), measured in concentrations ranging from 0.39 to 100 ng/µL in duplicates. Measurements were made using a microplate reader (Tecan Spark®, 20M, Bergman Diagnostika) with a bottom gain of 66. The calibration curve was created by plotting the known concentration against the fluorescence and performing power regression.

In addition, a calibration curve that made it possible to interpolate the fluorescence of lysed cells from the fluorescence of whole cells was also made.

Calibration curves were made during earlier studies that were part of the project MetaboProt and can be found in Appendix A.2.1.

2.4.5.4. mCherry calibration curve using western blot

To quantify the amount of mCherry in the western blot, a calibration curve was needed. The mCherry calibration curve was made using commercial mCherry (ABIN412973, antibodies-online GmbH) loaded onto an SDS-gel in concentrations ranging from 0.5 ng to 10 ng. Western blot was then then performed in the same manner as previously described in subsection 2.4.5.2.2, following the steps after soluble and insoluble proteins were separated.

The calibration curve was made by plotting the band intensities against the known concentrations and performing linear regression analysis. The calibration curve can be found in Appendix A.2.2.

2.4.6.Central carbon metabolite sampling

During the mCherry runs, samples for central carbon metabolite analysis were collected. These samples were further prepared for analysis of organic acids, amino acids, TCA metabolites, glycolysis metabolites, pyridine nucleotides, and nucleoside and deoxynucleoside phosphates. The quantification of the metabolites was done by Ion Chromatography Tandem Mass Spectrometry (IC-MS/MS). The method for the fast filtration-based sampling, quenching, and extraction is based on Thorfinnsdottir et al. (2023). The sampling points were at OD_{600} ~2.0, ~3.0, ~4.0 and ~5.0.

2.4.6.1. Fast-filtration sampling and quenching

A fast-filtration setup was used to sample in technical triplicates. The filtration setup consisted of a filtration manifold (Pall Corporation, 4206), a vacuum pump (ME 4R NT Diaphragm pump, Vacuubrand, 20731100), a vacuum controller (CVC 3000, Vacuubrand), and a waste collector. Filters (0.45 µm, PVDF Membrane, Merck Millipore, HVLP04700) were positioned onto the filtration manifold and saturated with mQ-H_2O. A volume corresponding to 5 units of OD_{600} was sampled. The samples were exposed to pressure 800 mbar below the ambient pressure before being washed with 10 mL mQ-H_2O (30 °C) and quenched in 10 mL quenching solution (mQ-H_2O: ACN (VWR, 83640.320): MeOH

(Merck, 1.06035.2500), 5:3:2, v/v) in 50 mL Falcon tubes, which had been kept at -20 °C in a low temperature circulation bath (GR150, Grant Instruments) filled with ethanol. After transferring to the quenching solution, the samples were immediately snap frozen in LN_2 and stored at -80 °C pending extraction.

2.4.6.2. Central carbon metabolite extraction

To extract the metabolites from the quenched samples, they were first thawed at -20 °C for 30 min in a low temperature circulation bath (GR150, Grant Instruments, Royston, UK) filled with ethanol. Thereafter, the samples were left in the circulation bath for 30 min, with occasional interruptions to be vortexed. The filters were discarded and cell debris removed by centrifugation (-9 °C, 4500 rcf, 10 min). 9.5 mL of the supernatants were transferred to new 50 mL Falcon tubes with a hole in the lid and snap-frozen in LN_2. Thereafter, the metabolites were concentrated by lyophilization (-105°C, 0.05 mbar, 18 h, Alpha 3-4 LSCbasic, Martin Christ Gefriertrocknungsanlagen GmbH).

The lyophilized metabolite extracts were reconstituted in 500 µL cold H_2O (VWR, 83645.320). Residual cell debris was removed by centrifugation (4 °C, 4500 rcf, 5 min), before transferring the supernatants to 10 kDa spin filtration tubes (VWR, 82031-350) and centrifuged (4 °C, 20817 rcf, 10 min). Residual volume was transferred to new spin filters and centrifuged again. 110 µL of the sample, spiked with 10 µL ^{13}C metabolite extracts, was transferred to inserts with plastic springs (150 µL, Waters, WAT094171) in individual vials (2 mL, Waters 186000848) with pre-slit caps (Waters, 186000305).

The ^{13}C metabolite extracts were prepared from yeast cultivated in shake flasks (30 °C, 200 rpm) in a minimal medium containing glucose labelled with U-^{13}C (99%, Cambridge Isotope Laboratories, CLM-1396-10).

2.4.6.3. Quantification of central carbon metabolites using IC-MS/MS

IC-MS/MS was performed according to Stafsnes et al. (2018) with some modifications. The concentration of the central carbon metabolites in *E. coli* was quantified using IC-MS/MS. The IC separation was carried out using the Thermo Scientific Dionex™ Integrion™ HPIC™ RFIC system with DI-water, supplemented with a makeup solvent of 90% ACN in DI-H_2O containing 0.01 % NH_4OH, delivered by an external AXP-MS pump at 0.1 mL/min, combined with the eluent via a low dead volume mixing tee and passed through a grounding union before entering the MS. The system had a Dionex™ IonPac™ AS11-HC-4 µm 2x250 mm IC column (Thermo Scientific, 078035) with a Dionex™ IonPac™ AG11-HC-4 µm 2x50 mm Guard column (Thermo Scientific, 078036). The system was equipped with an AS-AP thermostated autosampler, column oven, degasser, CR-TC, and an ADRS 600 2 mm suppressor and conductivity detector. The gradient conditions were as follows: an initial 4 mM potassium hydroxide was held for 1 min, increased to 12 mM at 5 min, to 20 mM at 13 min, 70 mM at 22 min, held at 70 mM for 7.5 min, followed by a rapid increase to 100 mM at 31 min, held at 100 mM for 5 min, decreased to 4 mM over 4 min, and finally held for 10 min to re-equilibrate the column. The total run time was 50 min. The injection volume was 25 µL with two times overfill.

The MS analysis was performed using a Waters Xevo TQ-S triple-quadruple MS in negative electrospray ionization mode with a capillary voltage of 2.5kV and ion source temperature of 150 °C. The desolvation gas was nitrogen, flowing at 800 L/h at 300 °C. The same collision energy for each MRM transition was used as described in Stafsnes et al. (2018), but the retention times were optimized for each compound both manually and using the

"Intellistart"-function in MassLynx 4.2. The MS was run in dynamic MRM mode and the retention time window for each compound was set to ±2 min of the expected retention time. Downstream data processing was performed in MassLynx 4.2

An ESTD was prepared to make a standard curve, making it possible to interpolate the concentration from the response acquired from the IC-MS/MS. The ESTD mix was prepared from analytical grade standards (Sigma Aldrich) mixed in mQ-H_2O. The ESTD contained 55 different central carbon metabolites in a concentration range of 117.19 – 15000 mM or double as much for selected metabolites.

2.5. Data processing, statistical analysis, and visualization

Cultivation data from bench-top bioreactors were plotted using Matplotlib v3.7.1 (Hunter, 2007). Concentrations of mCherry, pyridine nucleotides, and exometabolites were also plotted using Matplotlib v3.7.1.

Pyridine nucleotide data processing was performed as described by Rost et al. (2020), with modifications. MS data were inspected and processed in the TargetLynx application manager of the MassLynx 4.2 software (Waters). The concentration of the metabolites was quantified by interpolating from calibration curves generated using linear regression with 1/x weighting. The response factors of the ESTD and processed samples were corrected for using the response factor of the corresponding ISTD-isotopologue. The quantified data were manually adjusted by modifying the area and baseline of the integrated peaks when necessary. The concentrations were corrected for dilutions performed during sample processing and normalized by CDW. Potential outliers in the sub-sample sets were identified and rejected by Dixon's Q test with a 95 % confidence interval, as described in Appendix E.1. The data were further autoscaled, mean-centered and divided by the square root of the standard deviation of each variable, and visualized using MetaboAnalyst 5.0 (Pang et al., 2021).

3. Results

As part of the research project MetaboProt, the aim of this thesis was to study the effect that oxygen limitation had on the redox state and the capability of *E. coli* to produce RPs. The strains studied were the *E. coli* BL21 WT and the recombinant strain *E. coli* BL21 A2mCh. Negative controls, a strain with the plasmid, but without the mCherry encoding gene, was omitted due to the mCherry containing strain and the negative control having similar growth patterns (Everson, 2022; García-Calvo et al., 2023; Humlebrekk, 2022; Mæhlum, 2021; Mathiassen, 2022). For more information on the expression vector, see subsection 2.1, and the plasmid map is presented in Appendix G.

3.1. Preliminary batch cultivations

Prior to the proper cultivations were performed, the media was optimized. Additionally, testing of which temperature to cultivate at was performed.

The tested media were the M9-MtPr media 1 and 2, a chemically defined minimal medium, as shown in Table 2.8 and Table 2.10, respectively. Media 1 had higher concentrations of the trace minerals, with media 2 having some additional trace minerals. Media 1 was run first at both 30 °C and 37 °C using one biological replicate. Based on the findings from these cultivations, medium 2 was run at 37 °C using biological duplicates. As precipitation was observed when testing media 1, media 2 was run with and without the addition of EDTA. The resulting cultivation plots created can be viewew in in Figure B.1 in Appendix B.

It was found that the usage of media 2, both with and without the addition of EDTA, gave *E. coli* roughly twice the growth rate observed in media 1 at the same temperature (Table 3.1).

Table 3.1: The growth rate (μ) of *E. coli* BL21 WT and A2mCh using different medium, temperature, and the presence (+) or absence (-) of EDTA. One biological replicate was used when testing M9-MtPr medium 1, while M9-MtPr medium 2 was tested using biological duplicates. An example calculation to determine the growth rate can be viewed in Appendix A.3.

Strain	Medium	Temperature [°C]	EDTA	μ [h^{-1}]
WT	M9-MtPr 1	30	-	0.34
WT	M9-MtPr 1	37	-	0.37
A2mCh	M9-MtPr 1	30	-	0.33
A2mCh	M9-MtPr 1	37	-	0.33
WT	M9-MtPr 2	37	-	0.66 ± 0.00
WT	M9-MtPr 2	37	+	0.73 ± 0.04

Based on the data presented in Table 3.1, it was decided to use M9-MtPr medium 2 at 37 °C without EDTA for the following WT runs. EDTA was omitted due to its seemingly negligible effect on the growth rate and as EDTA has previously been shown to potentially be toxic to *E. coli* (Rantala et al., 2011). For the A2mCh runs, it was decided to use the M9-MtPr medium 2 at 30 °C, as a lower temperature is ideal for RP expression (Rosano & Ceccarelli, 2014). Investigation into which OD_{600} value, 0.5 or 1, to induce mCherry

production were also performed (Figure B.2 in Appendix B). As there was a negligible difference in the growth pattern between the cultivations, it was decided to induce mCherry production at OD_{600} ~ 0.5.

3.2. Batch cultivations

The effects of oxygen limitation on the redox state of *E. coli* BL21 WT and A2mCh strains were investigated using batch cultivations in 1 L bench-top bioreactors. Additionally, the effect this had on the production of RPs, namely mCherry, in the A2mCh strain was also evaluated.

3.2.1. Cultivation of *E. coli* BL21 WT

The cultivation of *E. coli* BL21 WT was performed with and without oxygen limitation in biological triplicates. As the biological triplicates were reproducible, Figure 3.1 presents the cultivation plots of one representative replicate for each condition. The remaining cultivation plots can be viewed in Appendix C.1. Prior to the onset of oxygen limitation the cultivations behaved similarly. After the onset of oxygen limitation the growth patterns differed. The non-limited cultivations grew with the same growth rate throughout the cultivation, while the growth rate was reduced by more than half in the oxygen-limited cultivations post-limitation. The growth rates are presented in Table 3.2. However, none of the cultivations reached glucose limitation. Thus, the reduced growth rate was most likely due to oxygen limitation.

Table 3.2 also presents the biomass at stationary phase, calculated from the cultivations shown in Figure B.1e, f, and Figure B.3a (Appendix B). From these, it was found that no oxygen limitation supported a biomass that was more than twice as great as the one reached in the stationary phase under oxygen limitation, most likely due to depletion of glucose.

Table 3.2: The biomass at stationary phase and growth rate (μ) before and after oxygen limitation for the cultivation runs of *E. coli* BL21 WT under oxygen limitation and no oxygen limitation. Where applicable, the percentage reduction is shown. The growth rate was calculated as presented in Appendix A.3. The biomass at stationary phase was calculated from the cultivations presented in Figure B.**1**e, f, and Figure B.**3**a (Appendix B).

Condition	Biomass at stationary phase [g CDW/L]	μ [g CDW/h]		
		Before oxygen limitation	After oxygen limitation	% reduction
O_2-lim	2.28 ± 0.10	0.56 ± 0.042	0.20 ± 0.011	64
No O_2-lim	6.82 ± 0.18	0.62 ± 0.0031	-	-

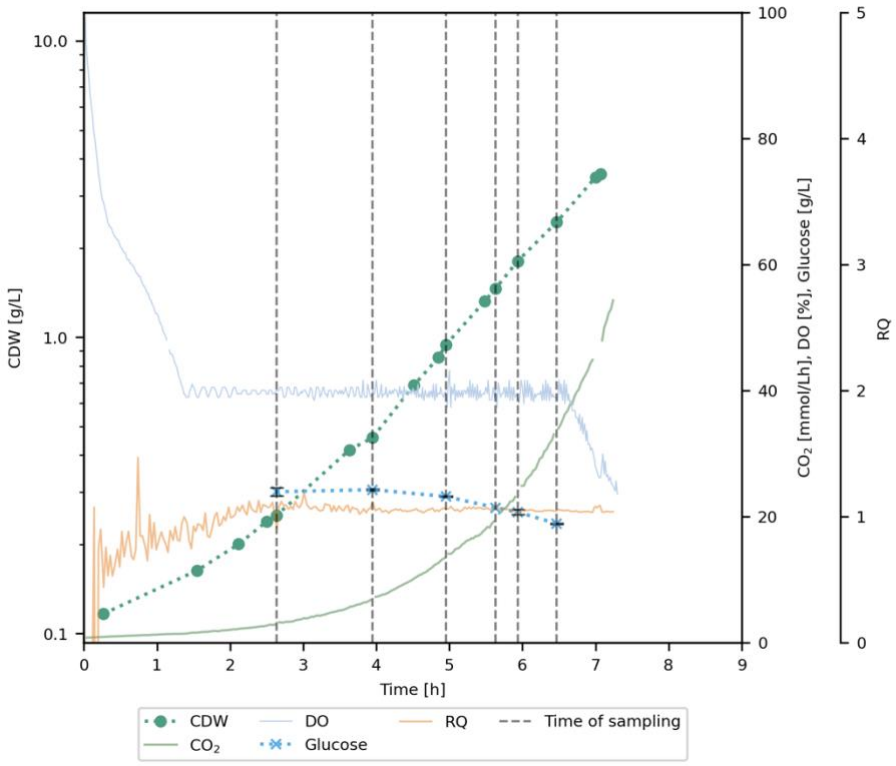

a) *E. coli* BL21 WT-I, no oxygen limitation.

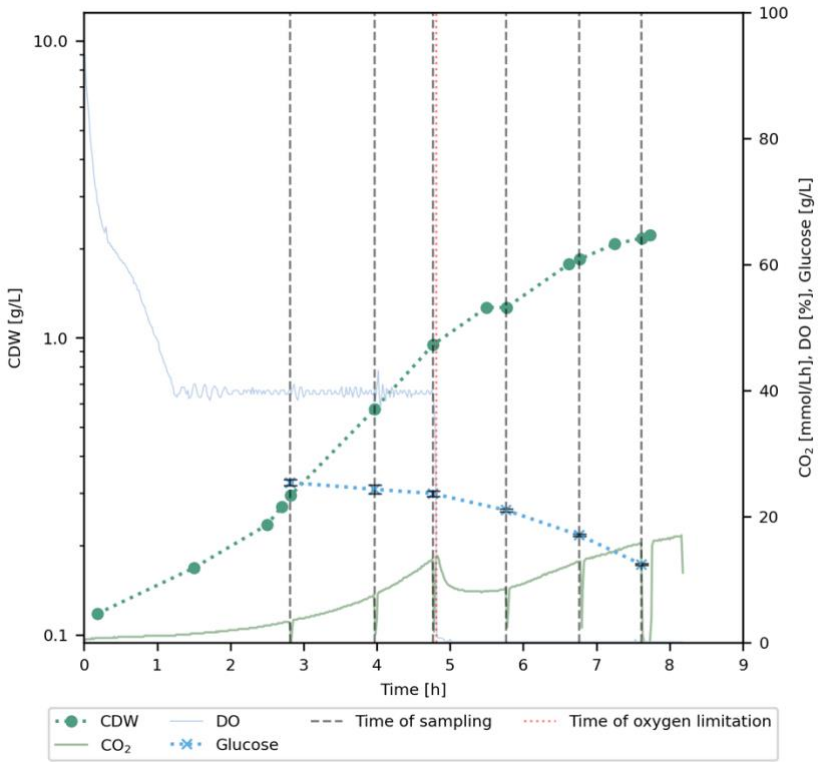

b) *E. coli* BL21 WT-I, oxygen limitation.

Figure 3.1: Representative cultivation plots for *E. coli* BL21 WT of the biological triplicates grown under no oxygen limitation (a) and oxygen limitation (b). The dissolved oxygen (DO, light blue line), CO_2 off-gas (green line) and respiratory quotient (RQ, yellow line) were measured online (RQ not

measured for (b) due to instrument malfunction). Cell dry weight (CDW, green dotted line) was calculated from the measured OD_{600} (see Appendix A.1 for how to calculate CDW from OD_{600}). Glucose (blue dotted line) was sampled for in technical quadruplicates, along with other exometabolites and pyridine nucleotides, as indicated by the vertical, black dashed lines. The cultivations were performed using 1 L bench-top bioreactor with M9-MtPr medium 2 (Table **2.10**) at 37 °C. The pH was constantly adjusted to 7.00. For (b) the oxygen cascade was turned off and agitation set to 400 rpm, to simulate oxygen limitation, when CDW was at 0.868 g/L (OD_{600} ~ 2.0), while for (a) the dissolved oxygen was kept above 40 %. The induction of oxygen limitation is indicated by the vertical, red dashed line. The concentration of glucose at the start of the cultivation for plot a) and b) was omitted due to the quantified concentration being much lower than the concentration at T1. Roman numerals indicate the biological replicate.

3.2.2.Cultivation of *E. coli* BL21 A2mCh

The cultivations of *E. coli* BL21 A2mCh were performed with and without oxygen limitation in biological triplicates. As the biological triplicates were reproducible, Figure 3.2 presents the cultivation plots of one representative replicate for each condition. The remaining cultivation plots can be viewed in Appendix C.2. The induction of mCherry production did not appear to affect the growth rate as the non-limited cultivations grew at the same growth rate throughout the cultivation. The oxygen-limited cultivations grew at the same growth rate until oxygen limitation was applied, which reduced the growth rate by more than half. The growth rates are presented in Table 3.3. As none of the cultivations reached glucose limitation, the reduced growth rate was most likely caused by oxygen limitation.

Table 3.3 also presents the biomass at stationary phase, calculated from the cultivations presented in Figure B.2 and Figure B.3b (Appendix B). From these cultivations, it was found that no oxygen limitation supported a biomass that was more than twice as great as the one reached in the stationary phase under oxygen limitation, most likely due to glucose depletion.

Table 3.3: The biomass at stationary phase and growth rate (μ) before and after the induction of mCherry production and after oxygen limitation for the cultivation runs for *E. coli* BL21 A2mCh under oxygen limitation and no oxygen limitation. Where applicable, the percentage reduction between (1) before and after induction, (2) before induction and after oxygen limitation, and (3) after induction and after oxygen limitation is shown. The growth rates were calculated as presented in Appendix A.3. The biomass at stationary phase was calculated from the cultivations presented in Figure B.**2** and Figure B.**3**b (Appendix B).

Condition		μ [g CDW/h]			% reduction		
	Biomass at stationary phase [g CDW/L]	Before induction	After induction	After oxygen limitation	1	2	3
O_2-lim	3.02	0.34 ± 0.012	0.34 ± 0.0023	0.15 ± 0.0078	0	55	55
No O_2-lim	7.59 ± 0.012	0.31 ± 0.017	0.33 ± 0.024	-	-6	-	-

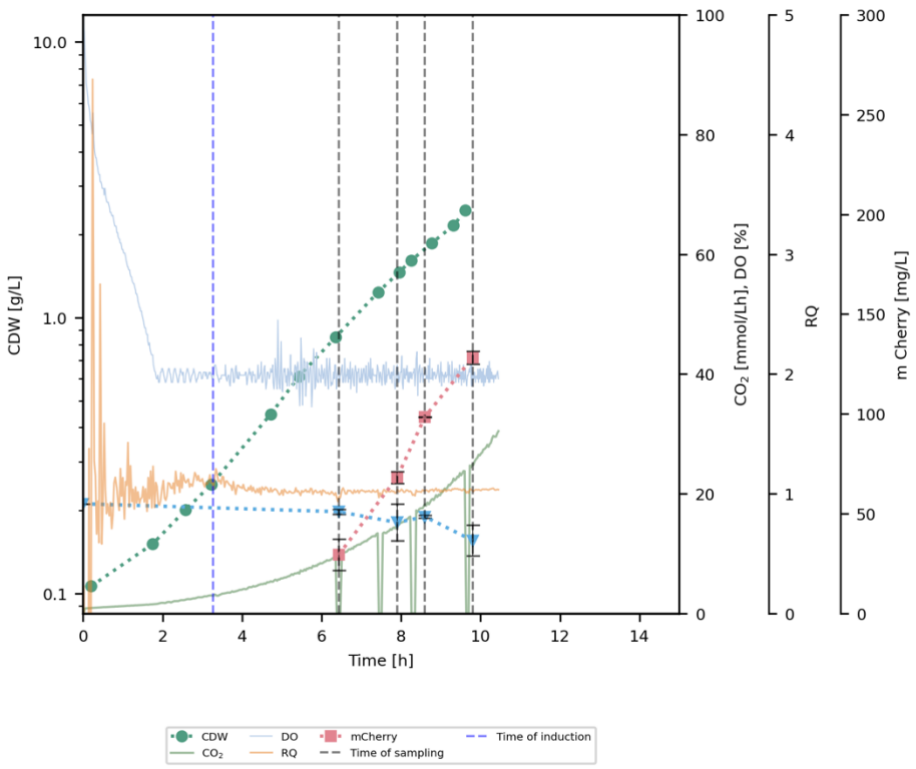

a) *E. coli* BL21 A2mCh-II, no oxygen limitation.

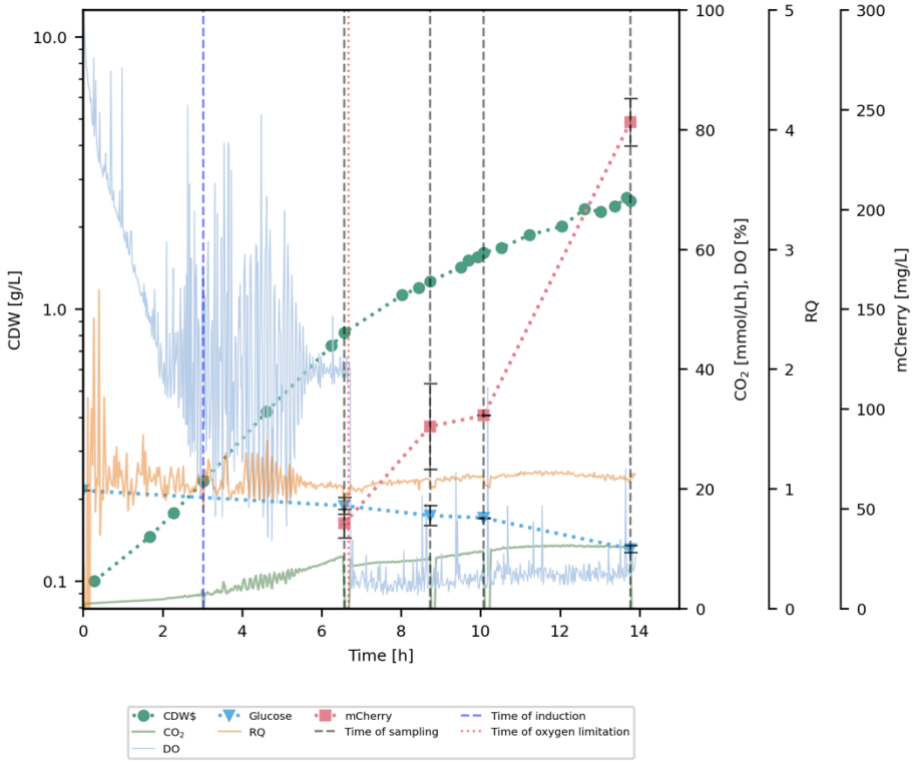

b) *E. coli* BL21 A2mCh-I, oxygen limitation.

Figure 3.2: Representative cultivation plots for E. coli BL21 A2mCh of the biological duplicates and triplicates under no oxygen limitation (a) and oxygen limitation (b), respectively. The dissolved oxygen (DO, light blue line), CO_2 off-gas (green line) and respiratory quotient (RQ, yellow line) was

measured online. Cell dry weight (CDW, green dotted line) was calculated from the measured OD_{600} (see Appendix A.1 for how to calculate CDW from OD_{600}). Glucose (blue dotted line) was sampled for in technical quadruplicates, along with other exometabolites, pyridine nucleotides and central carbon metabolites, as indicated by the vertical, black dashed lines. The concentration of mCherry (salmon pink dotted line) was measured in technical duplicates for only oxygen-limited A2mCh-I and control A2mCh-II, using western blot. The cultivations were performed using 1L bench-top bioreactor with M9-MtPr medium 2 (Table 2.10) at 30 °C. The pH was constantly adjusted to 7.00. For (b) the oxygen cascade was turned off and agitation set to 400 rpm, to simulate oxygen limitation, when CDW was at 0.8515 g/L (OD_{600} ~ 2.0), while for (a) the dissolved oxygen was kept above 40 %. The induction of oxygen limitation is indicated by the vertical, red dashed line. The production of mCherry was induced when the CDW was at 0.2491 g/L (OD_{600} ~0.5), indicated by the vertical, blue dashed line. Roman numerals indicate the biological replicate.

Due to time issues and limited material, the concentration of mCherry measured by western blot was reported only for *E. coli* BL21 WT-II and A2mCh-II, described in depth in subsection 3.2.2.1

3.2.2.1. Comparison of the production of mCherry in *E. coli* BL21 A2mCh

The amount of mCherry was quantified using western blot because the chromophore of mCherry needs oxygen to mature and fluoresce, which there is a lack of after the onset of oxygen limitation. Using the western blot, the concentration of mCherry (Figure 3.3) was obtained by interpolating band intensity values, using a calibration curve prepared with commercial pure mCherry run simultaneously with the samples, as presented in Appendix A.2.2.

Figure 3.3 presents the concentration of mCherry as both mg/L (a) and mg/g CDW (b), measured by the western blot. Under no oxygen limitation, A2mCh had a steady increase of mCherry, more than a four-fold increase from T1 to T4. Oxygen-limited A2mCh had a higher production of mCherry, close to a six-fold increase from T1 to T4. Prior to the onset of oxygen limitation (T1), both cultivations had similar concentrations of mCherry. Looking at the concentration of mCherry in terms of CDW, the specific concentration was highest at T2 for the control cultivation. From T1 to T4, the control had close to a 1.5-fold increase in the specific concentration of mCherry. Oxygen-limited A2mCh had a high variability in the specific concentration of mCherry at T2 and T3 between the technical replicates. The oxygen-limited cultivation had close to a two-fold increase in mCherry per CDW. Even though the fold increase was similar for the two cultivations, the specific concentration of mCherry for the limited cultivation appeared close to twice as high at T4 compared to the control.

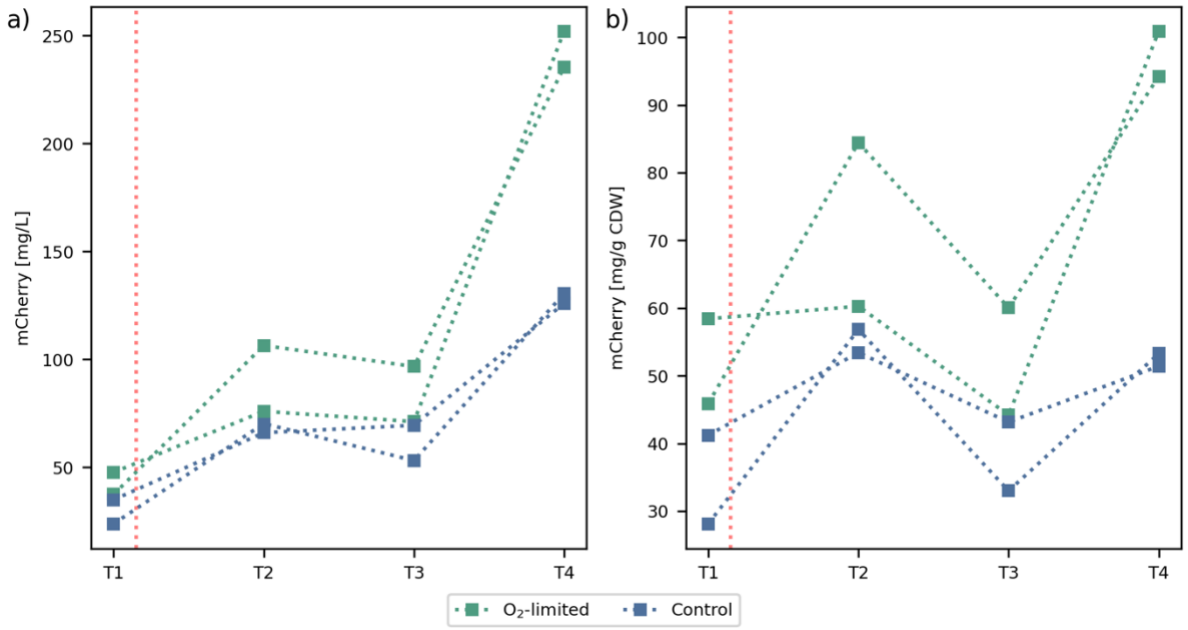

Figure 3.3: Concentration (mg/L (a) and mg/g CDW (b)) of mCherry at the different sampling points. Samples were taken in technical duplicates, given by the two lines for each condition. The red dotted line represents the onset of oxygen limitation in the O_2-limited cultivations. The concentration of mCherry was quantified by western blot, using Software Image Lab 6.0.1. The western blots and SDS-PAGEs used to confirm the presence of mCherry are presented in Appendix D.

The yields and specific production rates of mCherry in the different phases were calculated, presented in Table 3.4. In the whole mCherry producing phase, the oxygen-limited cultivation had close to a 1.5-fold increase in mCherry yield, compared to the control cultivation. However, the yield differed between the different phases, showing no clear trend of the limited cultivation having a lower yield than the control cultivation. This is also the case regarding the specific production rate. In some phases, the control had a higher specific production rate, such as in T1-T2, but in other cases the oxygen-limited had a higher specific production rate, such as in T3-T4. In the whole mCherry producing phase, T1-T4, the control and the oxygen-limited cultivation displayed similar specific production rates at 18.3 and 18.2 mg/g CDW/h, respectively.

Table 3.4: Yield ($Y_{mCh/s}$) and specific production rate of mCherry (q_{mCh}) in between the different time points. The production of mCherry was induced between T0 and T1. Oxygen limitation was initiated right after T1. T1-T4 represents the mCherry producing phase after oxygen limitation. Values are calculated from technical duplicates measured from one biological replicate in both cultivation conditions.

Condition	Time interval	$Y_{mCh/s}$ [mg/g Glc]	q_{mCh} [mg/g CDW/h]
No O_2-lim	T0-T1	22.2 ± 5.9	7.69 ± 2.10
	T1-T2	31.4 ± 8.8	109 ± 49
	T2-T3	8.01 ± 0.94	67.4 ± 30.0
	T3-T4	10.8 ± 1.0	30.6 ± 3.4
	T1-T4	24.2 ± 2.7	18.3 ± 1.3
O_2-lim	T0-T1	16.7 ± 2.8	11.2 ± 2.1
	T1-T2	24.9 ± 14.7	46.7 ± 35.7
	T2-T3	13.9 ± 54.6	22.9 ± 61.7
	T3-T4	32.9 ± 2.6	56.7 ± 20.2
	T1-T4	32.7 ± 0.7	18.2 ± 2.6

The concentration of mCherry was also quantified by measuring the fluorescence and interpolating the concentration using the standard curve in Appendix A.2.1. The difference in the volumetric concentration (mg/L) of mCherry quantified from fluorescence and western blot is presented in Appendix A.2.3.

3.2.3.Oxygen limitation led to an elevated overflow metabolism

The different overflow metabolites were quantified by HPLC, namely the organic acids acetate, citrate, ethanol, formate, fumarate, lactate, pyruvate, and succinate. The concentrations of the different organic acids are presented in Figure 3.4, plotted against CDW at the different time points. Negligible amounts (10^{-3} g/L) of citrate and fumarate, although quantified, were omitted. The overflow metabolisms of *E. coli* BL21 WT and A2mCh can be viewed in Figure 3.4. The WT and A2mCh were cultivated at different temperatures, 37 °C and 30 °C, respectively, which could explain some of the difference observed.

Figure 3.4 presents that the WT control had practically no excretion of all the organic acids, except for succinate. The extracellular concentration of succinate increased from the start of cultivation and plateaued when the CDW reached ~1.0 g/L. The WT under oxygen limitation had an increase in the concentrations of extracellular acetate, ethanol, formate, and lactate after the onset of oxygen limitation (CDW ~1.0 g/L). The secretion profile of succinate was similar for the control and the oxygen-limited WT until the point of oxygen limitation, where oxygen-limited cultivations reached an extracellular concentration of succinate that was twice as high as the control.

The excretion profile of the metabolites of A2mCh were different from metabolite to metabolite, as it was for the WT. For most metabolites, oxygen-limited cultivations had a higher excretion profile than control cultivations. Control cultivations of A2mCh excreted lactate and succinate, but showed little to no excretion of acetate, formate, and pyruvate. Oxygen-limited cultivations excreted acetate, lactate, pyruvate, and succinate, but little to no formate. The O_2-limited A2mCh showed an increase of excreted pyruvate from the penultimate to the last sampling point. However, this increase did have a big standard deviation due to the biological replicates not being similar, even though the technical replicates of each were. The excretion of acetate greatly increased after the onset of oxygen limitation, more than six times greater than that of the control cultivation. The control cultivations of A2mCh showed an increase in the extracellular concentration of acetate throughout the cultivation, but at a much smaller concentration.

The excretion profiles for ethanol were similar between the two cultivation conditions of A2mCh. The highest concentration of ethanol was reached before the onset of oxygen limitation and dropped throughout the cultivations. However, these high levels of ethanol are most likely due to the inducer being dissolved in ethanol. At the last sampling point, the oxygen-limited cultivations had a slightly higher extracellular concentration of ethanol compared to the control cultivations.

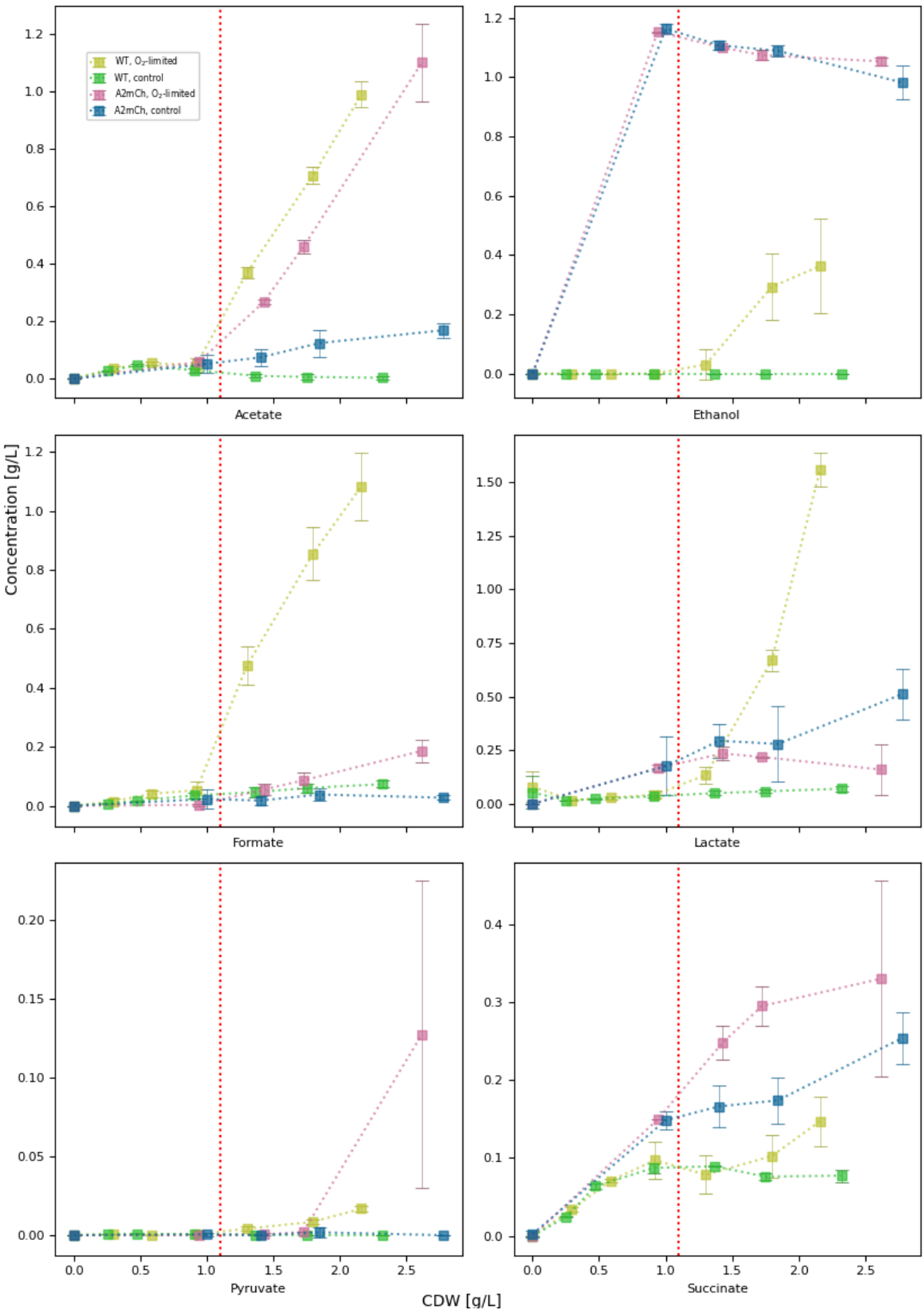

Figure 3.4: Concentration (g/L) of the overflow metabolites acetate, ethanol, formate, lactate, pyruvate, and succinate plotted against CDW (g/L). Samples were obtained as described in subsection 2.4.3 and quantified using an Alliance HPLC (Waters) with a Hi-Plex H 300 x 7.7 mm column (Agilent Technologies, PL1170-6830), detected by a refractive index (RI) and a UV/Vis

detector. The metabolites were sampled from 1 L bioreactors containing *E. coli* BL21 WT at 37 °C and A2mCh at 30 °C, which were cultivated either with oxygen limitation (yellow and pink dotted lines, respectively) or without oxygen limitation (green and blue dotted lines, respectively). The red dotted line represents when oxygen limitation was initiated.

3.2.4. Biomass yield and carbon recovery of *E. coli* BL21

Table 3.5 presents the biomass and overflow metabolite yield on glucose in the different phases for *E. coli* BL21 WT and A2mCh under the cultivations described in subsection 3.2.1 and 3.2.2. It also presents the carbon recovery for the different phases. The % carbon recovery was calculated on a g/L basis. It was assumed that the molecular weight for the biomass was 27.4 g/mol, from the biomass formula $CH_{1.8}O_{0.5}N_{0.2}$ and 10 % estimated ashes (Doran, 1995). The flows considered for the mass balance equation were glucose as substrate and biomass, CO_2, mCherry and the overflow metabolites as the products, either consumed or produced between two time points.

Both the oxygen-limited and non-limited cultivations of the WT showed similar biomass yields in the T0-T3 phase, prior to the onset of oxygen limitation. In T3-T6, the limited cultivations showed a reduction in biomass yield. This correlates with an insufficient supply of oxygen leading to a shift in metabolism, seen as the increase in organic acid secretion. Looking at the whole cultivation, the non-limited WT showed a biomass yield that was more than twice that of the oxygen-limited WT. In the phase corresponding to the oxygen-limited phase, the non-limited A2mCh had a higher biomass yield than was observed for the oxygen-limited A2mCh. For the whole cultivation, the non-limited A2mCh showed a higher biomass yield than the limited A2mCh.

The organic acid yield showed a 40-fold increase in the WT strain in the oxygen-limited phase as opposed to the control. For the A2mCh strain, the organic acid yield was found to double in the oxygen-limited phase compared to the control.

A varying amount of the carbon was accounted for in the different phases. In the cultivations of the WT, between 53 and 76 % of the carbon was accounted for in the different phases and conditions. For the cultivations using A2mCh, between 84 and 119 % of the carbon was accounted for in the different phases and conditions.

Table 3.5: The biomass yield ($Y_{biomass/s}$), overflow metabolite yield ($Y_{acid/s}$), and % carbon recovery between sampling points observed for *E. coli* BL21 WT and A2mCh under oxygen limitation and no oxygen limitation. For WT: T0-T3 represents the phase before oxygen limitation; T3-T6 represents the phase after oxygen limitation; T0-T6 represent the whole cultivation. For A2mCh: T2-T4 represents either the oxygen-limited phase or the non-limited phase, depending upon condition stated; T1-T4 represents the mCherry production phase; T0-T4 represents the whole cultivation. For the yield, all strains and conditions had three biological replicates, except for A2mCh under oxygen limitation, which had two biological replicates. Where no standard deviation is stated, samples were not included due to negative values for glucose consumption in the given phase. Ethanol is not included in the organic acid yield for A2mCh.

Strain	Condition	Phase	$Y_{biomass/s}$ [g CDW/g Glc]	$Y_{acid/s}$ [g/g Glc]	% Carbon recovery
WT	No O_2-lim	T0-T3	0.33	0.083	62
		T3-T6	0.42 ± 0.43	0.011 ± 0.007	69
		T0-T6	0.52 ± 0.16	0.041 ± 0.019	76
WT	O_2-lim	T0-T3	0.34 ± 0.02	0.045 ± 0.036	53
		T3-T6	0.13 ± 0.01	0.44 ± 0.01	65

		T0-T6	0.19 ± 0.00	0.54 ± 0.32	65
A2mCh	No O_2-lim	T2-T4	0.39 ± 0.07	0.12 ± 0.03	84
		T1-T4	0.48 ± 0.20	0.11 ± 0.00	92
		T0-T4	0.48 ± 0.01	0.24 ± 0.12	119
A2mCh	O_2-lim	T2-T4	0.32 ± 0.13	0.28 ± 0.06	103
		T1-T4	0.28 ± 0.07	0.25 ± 0.02	86
		T0-T4	0.34 ± 0.11	0.28 ± 0.09	108

3.3. Analysis of metabolism of *E. coli BL21*

During the batch cultivations described in subsections 3.2.1 and 3.2.2, samples were collected for analysis of both pyridine nucleotides and central carbon metabolites. The pyridine nucleotides consists of the precursors of $NAD(P)^+$/NAD(P)H and other metabolites important for the shuttle of energy in the cells. The central carbon metabolites consisted of organic acids, amino acids, TCA cycle metabolites, glycolysis metabolites, pyridine nucleotides, and nucleoside and deoxynucleoside phosphates. *E. coli* BL21 A2mCh was analysed under oxygen limitation and no oxygen limitation, to evaluate how limitation affected cells under RPP metabolic burden, compared to no oxygen limitation. The WT was also included, making it possible to compare the metabolism of the recombinant strain to that of the WT. However, WT cultivations were not sampled for central carbon metabolites, unlike A2mCh.

Due to time limitations the central carbon metabolites were not quantified and thus will not be presented.

3.3.1. Principal component analysis (PCA) of pyridine nucleotides

The pyridine nucleotides, their precursors, and other energy metabolites were extracted from cell pellets and quantified using zwitterionic HILIC MS/MS. As NAM, NA, 1-mNAM, NMN and ADPR were outside of the limit of quantification, these are not reported on.

To investigate the trend of how the pyridine nucleotide pools of the different strains, conditions, and time points differed, 2D score plots were generated by PCA using concentration values for each analysed metabolite. Figure 3.5 presents the 2D score plot of all the biological triplicates of cultivation of strains at all time points. The 2D score plot explains 84.6 % of the variance, where 58.9 % of the variance is explained by PC1 and 25.7 % of the variance is explained by PC2. Although the strains were cultivated at different temperatures, this likely did not contribute to the observed separation. This is evident by the WT samples at T1 being clustered together with samples of A2mCh from T1 and T2, indicating separation based on strain rather than temperature. This indication is further strengthened as all samples from A2mCh are placed on the top right half of the plot, while WT is placed on the bottom left of the plot. In other words, some of the difference seen in the pyridine nucleotide pools are due the samples being from different strains of *E. coli* BL21. The separation could also be due to time. This is evident as samples from early in the cultivations are placed on the top left of the 2D score plot, while samples from later in the cultivations are scattered towards the bottom right.

To further highlight the effect of time on separation, a 2D score plot only containing the samples from the cultivations of the WT strain was generated (Figure 3.6). For the WT, 83.3 % of the variance is explained by the 2D score plot, where 48.2 % is explained by PC1, and 35.1 % is explained by PC2. In this plot, T1 is separated from T2 and T3 along PC1. A separation based on time is also observed as early time points are placed in the top

of the plot, while later time points are placed in descending order. After the onset of oxygen limitation, T4 and onward for the limited cultivations, there is a greater separation between the time points. This is apparent as T5 and T6 for the limited cultivations are placed further down in the plot than T5 and T6 for the control cultivations. This can also be seen for T4, although the separation is not as clear. This indicates that the effect of oxygen limitation takes time to set in. This is further highlighted in Figure F.1a (Appendix F), where the data from the two last time points of the cultivations of the WT are presented in a 2D score plot.

The same trend was observed for A2mCh, in that there was a time-dependent separation of the samples. Moreover, the effect of oxygen limitation took some time to set in, but the oxygen-dependent separation was not as prominent for A2mCh as it was for the WT. This is evident from the 2D score plots in Figure F.1b and c (Appendix F).

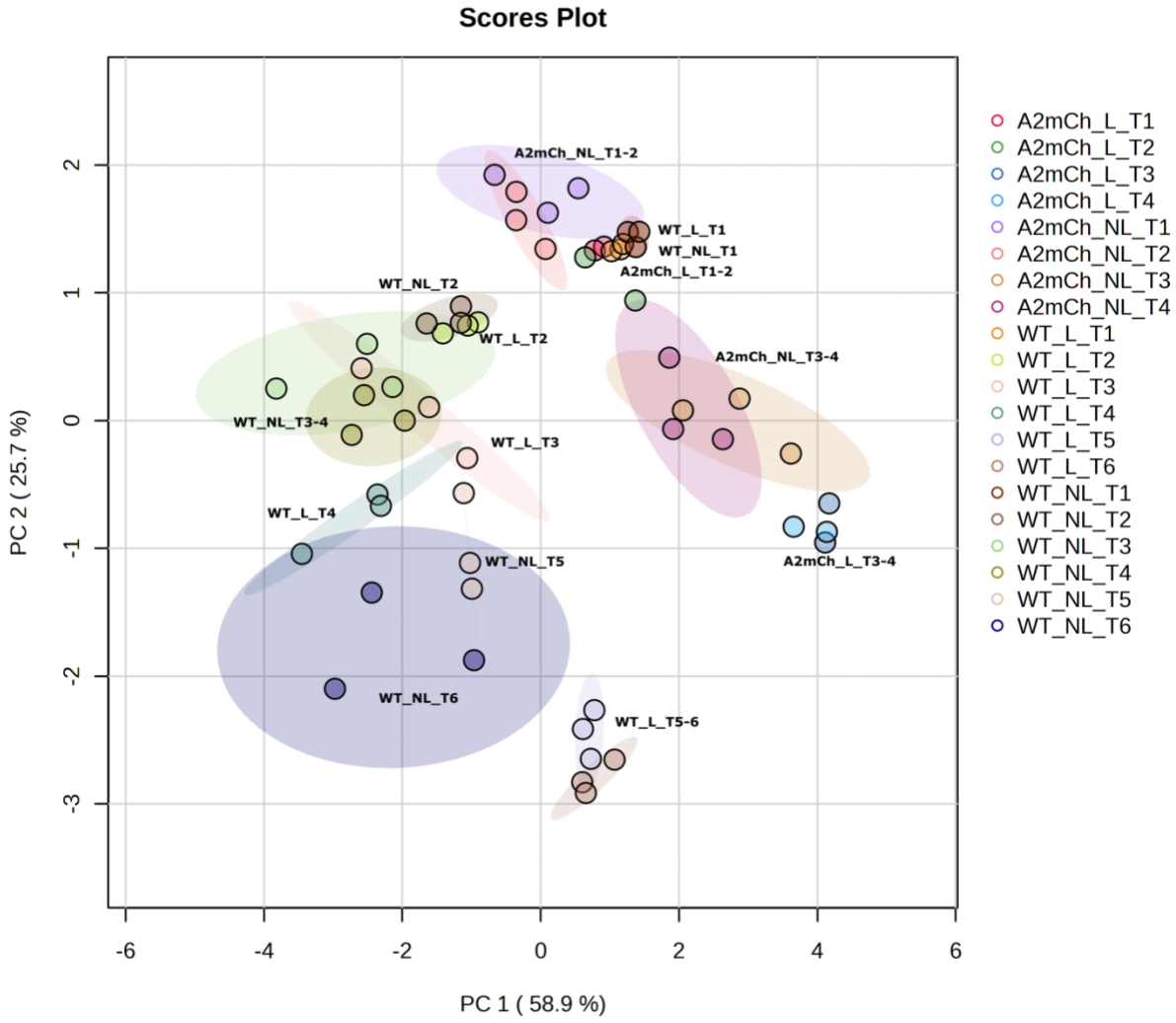

Figure 3.5: 2D score plots, generated by PCA, of biological triplicates of both cultivation conditions of *E. coli* BL21 WT and A2mCh, grouped by strain, condition, and time point. The plot is based on the pyridine nucleotide pools, quantified by zwitterionic HILIC-MS/MS, and processed as described in subsection 2.4.4.2. The PCA was performed on autoscaled data, using MetaboAnalyst 5.0 (Pang et al., 2021).

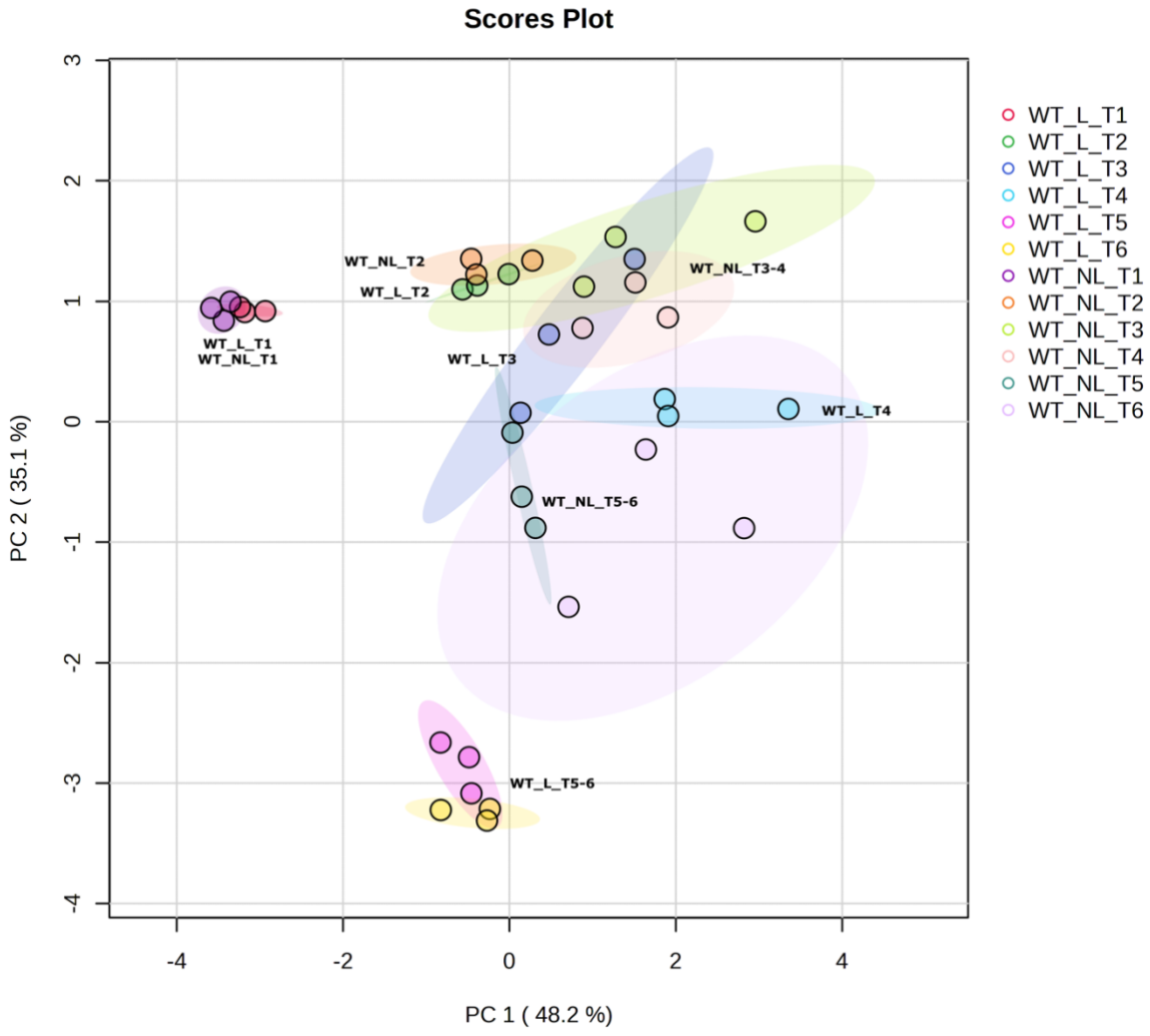

Figure 3.6: 2D score plots, generated by PCA, of biological triplicates of both cultivation conditions of *E. coli* BL21 WT, grouped by condition, and time point. The plot is based on the pyridine nucleotide pools, quantified by zwitterionic HILIC-MS/MS, and processed as described in subsection 2.4.4.2. The PCA was performed on autoscaled data, using MetaboAnalyst 5.0 (Pang et al., 2021).

3.3.2.The pyridine nucleotides through the cultivations

In

Figure 3.7, the concentration of NR, NaMN, NAD^+, NADH, $NADP^+$, NADPH, and FAD, including the ratios NADH/NAD^+ and NADPH/$NADP^+$, are plotted as bar charts at the different time points for the different strains and conditions. NAD^+, NADH, $NADP^+$, and NADPH were generally in much higher abundance than the pyridine nucleotide precursors NR and NaMN, and FAD, one to two orders of magnitude higher. For both cultivation conditions of the WT, a steady increase of both NR and NaMN could be observedfrom the first to the last time point. However, the concentration of NR at T6 was more than 1.5 times greater for the oxygen-limited cultivation compared to the control, with the marked increase happening at T5. The same trend could be seen for A2mCh, a marked increase at the two last time points, and the increase being greater for the oxygen-limited cultivation than the control. A higher concentration of NR was also observed in A2mCh than in the WT strain. Conversely, the opposite is seen for NaMN. The concentration of NaMN at the last

time points was higher for the control cultivations than for the oxygen-limited cultivations and the WT had a higher intracellular concentration of NaMN than A2mCh had.

The changes in FAD concentrations between the strains were seemingly the same, but at greater concentrations in the WT. Additionally, the onset of oxygen limitation had little to no effect on the accumulation of FAD. For the WT, FAD increased from T1 to T4, decreased at T5, and increased again at T6. For A2mCh, FAD increased from T1 to T2, decreased at T3 and increased at T4.

The trends of the accumulation of $NAD(P)^+$ and NAD(P)H were more varying. For the WT, there was an increase in NAD^+ and NADH from T1 to T4. At T5, both decreased. However, the decrease was greater for the oxygen-limited WT than the control cultivation. Additionally, NADH increased at T6 for the control. This was also seen in the ratios of NADH to NAD^+, where an increase in the ratios at T5 was observed, but a decrease at T6 for the control cultivations and not for the oxygen-limited. This could be due to the lower ability of the oxygen-limited WT cultivations to reoxidise NADH to NAD^+. For A2mCh, a drop in the concentration of NAD^+ and NADH from T2 to T3 could be observed. The concentration of NADH stayed constant, while the concentration of NAD^+ increased slightly from T3 to T4., both in oxygen-limited and control cultivations. There appeared to be little variation in the ratios of NADH to NAD^+ for both conditions, indicating similar abilities to reoxidise NADH.

For the oxygen-limited WT cultivations, a drastic drop in $NADP^+$ and NADPH could be seen from T4 to T5. For the control cultivations of the WT, this drop was also found for $NADP^+$, but not in the NADPH concentration. This led to the oxygen-limited cultivations of the WT to have lower ratios of NADPH to $NADP^+$ than the control cultivations at the two last time points. The same trend was observed for both cultivations of A2mCh, with both the concentration of $NADP^+$ and NADPH dropping from T2 to T3 and staying low. However, the drop in NADPH for the oxygen-limited cultivations of A2mCh was greater than that of the control cultivations. This led the ratios of NADPH to $NADP^+$ to drop at T3 and to stay low for the oxygen-limited cultivations of A2mCh, but to remain constant in the control cultivations of A2mCh.

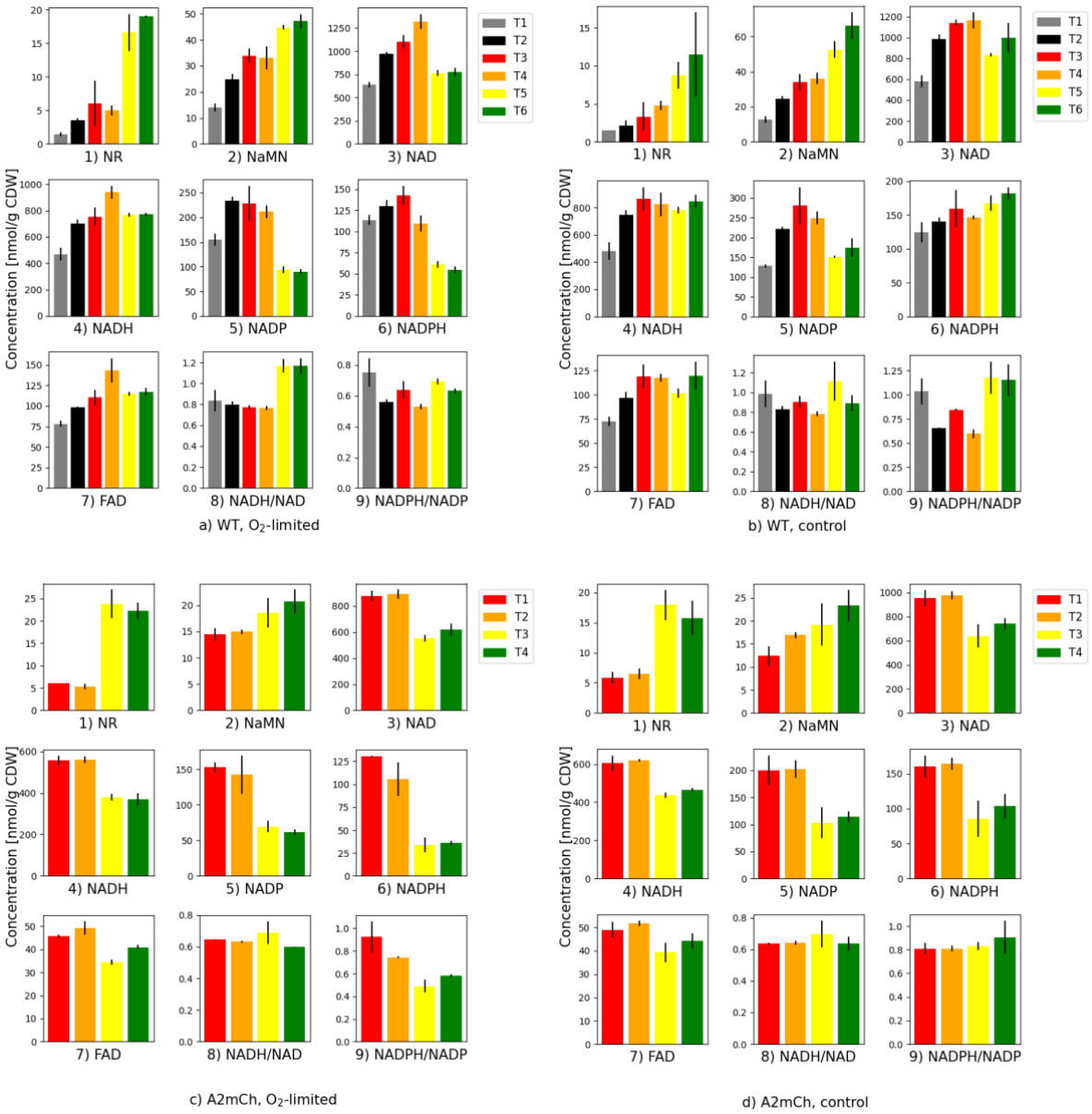

Figure 3.7: The concentrations [nmol/g CDW] of different pyridine nucleotides, some of their precursors and one other energy metabolites of *E. coli* BL21 WT (a, b) and A2mCh (c, d) under oxygen limitation (a, c) and a control with no oxygen limitation (b, d). The ratio of NADH to NAD and NADPH to NADP is also shown. The WT was sampled for the metabolite analyses at six different time points. The three first were prior to oxygen limitation being induced, and the three last were after it was induced. A2mCh was sampled for the metabolites at four different time points. The first was prior to oxygen limitation being induced, while the three last were after. The production of mCherry for the A2mCh strain was induced prior to all sampling points. For the control, the sampling points were matched with the corresponding strain under limited conditions according to their OD_{600}-values. WT T3 corresponds to A2mCh T1, based on OD_{600} values they were sampled at. All samples were taken in biological triplicates, except A2mCh O_2-limited, which was taken in biological duplicates. All biological replicates were sampled in technical triplicates. The concentrations were measured and quantified using zwitterionic HILIC-MS/MS.

4. Discussion

Through the work of this thesis, the redox homeostasis of *E. coli* BL21 WT and the recombinant strain A2mCh, including the RPP of A2mCh, has been investigated under conditions where the electron acceptor O_2 was limited. This has been done through cultivations, quantification of overflow metabolites, and quantification of pyridine nucleotides and their precursors. Samples were also collected for central carbon metabolite quantification, but due to time constraints these experiments were not completed.

4.1. Growth characteristics and mCherry production

Through the cultivations of both *E. coli* BL21 WT and A2mCh under oxygen limitation and no limitation, limiting the amount of oxygen present decreased bacterial growth rate and induced by-product formation. Additionally, the amount of mCherry produced was positively affected by the limiting of oxygen.

4.1.1. The onset of oxygen limitation affected growth characteristics

When altering the availability of oxygen, one would expect that the metabolism of *E. coli* will adjust accordingly to meet the new conditions. When oxygen is limited or not present, *E. coli* cannot fully oxidize glucose. Consequently, a lower energy output to fuel growth is acquired (Unden & Bongaerts, 1997). This was demonstrated through the work of this thesis, as both A2mCh and WT displayed a reduction in biomass accumulation during oxygen limitation (Table 3.2 and Table 3.3). Other studies, working with different *E. coli* strains, have also shown a reduction in biomass as the DO is decreased (Krishna Rao et al., 2008; Li et al., 1992). A reduction in growth rate was also observed when oxygen limitation was initiated. For the WT, oxygen limitation led to a 64 % reduction in growth rate, while A2mCh saw a 55 % reduction. These results indicate that in situations where oxygen limitation occurs, intentionally or not, it will detrimentally affect the ability of *E. coli* to support a high growth rate.

Furthermore, It is expected that the metabolic burden correlated with plasmid maintenance would negatively impact biomass (Diaz Ricci & Hernandez, 2000). This was shown in a study by Ow et al. (2006), where *E. coli* DH5α harbouring a NS3 plasmid had a lower biomass at the stationary phase compared to the plasmid free *E. coli* DH5α amounting to a 34 % reduction. However, this was not the case in the work of this thesis. A2mCh was found to have a higher biomass than the WT, at 7.59 and 6.82 g CDW/L, respectively. This was also the case for the oxygen-limited cultivations, showing a maximum biomass of 3.02 and 2.82 g CDW/L for the recombinant and the wildtype strains, respectively. It is possible that some of the discrepancy seen between the expected outcome and the observed outcome could be due to batch-to-batch variability (Gnoth et al., 2007; Jenzsch et al., 2006). However, this is most likely not the case, as both A2mCh and the WT had relatively low standard deviations between biological replicates. Even though A2mCh could support a higher biomass than the WT, A2mCh grew slower. This is apparent from the cultivation plots in Figure 3.1 and Figure 3.2 and Figure B.1, Figure B.2, and Figure B.3 in Appendix B. The slower growth rate could be due to the metabolic burden induced by plasmid maintenance, despite the different cultivation temperatures of the WT and A2mCh. This

interpretation is possible as García-Calvo et al. (2023) cultivated the same strains of *E. coli* BL21, WT and A2mCh, where A2mCh reached a higher biomass at the stationary phase at a lower growth rate compared to WT. This was also seen in the study by Ow et al. (2006).

Another parameter to explore is how the induction of mCherry production affects the growth rate of A2mCh. Results showed that the growth rate before and after the induction of mCherry production did not differ (Table 3.3). The oxygen-limited cultivations displayed no alteration in growth rate, while the control cultivations had a 6 % increase, most likely due to batch-to-batch variability (Gnoth et al., 2007; Jenzsch et al., 2006). A study by Heyland et al. (2011) showed that inducing the production of RPs will negatively impact the growth rate of *E. coli* BL21. It is plausible that the effect of RPP on the growth rate had not been detected because A2mCh had not reached the exponential growth phase when the production of mCherry was induced.

4.1.2.Oxygen limitation increased the production of mCherry

Given the reduction in growth rate and biomass accumulation observed after the onset of oxygen limitation, it would be reasonable to assume that the accumulation of mCherry would also be negatively affected. This is because aerobiosis provides more energy to support protein production (Tripathi et al., 2009). Li et al. (1992) found that oxygen limitation had a negative impact on the volumetric activity of the recombinantly expressed β-galactosidase, compared to a constant DO of 50 %, in two of the four expression systems investigated. However, this study used another type of reporter protein, measuring expression in the form of protein activity, and K12 and TB1 strains of *E. coli*. Therefore, this study is not directly transferrable to the use of mCherry as a reporter and the BL21 strain as an expression host.

In the present study, the production of mCherry, both volumetric (mg/L) and specific (mg/g CDW) concentration, was greater under oxygen limitation than no oxygen limitation (Figure 3.3). On the other hand, when looking at the specific production rate of mCherry, there was no discernible difference between the production rate under oxygen limitation and no oxygen limitation (Table 3.4). The yield of mCherry on glucose shows a positive effect of oxygen limitation . This indicates that oxygen limitation will increase the yield of mCherry on glucose, meaning that there is a lower cost of substrate associated with the increased concentration of mCherry seen under oxygen limitation.

4.1.3.Varying degrees of carbon was recovered

As *E. coli* consumes glucose, it should be converted to different carbon compounds, either in the form of overflow metabolites, biomass, mCherry, or CO_2 off-gas. From these compounds it is possible to calculate how much of the carbon from the glucose was recovered in the quantified by-products, biomass, and product of interest. Such calculations were performed and are presented in subsection 3.2.4. These values revealed that a varying degree of the carbon was accounted for. This held true between strains, conditions, time points, and phases. The cultivation of A2mCh under oxygen limitation had the highest amount of carbon accounted for, with a value of 108 %. However, even within this cultivation, differing amounts of carbon was accounted for in between each time point. As little as 67 % was accounted for in T3-T4, and as much as 220 % was accounted for in T2-T3.

The varying degree of carbon recovery could be due to different challenges, one of which could be the HPLC data. The quantified concentration of glucose increased between some time points due to an unknown co-eluting compound close in retention time to glucose. Therefore, another and more specific method to quantify glucose should be implemented, such as enzymatic methods or capillary zone electrophoresis (Galant et al., 2015). Another problem could be the excretion of undetected compounds. A study done in 1978 showed that an *E. coli* B strain and some *E. coli* K-12 strains excreted the pyrimidine pathway metabolites uracil and orotic acid, respectively (Womack & Odonovan, 1978; Yates & Pardee, 1956). Therefore, it is possible that the strains used in this thesis excrete such metabolites and others that were not quantified. Another study by Valgepea et al. (2011) found that as the growth rate increase in *E. coli* K-12, so does the loss of carbon into compounds that were not sampled for. This could provide some of the answers as to why so much of the carbon was not accounted for in *E. coli* BL21 WT, but the onset of oxygen limitation most likely had some effect on the loss of carbon as well. This is evident from the fact that the limited WT had a lower carbon recovery than the control, even though it grew at a lower growth rate. However, few and low unidentified peaks were observed in the chromatograms from the HPLC. Therefore, the low carbon recovery is most likely due to the uncertainty in the glucose values.

4.1.4. Quantification of the reporter protein

When investigating the metabolism of the expression of RPs, it is of utmost importance that the protein expressed is easily qunatified. This is done by using reporter proteins, such as the fluorescent protein mCherry (Lambert, 2019; Shaner et al., 2007). However, a downside of mCherry, especially when investigating the effect of oxygen limitation on RPP, is the fact that the chromophore needs oxygen to mature and fluoresce (Chapagain et al., 2011). This is evident from Figure A.1 where the concentration of mCherry stagnated after the onset of oxygen limitation when quantified from the fluorescence, but increased when quantified from the western blot. This problem was circumvented by carrying out the quantification of mCherry by using a western blot. However, there are some challenges related to quantification of proteins through western blots since western blotting was originally a qualitative method, which has been adapted to become a quantitative method in recent years (Pillai-Kastoori et al., 2020).

Without proper experimental design, methodology, and technique, substantial errors can occur. This can in turn lead to misinterpretation of data (Pillai-Kastoori et al., 2020). However, steps to avoid this was taken. A specific primary antibody for mCherry was used, namely anti-mCherry antibody (Abcam, ab167453), in addition to a secondary antibody specific to the primary. Optimization of amount of secondary antibody was also performed. A 100 times higher dilution than what was recommended by the manufacturers was used, as the recommended led to reverse banding. On the other hand, the reverse banding could have been prevented by using a fluorescent secondary antibody, considered as the optimal detection method (Pillai-Kastoori et al., 2020).

4.2. Overflow metabolism of *E. coli*

Overflow metabolism is generally considered a problem, mostly related to the growth of cells under anaerobic conditions (Basan et al., 2015). The excretion of organic acids, namely acetate and lactate, is closely correlated to RPP and has a detrimental effect on the cells growth and protein production (Kim et al., 2015; Lara et al., 2006). Therefore, overflow metabolism is of interest to avoid. On the other hand, it is believed that overflow

metabolism is a mechanism which allows for the enhanced utilization of glucose when the respiratory capacity is fully saturated (Teixeira de Mattos & Neijssel, 1997).

In the present study, the WT and A2mCh showed differing overflow metabolisms under both conditions. Under oxygen limitation, both strains were found to have an elevated excretion of acetate compared to their controls, which excreted little to no acetate throughout cultivation (Figure 3.4). The oxygen-limited strains began to excrete acetate after limitation initiation, indicating that excretion was due to an insufficient amount of oxygen leading to incomplete oxidation of glucose (Enjalbert et al., 2017). In a study by Lara et al. (2019), results showed that *E. coli* grown under oxygen limitation had elevated acetate excretion compared to *E. coli* grown in fully aerated conditions. In our study, it was also found that the A2mCh strain had a slightly elevated acetate excretion in comparison to the WT strain. This was the case for both the oxygen-limited cultivations and the control cultivations. A study by Rozkov et al. (2004) that a plasmid-containing strain of *E. coli* K12 has an elevated acetate excretion in relation to its wildtype, up to a 90 % increase. This indicates that the elevated acetate secretion observed for the A2mCh strain could be due to plasmid-induced stress.

Both control strains secreted virtually no formate, while both oxygen-limited strains had increased secretion of formate after the onset of oxygen limitation. Formate is closely associated with oxygen limitation (Xu et al., 1999), as shown in a study by Lara et al. (2019), where *E. coli* was found to have an extracellular formate concentration of 0.85 g/L three hours after the onset of oxygen limitation. Interestingly, under oxygen limitation the A2mCh strains secreted five times less the amount of formate as the WT strain did at the last sampling point. This low amount of formate, relative to the oxygen-limited WT, could be due to the activity of formate hydrogenlyase, an enzyme converting formate to carbon dioxide and hydrogen (Yoshida et al., 2005).

The oxygen-limited WT showed an elevated excretion of lactate compared to its control, as is expected (Liu et al., 2011). On the other hand, A2mCh had a lower excretion of lactate compared to its control, which was unexpected. This could be due to a reuptake of lactate, as evident from the decreasing extracellular concentration of lactate from T2 to T4. The ability to take up lactate from the environment is induced by aerobiosis (Dong et al., 1993). As a decreasing extracellular concentration of lactate is seen for the oxygen-limited A2mCh strain, reuptake of lactate should not be possible. Therefore, the lowered lactate could be due to sampling error. When lactate is utilized it is oxidized to pyruvate (Dong et al., 1993). This is in accordance with the elevated levels of pyruvate at the last sampling point of oxygen-limited A2mCh, as none of the other strains and conditions saw this elevation. However, both the concentration of pyruvate and lactate at the last sampling point for the oxygen-limited A2mCh strain were relatively high and it is challenging to conclude with anything.

All strains and conditions showed excretion of succinate. A2mCh had higher secretion of succinate with the oxygen-limited cultivations excreting more than the control. This held true for the WT strain as well. The increase in succinate of the oxygen-limited cultivations compared to the controls could be due to the inhibition succinate dehydrogenase, an enzyme which converts succinate to fumarate, and the activation of fumarate reductase, an enzyme which converts fumarate to succinate, both caused by oxygen limitation (Lara et al., 2019). This also fits with the fact that no fumarate was excreted. However, to be sure, transcriptomics must be utilized.

The oxygen-limited WT showed some secretion of ethanol. On the other hand, it is not possible to determine the secretion of ethanol by the A2mCh strain, as this is contaminated by the dissolvent of the inducer. However, a slightly higher concentration of ethanol for the oxygen-limited A2mCh strain compared to the control at the last time point was observed. The elevated concentration of the secreted ethanol for both oxygen-limited cultivations indicate a shift from the TCA cycle to ethanol fermentation.

4.2.1. An increased overflow metabolism did not lead to less RPP

It is commonly thought that overflow metabolism, namely the production of acetate, is detrimental to the production of RPs (Eiteman & Altman, 2006; Vemuri, Altman, et al., 2006). An elevated excretion of acetate was seen under oxygen limitation when mCherry was produced compared to under no oxygen limitation. However, a lesser volumetric abundance of mCherry was not seen in this case. An increase in other overflow metabolites such as pyruvate and succinate was also observed in the oxygen-limited cultivations compared to controls. From this, it is plausible to suggest that an increased overflow metabolism was not as detrimental to the production of RPs in the present case. However, the overflow metabolism was found to be associated with a higher substrate cost.

The increased overflow metabolism not leading to a reduction in RPP could also be due to ethanol. A protocol developed by Chhetri et al. (2015) was found to increase the expression of RPs in *E. coli*. This protocol uses the addition of 3 % ethanol to give a marked increase in RPP. However, this method was based on T5 and T7 bacterial promoters. The concentration of ethanol used in the protocol is also much higher than the ones measured in the samples. Even though this is the case, it is possible that the amount of ethanol that the inducer was dissolved in could have a dampening effect on the otherwise well-known negative effect of overflow metabolism on RPP. The ethanol could work through a heat shock-like mechanism. A study by Chaudhuri et al. (2006) showed that ethanol induces a heat shock response in *E. coli*. Another study by Oganesyan et al. (2007) found that heat shock responses in *E. coli* will increase the solubility of RPs and therefore the quantifiable amount of RPs.

4.3. Pyridine nucleotides

The pyridine nucleotides were sampled for and analysed to give insight into the redox state of *E. coli*. From the PCAs, which can be viewed in subsection 3.3.1 and Appendix F, it was evident that the WT and A2mCh mostly differed in the last two sampling points (WT: T5 and T6; A2mCh: T3 and T4). Therefore, this discussion will firstly focus on why the sampling points did not differ much, followed by how the last two points differ.

4.3.1. The concentration of pyridine nucleotides did not differ significantly up until the two last time points

The concentration of NR increased both for the oxygen-limited WT and the control WT through the first four sampling points, being roughly 5 nmol/g CDW at T4. This increase in NR could either indicate an increased breakdown of NAD^+ to NR and other of the NAD^+ precursors, or a block of the later steps in the salvage pathways converting NR to the pyridine nucleotides (Osterman, 2009). Over the same time period, an increase in NaMN was measured. This could indicate that the synthesis of NAD^+ from NR is not blocked in the conversion from NR to NaMN, since NaMN is an intermediate precursor in this pathway. Another indication that the turnover is not blocked is seen as there were an increase in all

the pyridine nucleotides in the first four time point. However, this does not mean that there is not an increased breakdown of NAD^+ to NR, as the increase in NAD^+ could be due to the *de novo* pathway from aspartate (Osterman, 2009). Additionally, an increase in FAD through cultivation was measured from the first four sampling points. Since FAD is a cofactor important for the TCA cycle, one could speculate that the increase in FAD was due to an increased flux through the TCA cycle needed by the cells to grow exponentially. However, this is not clear as the concentration of the reduced form of FAD ($FADH_2$) was not measured.

Both the oxygen-limited and control A2mCh had similar concentrations of NR at T1 and T2 as the WT at T3 and T4, which were sampled at the same values of OD_{600}. This similarity in NR could indicate that the production of mCherry did not affect the salvage pathway of NR. Similar concentrations of NaMN between the different conditions of A2mCh were also seen, with a small increase from T1 to T2 for the control, but these were half of that of the WT at T3 and T4. This could indicate a lower synthesis of NAD^+ from NR. The concentrations of all the pyridine nucleotides were stable during the first two time points, which could indicate that there is some turnover from NAD^+ to NaMN through NR or another precursor of NaMN. However, there could also be synthesis of NAD^+ through the *de novo* pathway since the pyridine nucleotides are stable in concentration, while NaMN sees an increase. There is a slight increase in the concentration of FAD from T1 to T2. This could indicate an increased flux through the TCA, as FAD is a coenzyme in the enzymatic reaction converting succinate to fumarate (Kim & Winge, 2013).

4.3.2.The redox ratios tells us about the redox state of the cell

For the oxygen-limited WT, the $NADH/NAD^+$ ratios did not significantly change between the first four time points. This indicates that the redox state of *E. coli* did not change, not even some time after the onset of oxygen limitation. The $NADH/NAD^+$ ratio increased to ~1.2 at the last two time point. This correlates with the induction of oxygen limitation and thus the absence of an external electron acceptor to reoxidize all NADH to NAD^+ (Ahmad et al., 2022; Babcock, 1999). However, fermentation allows for reoxidization of NADH to NAD^+, but less effectively (du Plessis et al., 2015). For the control, the $NADH/NAD^+$ ratios decreased until T4, indicating a small reduction in redox state which could mean the oxygen availability improved as the cultivation went on (Thorfinnsdottir et al., 2023).

The $NADPH/NADP^+$ ratios for the oxygen-limited cultivations showed small differences through the first four time points of the cultivation, although not by much, with a maximum of 0.75 and a minimum of 0.5. Through the last two time points, the $NADPH/NADP^+$ ratios still differed. Maintaining a high $NADPH/NADP^+$ ratio is important to attain high reaction rates for biomass producing reactions (Zhang et al., 2015). The ratios found were similar to those found by Godoy et al. (2016) in a K12 strain of *E. coli* under low aeration. For the control, the $NADPH/NADP^+$ ratios differed more than those of the oxygen-limited for the first four time points, leading to a more unstable driving force for biomass producing reactions. Even though this is the case, practically no difference was found between the growth rates of the strains in different cultivation conditions prior to oxygen limitation. Zhang et al. (2015) found that the $NADPH/NADP^+$ ratio in the cytosol was significantly different than that in the whole cell of *Saccharomyces cerevisiae*. Even though *E. coli* does not have the same compartmentalisation as eukaryotes, they have functionally different regions (Cossins et al., 2011). It is possible that these regions have different $NADPH/NADP^+$ ratios, which leads to an ability to maintain a constant growth rate while the $NADPH/NADP^+$ ratio for the whole cell does not support high growth. At the last two

time points, an increase to ~1.15 in the NADPH/$NADP^+$ ratio was seen for the control, while it remained low for the oxygen-limited WT. This correlates with the fact that the control has a higher growth rate than the limited cultivations after the onset of oxygen limitation.

For the oxygen-limited A2mCh, the NADH/NAD^+ ratio was maintained at a constant level throughout the cultivation. This held true for the control as well. This could indicate that even when the availability of an external electron acceptor is limited, the A2mCh has the same ability to reoxidize NAD^+ by fermentation as if fully aerated. However, the NADH/NAD^+ ratios for A2mCh differed slightly from the WT, especially for the last two time points, where A2mCh had a ratio that was half that of the WT. For the controls, A2mCh also had lower NADH/NAD^+ ratios compared to the WT. This could indicate a lower repression of the TCA cycle in A2mCh compared to the WT, as a high redox ratio is correlated with the repression of the TCA cycle (Vemuri, Altman, et al., 2006). A study by Vemuri, Eiteman, et al. (2006) found that lowering the NADH/NAD^+ ratio increased RPP Therefore, one could speculate whether the lower NADH/NAD^+ ratios of A2mCh could be connected to the production of mCherry.

The NADPH/$NADP^+$ ratio decreased throughout cultivation for oxygen-limited A2mCh, while it stayed constant for the control. This decrease could be due to the metabolism shifting from a metabolism supporting both a relatively high growth rate and mCherry production, as can be seen for the control, to a metabolism supporting mCherry production at the expense of growth. This is evident from the growth rates, where the growth rate of oxygen-limited A2mCh was reduced after the onset of oxygen limitation, while the control had the same growth rate throughout cultivation. It has been shown by Özkan et al. (2005) that inducing the production of RP will alter the metabolic flux to one supporting more energy producing pathways. The addition of oxygen limitation will further interfere with the cells ability to produce energy. It is likely that this additive effect will further hamper the ability of *E. coli* to have a metabolic flux supporting the redox ratio, in the form of NADPH/$NADP^+$, needed to have a relatively high growth rate.

4.3.3.Oxygen limitation led to a reduction in the pyridine nucleotides

At the last two sampling points, a drop in the concentration of both $NAD(P)^+$ and NAD(P)H was measured for all strains and conditions, compared to the previous sampling point. For the WTs, the reduction in the pyridine nucleotides was markedly greater for the oxygen-limited. The reduction in the $NAD(P)^+$ and NAD(P)H for A2mCh was more similar between the two conditions, although being slightly greater for the oxygen-limited A2mCh. For both strains under oxygen limitation, the concentration of NADH did not drop as much as the concentration of NAD^+. A study by Wimpenny and Firth (1972) on various bacteria showed that when going from oxygen rich to oxygen poor condition the concentration of NADH stayed constant, while the concentration of NAD^+ dropped.

The decrease in pyridine nucleotides was also accompanied by an increase in the precursors NR and NaMN. This could point at an increased breakdown of the pyridine nucleotides at these time points as both NR and NaMN are breakdown products of the pyridine nucleotides (Osterman, 2009). This increase in NR and NaMN was seen for both the controls and the oxygen-limited cultivations. This could indicate that the increase is related to the biomass seen or at what growth phase the bacterial culture is in. Although this could be the case, some of the increase is more likely caused by oxygen limitation. This is evident from the oxygen-limited having a higher concentration of NR and a lower concentration of NaMN than the control, which was true for both the WT and A2mCh. In addition to oxygen

limitation leading to an increase in NR and in NaMN, but lower than that of the control, RPP also influenced NR and NaMN. The control of A2mCh displayed an elevated level of NR as compared to the WT control, and the level of NaMN was lower. This trend was also evident when comparing the oxygen-limited A2mCh and its control. Oxygen-limited A2mCh had the highest amount of NR, while the control had the highest amount of NaMN.

From these results, one could postulate that both oxygen limitation and RPP had a negative effect on the energy metabolism of *E. coli*. Both led to an accumulation of NR and NaMN, although oxygen limitation led to a higher accumulation of NaMN than RPP did, while RPP led to a higher accumulation of NR than oxygen limitation did. As described earlier, this could be due to steps later in the salvage pathways being blocked. However, this is hard to say for certain as the later intermediates of the pathway were not possible to quantify and some, such as nicotinic acid adenine dinucleotide, were not detected for.

4.4. Further work

To further investigate the effect of oxygen limitation, additional experiments and alterations should be performed. Listed are some recommendations:

- The use of another reporter protein. As the chromophore of mCherry needs oxygen to fluoresce, another reporter protein should be used.
- Perform IC-MS/MS analysis and quantify the central carbon metabolites. This would give more insight into the metabolic state of the cell and it would make it possible to compare the concentration of the overflow metabolites with the concentration of the corresponding intracellular metabolites.
- Measure glucose by another method than HPLC, as an unknow co-eluting compound interfered with the peak of glucose. Glucose could be quantified through enzymatic kits or capillary zone electrophoresis.
- Conduct fluxomic analyses and combine with metabolic profiling to give more information on the metabolic pathway activities.
- Run cultivations for longer, incorporating the same sampling methods as used in this thesis, to get insight into the metabolic state at stationary phase. This could give insight of the expression of RPs when energy is not used on growth.
- Investigate the effect of oxygen limitation in a fed-batch system. Fed-batch systems allows cultures to reach high cell concentrations. As fed-batch systems are more like the industrial standard, how oxygen limitation affects the metabolism of *E. coli* in these systems would be interesting to investigate.
- Repeat cultivations as is but simulate oxygen limitation by using nitrogen as sparge air. This would simulate complete oxygen limitation, as no external electron acceptor would be available.

Conclusion

The data and results in this thesis underline the known effect that oxygen limitation has on the growth characteristics of *E. coli* BL21. However, the induction of mCherry production seemingly did not have an effect on the growth characteristics of the recombinant A2mCh strain, in contrast to what is found by other researchers.

The onset of oxygen limitation was found to induce overflow metabolism in both the WT and the A2mCh strain. This greatly affected the yield of biomass, as much more glucose was used to produce overflow metabolites. The overflow metabolism was exacerbated by the induction of mCherry production in connection to the secretion of pyruvate and succinate. However, the WT strain excreted more of some of the overflow metabolites, namely formate and lactate, when exposed to oxygen limitation.

Oxygen limitation had opposing effects on the production of mCherry. During oxygen limitation both a higher volumetric and specific concentration of mCherry was observed, which was unexpected. The yield of mCherry on glucose was higher when oxygen limitation was imposed as opposed to when it was not. However, the observed specific production rates of mCherry were similar when oxygen limitation was imposed and when it was not imposed.

A time-delay was observed between the initiation of oxygen limitation and when it affected the redox state of *E. coli* in the cultivations. After the delay, an increase in the precursors of $NAD(P)^+$ and NAD(P)H and a decrease in $NAD(P)^+$ and NAD(P)H was observed. The oxidized form had a greater decrease than the reduced form, indicating that the cells were unable to reoxidize the metabolites. The same trends were seen for the control cultivations, although not as prominent, indicating that they were able of reoxidizing NAD(P)H to $NAD(P)^+$.

From an industrial point of view, the above results indicate different things. Regarding the production of RPs, oxygen limitation leads to a higher concentration at the same biomass. However, it takes just as long to produce the same levels of RPs, seen from the specific production rates. On the other hand, the higher production of the RPs is associated with a lower cost of substrates, with some of the substrate being metabolised into by-products such as succinate and pyruvate. In contrast, when non-homogenous aeration happens, it takes some time before it affects the redox state of the cells.

Bibliography

Ahmad, M., Wolberg, A., & Kahwaji, C. (2022). Biochemistry, Electron Transport Chain. *StatPearls [Internet]. Treasure Island (FL): StatPearls Publishing*. https://www.ncbi.nlm.nih.gov/books/NBK526105/

Andersson, L., Yang, S., Neubauer, P., & Enfors, S. O. (1996, May 15). Impact of plasmid presence and induction on cellular responses in fed batch cultures of Escherichia coli. *J Biotechnol, 46*(3), 255-263. https://doi.org/10.1016/0168-1656(96)00004-1

Arsene, F., Tomoyasu, T., & Bukau, B. (2000, Apr 10). The heat shock response of Escherichia coli. *Int J Food Microbiol, 55*(1-3), 3-9. https://doi.org/10.1016/s0168-1605(00)00206-3

Babcock, G. T. (1999, Nov 9). How oxygen is activated and reduced in respiration. *Proc Natl Acad Sci U S A, 96*(23), 12971-12973. https://doi.org/10.1073/pnas.96.23.12971

Bakke, I., Berg, L., Aune, T. E., Brautaset, T., Sletta, H., Tondervik, A., & Valla, S. (2009, Apr). Random mutagenesis of the PM promoter as a powerful strategy for improvement of recombinant-gene expression. *Appl Environ Microbiol, 75*(7), 2002-2011. https://doi.org/10.1128/AEM.02315-08

Balzer, S., Kucharova, V., Megerle, J., Lale, R., Brautaset, T., & Valla, S. (2013, Mar 18). A comparative analysis of the properties of regulated promoter systems commonly used for recombinant gene expression in Escherichia coli. *Microb Cell Fact, 12*(1), 26. https://doi.org/10.1186/1475-2859-12-26

Basan, M., Hui, S., Okano, H., Zhang, Z., Shen, Y., Williamson, J. R., & Hwa, T. (2015, Dec 3). Overflow metabolism in Escherichia coli results from efficient proteome allocation. *Nature, 528*(7580), 99-104. https://doi.org/10.1038/nature15765

Bentley, W. E., Mirjalili, N., Andersen, D. C., Davis, R. H., & Kompala, D. S. (1990). Plasmid-encoded protein: the principal factor in the "metabolic burden" associated with recombinant bacteria. *Biotechnology and bioengineering, 35*(7), 668-681.

Berg, L., Lale, R., Bakke, I., Burroughs, N., & Valla, S. (2009). The expression of recombinant genes in Escherichia coli can be strongly stimulated at the transcript production level by mutating the DNA-region corresponding to the 5′-untranslated part of mRNA. *Microbial biotechnology, 2*(3), 379-389.

Blatny, J. M., Brautaset, T., Winther-Larsen, H. C., Karunakaran, P., & Valla, S. (1997). Improved broad-host-range RK2 vectors useful for high and low regulated gene expression levels in gram-negative bacteria. *Plasmid, 38*(1), 35-51. https://doi.org/10.1006/plas.1997.1294

Brinas, L., Zarazaga, M., Saenz, Y., Ruiz-Larrea, F., & Torres, C. (2002, Oct). Beta-lactamases in ampicillin-resistant Escherichia coli isolates from foods, humans, and healthy animals. *Antimicrob Agents Chemother, 46*(10), 3156-3163. https://doi.org/10.1128/AAC.46.10.3156-3163.2002

Chapagain, P. P., Regmi, C. K., & Castillo, W. (2011, Dec 21). Fluorescent protein barrel fluctuations and oxygen diffusion pathways in mCherry. *J Chem Phys, 135*(23), 235101. https://doi.org/10.1063/1.3660197

Chaudhuri, S., Jana, B., & Basu, T. (2006). Why does ethanol induce cellular heat-shock response? *Cell biology and toxicology, 22*, 29-37.

Chen, R. (2012, Sep-Oct). Bacterial expression systems for recombinant protein production: E. coli and beyond. *Biotechnol Adv, 30*(5), 1102-1107. https://doi.org/10.1016/j.biotechadv.2011.09.013

Chhetri, G., Kalita, P., & Tripathi, T. (2015, 2015/01/01/). An efficient protocol to enhance recombinant protein expression using ethanol in Escherichia coli. *MethodsX, 2*, 385-391. https://doi.org/10.1016/j.mex.2015.09.005

Clark, D. P. (1989, Sep). The fermentation pathways of Escherichia coli. *FEMS Microbiol Rev, 5*(3), 223-234. https://doi.org/10.1016/0168-6445(89)90033-8

Cossins, B. P., Jacobson, M. P., & Guallar, V. (2011, Jun). A new view of the bacterial cytosol environment. *PLoS Comput Biol, 7*(6), e1002066. https://doi.org/10.1371/journal.pcbi.1002066

Dean, R. B., & Dixon, W. J. (1951). Simplified Statistics for Small Numbers of Observations. *Analytical chemistry, 23*(4), 636-638. https://doi.org/DOI 10.1021/ac60052a025

Diaz Ricci, J. C., & Hernandez, M. E. (2000, 2000/01/01). Plasmid effects on Escherichia coli metabolism. *Crit Rev Biotechnol, 20*(2), 79-108. https://doi.org/10.1080/07388550008984167

Dong, J. M., Taylor, J. S., Latour, D. J., Iuchi, S., & Lin, E. C. (1993, Oct). Three overlapping lct genes involved in L-lactate utilization by Escherichia coli. *J Bacteriol, 175*(20), 6671-6678. https://doi.org/10.1128/jb.175.20.6671-6678.1993

Doran, P. M. (1995). *Bioprocess engineering principles*. Elsevier.

du Plessis, S. S., Agarwal, A., Mohanty, G., & van der Linde, M. (2015, Mar-Apr). Oxidative phosphorylation versus glycolysis: what fuel do spermatozoa use? *Asian J Androl, 17*(2), 230-235. https://doi.org/10.4103/1008-682X.135123

Durland, R. H., Toukdarian, A., Fang, F., & Helinski, D. R. (1990, Jul). Mutations in the trfA replication gene of the broad-host-range plasmid RK2 result in elevated plasmid copy numbers. *J Bacteriol, 172*(7), 3859-3867. https://doi.org/10.1128/jb.172.7.3859-3867.1990

Efstathiou, C. E. (2006, Jul 15). Estimation of type I error probability from experimental Dixon's "Q" parameter on testing for outliers within small size data sets. *Talanta, 69*(5), 1068-1071. https://doi.org/10.1016/j.talanta.2005.12.031

Eiteman, M. A., & Altman, E. (2006, Nov). Overcoming acetate in Escherichia coli recombinant protein fermentations. *Trends Biotechnol, 24*(11), 530-536. https://doi.org/10.1016/j.tibtech.2006.09.001

Enjalbert, B., Millard, P., Dinclaux, M., Portais, J. C., & Letisse, F. (2017, Feb 10). Acetate fluxes in Escherichia coli are determined by the thermodynamic control of the Pta-AckA pathway. *Sci Rep, 7*(1), 42135. https://doi.org/10.1038/srep42135

Everson, N. S. P. (2022). Metabolic Profiling of *Escherichia coli* BL21 During Recombinant Protein Production with Varying Expression Vector Characteristics [Master's thesis].

Feizollahzadeh, S., Kouhpayeh, S., Rahimmansh, I., Khanahmad, H., Sabzehei, F., Ganjalikhani-Hakemi, M., Andalib, A., Hejazi, Z., & Rezaei, A. (2017). The Increase in Protein and Plasmid Yields of E. coli with Optimized Concentration of Ampicillin as Selection Marker. *Iran J Biotechnol, 15*(2), 128-134. https://doi.org/10.15171/ijb.1467

Figurski, D. H., & Helinski, D. R. (1979, Apr). Replication of an origin-containing derivative of plasmid RK2 dependent on a plasmid function provided in trans. *Proc Natl Acad Sci U S A, 76*(4), 1648-1652. https://doi.org/10.1073/pnas.76.4.1648

Galant, A. L., Kaufman, R. C., & Wilson, J. D. (2015, Dec 1). Glucose: Detection and analysis. *Food Chem, 188*, 149-160. https://doi.org/10.1016/j.foodchem.2015.04.071

García-Calvo, L., Rane, D. V., Everson, N., Humlebrekk, S. T., Mathiassen, L. F., Mæhlum, A. H. M., Malmo, J., & Bruheim, P. (2023, 2023-March-13). Central carbon metabolite profiling reveals vector-associated differences in the recombinant protein production host Escherichia coli BL21 [Original Research]. *Frontiers in Chemical Engineering, 5*. https://doi.org/10.3389/fceng.2023.1142226

Gawin, A., Valla, S., & Brautaset, T. (2017, Jul). The XylS/Pm regulator/promoter system and its use in fundamental studies of bacterial gene expression, recombinant protein production and metabolic engineering. *Microb Biotechnol, 10*(4), 702-718. https://doi.org/10.1111/1751-7915.12701

Ghim, C. M., Lee, S. K., Takayama, S., & Mitchell, R. J. (2010, Jul). The art of reporter proteins in science: past, present and future applications. *BMB Rep, 43*(7), 451-460. https://doi.org/10.5483/bmbrep.2010.43.7.451

Gill, R. T., Valdes, J. J., & Bentley, W. E. (2000, Jul). A comparative study of global stress gene regulation in response to overexpression of recombinant proteins in Escherichia coli. *Metab Eng, 2*(3), 178-189. https://doi.org/10.1006/mben.2000.0148

Glick, B. R. (1995, 1995/01/01/). Metabolic load and heterologous gene expression. *Biotechnol Adv, 13*(2), 247-261. https://doi.org/10.1016/0734-9750(95)00004-a

Gnoth, S., Jenzsch, M., Simutis, R., & Lubbert, A. (2007, Oct 31). Process Analytical Technology (PAT): batch-to-batch reproducibility of fermentation processes by robust process operational design and control. *J Biotechnol, 132*(2), 180-186. https://doi.org/10.1016/j.jbiotec.2007.03.020

Godoy, M. S., Nikel, P. I., Cabrera Gomez, J. G., & Pettinari, M. J. (2016, Jan 1). The CreC Regulator of Escherichia coli, a New Target for Metabolic Manipulations. *Appl Environ Microbiol, 82*(1), 244-254. https://doi.org/10.1128/AEM.02984-15

Goeddel, D. V., Kleid, D. G., Bolivar, F., Heyneker, H. L., Yansura, D. G., Crea, R., Hirose, T., Kraszewski, A., Itakura, K., & Riggs, A. D. (1979, Jan). Expression in Escherichia coli of chemically synthesized genes for human insulin. *Proc Natl Acad Sci U S A, 76*(1), 106-110. https://doi.org/10.1073/pnas.76.1.106

Goodman, M. F. (2000, Apr). Coping with replication 'train wrecks' in Escherichia coli using Pol V, Pol II and RecA proteins. *Trends Biochem Sci, 25*(4), 189-195. https://doi.org/10.1016/s0968-0004(00)01564-4

Harcum, S. W., & Haddadin, F. T. (2006, Oct). Global transcriptome response of recombinant Escherichia coli to heat-shock and dual heat-shock recombinant protein induction. *J Ind Microbiol Biotechnol, 33*(10), 801-814. https://doi.org/10.1007/s10295-006-0122-3

Heyland, J., Blank, L. M., & Schmid, A. (2011, Sep 10). Quantification of metabolic limitations during recombinant protein production in Escherichia coli. *J Biotechnol, 155*(2), 178-184. https://doi.org/10.1016/j.jbiotec.2011.06.016

Hoffmann, F., & Rinas, U. (2001, Dec). On-line estimation of the metabolic burden resulting from the synthesis of plasmid-encoded and heat-shock proteins by monitoring respiratory energy generation. *Biotechnol Bioeng, 76*(4), 333-340. https://doi.org/10.1002/bit.10098

Humlebrekk, S. T. (2022). Physiological and Metabolic Consequences of Expression Vector Presence in *Escherichia coli* [Master's thesis].

Hunter, J. D. (2007, May-Jun). Matplotlib: A 2D graphics environment. *Computing in science & engineering, 9*(3), 90-95. https://doi.org/Doi 10.1109/Mcse.2007.55

Itakura, K., Hirose, T., Crea, R., Riggs, A. D., Heyneker, H. L., Bolivar, F., & Boyer, H. W. (1977, Dec 9). Expression in Escherichia coli of a chemically synthesized gene for the hormone somatostatin. *Science, 198*(4321), 1056-1063. https://doi.org/10.1126/science.412251

Jensen, P. R., & Michelsen, O. (1992, Dec). Carbon and energy metabolism of atp mutants of Escherichia coli. *J Bacteriol, 174*(23), 7635-7641. https://doi.org/10.1128/jb.174.23.7635-7641.1992

Jenzsch, M., Simutis, R., & Lubbert, A. (2006, Apr). Optimization and control of industrial microbial cultivation processes. *Engineering in Life Sciences, 6*(2), 117-124. https://doi.org/10.1002/elsc.200620901

Johnson, I. S. (1983, Feb 11). Human insulin from recombinant DNA technology. *Science, 219*(4585), 632-637. https://doi.org/10.1126/science.6337396

Kanehisa, M. (2019, Nov). Toward understanding the origin and evolution of cellular organisms. *Protein Sci, 28*(11), 1947-1951. https://doi.org/10.1002/pro.3715

Kanehisa, M., Furumichi, M., Sato, Y., Kawashima, M., & Ishiguro-Watanabe, M. (2023, Jan 6). KEGG for taxonomy-based analysis of pathways and genomes. *Nucleic Acids Res, 51*(D1), D587-D592. https://doi.org/10.1093/nar/gkac963

Kanehisa, M., & Goto, S. (2000, Jan 1). KEGG: kyoto encyclopedia of genes and genomes. *Nucleic Acids Res, 28*(1), 27-30. https://doi.org/10.1093/nar/28.1.27

Kim, H. J., & Winge, D. R. (2013, May). Emerging concepts in the flavinylation of succinate dehydrogenase. *Biochim Biophys Acta, 1827*(5), 627-636. https://doi.org/10.1016/j.bbabio.2013.01.012

Kim, T. S., Jung, H. M., Kim, S. Y., Zhang, L., Li, J., Sigdel, S., Park, J. H., Haw, J. R., & Lee, J. K. (2015, Jul). Reduction of Acetate and Lactate Contributed to Enhancement of a Recombinant Protein Production in E. coli BL21. *J Microbiol Biotechnol, 25*(7), 1093-1100. https://doi.org/10.4014/jmb.1503.03023

Kirk, O., Borchert, T. V., & Fuglsang, C. C. (2002, Aug). Industrial enzyme applications. *Curr Opin Biotechnol, 13*(4), 345-351. https://doi.org/10.1016/s0958-1669(02)00328-2

Kost, T. A., Condreay, J. P., & Jarvis, D. L. (2005, May). Baculovirus as versatile vectors for protein expression in insect and mammalian cells. *Nat Biotechnol, 23*(5), 567-575. https://doi.org/10.1038/nbt1095

Krishna Rao, D. V., Ramu, C. T., Rao, J. V., Narasu, M. L., & Bhujanga Rao, A. K. (2008, Sep). Impact of dissolved oxygen concentration on some key parameters and production of rhG-CSF in batch fermentation. *J Ind Microbiol Biotechnol, 35*(9), 991-1000. https://doi.org/10.1007/s10295-008-0374-1

Kumar, J., Chauhan, A. S., Shah, R. L., Gupta, J. A., & Rathore, A. S. (2020, Aug). Amino acid supplementation for enhancing recombinant protein production in E. coli. *Biotechnol Bioeng, 117*(8), 2420-2433. https://doi.org/10.1002/bit.27371

Kusnadi, A. R., Nikolov, Z. L., & Howard, J. A. (1997, Dec 5). Production of recombinant proteins in transgenic plants: Practical considerations. *Biotechnol Bioeng, 56*(5), 473-484. https://doi.org/10.1002/(SICI)1097-0290(19971205)56:5<473::AID-BIT1>3.0.CO;2-F

Kvitvang, H. F., & Bruheim, P. (2015, Aug 15). Fast filtration sampling protocol for mammalian suspension cells tailored for phosphometabolome profiling by capillary ion chromatography - tandem mass spectrometry. *J Chromatogr B Analyt Technol Biomed Life Sci, 998-999*, 45-49. https://doi.org/10.1016/j.jchromb.2015.06.018

Lambert, T. J. (2019, Apr). FPbase: a community-editable fluorescent protein database. *Nat Methods, 16*(4), 277-278. https://doi.org/10.1038/s41592-019-0352-8

Lara, A. R., Galindo, E., Ramirez, O. T., & Palomares, L. A. (2006, Nov). Living with heterogeneities in bioreactors: understanding the effects of environmental gradients on cells. *Mol Biotechnol, 34*(3), 355-381. https://doi.org/10.1385/MB:34:3:355

Lara, A. R., Jaen, K. E., Folarin, O., Keshavarz-Moore, E., & Buchs, J. (2019, Oct 15). Effect of the oxygen transfer rate on oxygen-limited production of plasmid DNA by Escherichia coli. *Biochemical Engineering Journal, 150*, 107303. https://doi.org/ARTN 10730310.1016/j.bej.2019.107303

Lee, S. Y. (1996, Mar). High cell-density culture of Escherichia coli. *Trends Biotechnol, 14*(3), 98-105. https://doi.org/10.1016/0167-7799(96)80930-9

Li, X., Robbins, J. W., Jr., & Taylor, K. B. (1992, Jan). Effect of the levels of dissolved oxygen on the expression of recombinant proteins in four recombinant Escherichia coli strains. *J Ind Microbiol, 9*(1), 1-9. https://doi.org/10.1007/BF01576362

Lim, B., Miyazaki, R., Neher, S., Siegele, D. A., Ito, K., Walter, P., Akiyama, Y., Yura, T., & Gross, C. A. (2013, Dec). Heat shock transcription factor sigma32 co-opts the signal recognition particle to regulate protein homeostasis in E. coli. *PLoS Biol, 11*(12), e1001735. https://doi.org/10.1371/journal.pbio.1001735

Lin, H., Hoffmann, F., Rozkov, A., Enfors, S. O., Rinas, U., & Neubauer, P. (2004). Change of extracellular cAMP concentration is a sensitive reporter for bacterial fitness in high-cell-density cultures of Escherichia coli. *Biotechnology and bioengineering, 87*(5), 602-613.

Liu, H., Kang, J., Qi, Q., & Chen, G. (2011, May). Production of lactate in Escherichia coli by redox regulation genetically and physiologically. *Appl Biochem Biotechnol, 164*(2), 162-169. https://doi.org/10.1007/s12010-010-9123-9

Losen, M., Frolich, B., Pohl, M., & Buchs, J. (2004, Jul-Aug). Effect of oxygen limitation and medium composition on Escherichia coli fermentation in shake-flask cultures. *Biotechnol Prog, 20*(4), 1062-1068. https://doi.org/10.1021/bp034282t

Lu, W., Wang, L., Chen, L., Hui, S., & Rabinowitz, J. D. (2018, Jan 20). Extraction and Quantitation of Nicotinamide Adenine Dinucleotide Redox Cofactors. *Antioxid Redox Signal, 28*(3), 167-179. https://doi.org/10.1089/ars.2017.7014

Mæhlum, A. H. M. (2021). Growth Characterization and Mass Spectrometric Metabolic Profiling of *Escherichia coli* During Recombinant Protein Production [Master's thesis].

Magasanik, B. (1961). Catabolite repression. Cold Spring Harbor symposia on quantitative biology,

Majchrzak, M., Bowater, R. P., Staczek, P., & Parniewski, P. (2006, Dec 8). SOS repair and DNA supercoiling influence the genetic stability of DNA triplet repeats in Escherichia coli. *J Mol Biol, 364*(4), 612-624. https://doi.org/10.1016/j.jmb.2006.08.093

MarketsandMarkets. (2023). *Recombiant Proteins Market by Product (Growth Factorsm Chemokines, Structural Proteins, Membrane Proteins), Application (Drug Discovery*

& Development, Biopharma Production, Research, Diagnostics), End User (Biotech, CROs) & Region - Global Forecast to 2027

Mathiassen, L. F. (2022). Growth characteristics and metabolic changes in recombinant *Escherichia coli* with different plasmid copy numbers and expression system strengths [Master's thesis].

Mattanovich, D., Branduardi, P., Dato, L., Gasser, B., Sauer, M., & Porro, D. (2012). Recombinant Protein Production in Yeasts. In A. Lorence (Ed.), *Recombinant Gene Expression* (pp. 329-358). Humana Press. https://doi.org/10.1007/978-1-61779-433-9_17

Michel, B. (2005, Jul). After 30 years of study, the bacterial SOS response still surprises us. *PLoS Biol, 3*(7), e255. https://doi.org/10.1371/journal.pbio.0030255

Miki, B., & McHugh, S. (2004, Feb 5). Selectable marker genes in transgenic plants: applications, alternatives and biosafety. *J Biotechnol, 107*(3), 193-232. https://doi.org/10.1016/j.jbiotec.2003.10.011

Nakamura, M., Bhatnagar, A., & Sadoshima, J. (2012, Aug 17). Overview of pyridine nucleotides review series. *Circ Res, 111*(5), 604-610. https://doi.org/10.1161/CIRCRESAHA.111.247924

Ni, Y., & Chen, R. (2009, Nov). Extracellular recombinant protein production from Escherichia coli. *Biotechnol Lett, 31*(11), 1661-1670. https://doi.org/10.1007/s10529-009-0077-3

O'Beirne, D., & Hamer, G. (2000a, Oct). Oxygen availability and growth of Escherichia coli W3110: Dynamic responses to limitation and starvation. *Bioprocess Engineering, 23*(4), 381-387. https://doi.org/DOI 10.1007/s004499900177

O'Beirne, D., & Hamer, G. (2000b, Nov). Oxygen availability and the growth of Escherichia coli W3110: A problem exacerbated by scale-up. *Bioprocess Engineering, 23*(5), 487-494. https://doi.org/DOI 10.1007/s004499900185

Oganesyan, N., Ankoudinova, I., Kim, S. H., & Kim, R. (2007, Apr). Effect of osmotic stress and heat shock in recombinant protein overexpression and crystallization. *Protein Expr Purif, 52*(2), 280-285. https://doi.org/10.1016/j.pep.2006.09.015

Osterman, A. (2009, Aug). Biogenesis and Homeostasis of Nicotinamide Adenine Dinucleotide Cofactor. *EcoSal Plus, 3*(2). https://doi.org/10.1128/ecosalplus.3.6.3.10

Overton, T. W. (2014, May). Recombinant protein production in bacterial hosts. *Drug Discov Today, 19*(5), 590-601. https://doi.org/10.1016/j.drudis.2013.11.008

Ow, D. S.-W., Nissom, P. M., Philp, R., Oh, S. K.-W., & Yap, M. G.-S. (2006, 2006/07/03/). Global transcriptional analysis of metabolic burden due to plasmid maintenance in Escherichia coli DH5α during batch fermentation. *Enzyme and Microbial Technology, 39*(3), 391-398. https://doi.org/10.1016/j.enzmictec.2005.11.048

Özkan, P., Sariyar, B., Ütkür, F. Ö., Akman, U., & Hortaçsu, A. (2005, 2005/01/01/). Metabolic flux analysis of recombinant protein overproduction in Escherichia coli. *Biochemical Engineering Journal, 22*(2), 167-195. https://doi.org/10.1016/j.bej.2004.09.012

Palomares, L. A., Estrada-Mondaca, S., & Ramirez, O. T. (2004). Production of recombinant proteins: challenges and solutions. *Methods Mol Biol, 267*, 15-52. https://doi.org/10.1385/1-59259-774-2:015

Pang, Z. Q., Chong, J., Zhou, G. Y., Morais, D. A. D., Chang, L., Barrette, M., Gauthier, C., Jacques, P. E., Li, S. Z., & Xia, J. G. (2021, Jul 2). MetaboAnalyst 5.0: narrowing the gap between raw spectra and functional insights. *Nucleic Acids Research, 49*(W1), W388-W396. https://doi.org/10.1093/nar/gkab382

Perederina, A., Svetlov, V., Vassylyeva, M. N., Tahirov, T. H., Yokoyama, S., Artsimovitch, I., & Vassylyev, D. G. (2004, Aug 6). Regulation through the secondary channel--structural framework for ppGpp-DksA synergism during transcription. *Cell, 118*(3), 297-309. https://doi.org/10.1016/j.cell.2004.06.030

Pillai-Kastoori, L., Schutz-Geschwender, A. R., & Harford, J. A. (2020, Mar 15). A systematic approach to quantitative Western blot analysis. *Anal Biochem, 593*, 113608. https://doi.org/10.1016/j.ab.2020.113608

Pollak, N., Dolle, C., & Ziegler, M. (2007, Mar 1). The power to reduce: pyridine nucleotides--small molecules with a multitude of functions. *Biochem J, 402*(2), 205-218. https://doi.org/10.1042/BJ20061638

Puetz, J., & Wurm, F. M. (2019, Aug). Recombinant Proteins for Industrial versus Pharmaceutical Purposes: A Review of Process and Pricing. *Processes, 7*(8), 476. https://doi.org/ARTN 476 10.3390/pr7080476

Rantala, A., Utriainen, M., Kaushik, N., Virta, M., Valimaa, A. L., & Karp, M. (2011, May). Luminescent bacteria-based sensing method for methylmercury specific determination. *Anal Bioanal Chem, 400*(4), 1041-1049. https://doi.org/10.1007/s00216-011-4866-x

Recombinant Protein. (2006). In *Encyclopedic Reference of Genomics and Proteomics in Molecular Medicine* (pp. 1609-1609). Springer Berlin Heidelberg. https://doi.org/10.1007/3-540-29623-9_8485

Rorabacher, D. B. (1991). Statistical treatment for rejection of deviant values: critical values of Dixon's" Q" parameter and related subrange ratios at the 95% confidence level. *Analytical chemistry, 63*(2), 139-146.

Rosano, G. L., & Ceccarelli, E. A. (2014). Recombinant protein expression in Escherichia coli: advances and challenges. *Front Microbiol, 5*, 172. https://doi.org/10.3389/fmicb.2014.00172

Rosano, G. L., Morales, E. S., & Ceccarelli, E. A. (2019, Aug). New tools for recombinant protein production in Escherichia coli: A 5-year update. *Protein Sci, 28*(8), 1412-1422. https://doi.org/10.1002/pro.3668

Rost, L. M., Shafaei, A., Fuchino, K., & Bruheim, P. (2020, May 1). Zwitterionic HILIC tandem mass spectrometry with isotope dilution for rapid, sensitive and robust quantification of pyridine nucleotides in biological extracts. *J Chromatogr B Analyt Technol Biomed Life Sci, 1144*, 122078. https://doi.org/10.1016/j.jchromb.2020.122078

Rozkov, A., Avignone-Rossa, C. A., Ertl, P. F., Jones, P., O'Kennedy, R. D., Smith, J. J., Dale, J. W., & Bushell, M. E. (2004, Dec 30). Characterization of the metabolic burden on Escherichia coli DH1 cells imposed by the presence of a plasmid containing a gene therapy sequence. *Biotechnol Bioeng, 88*(7), 909-915. https://doi.org/10.1002/bit.20327

Rudge, S. R., & Ladisch, M. R. (2020). Industrial Challenges of Recombinant Proteins. In A. C. Silva, J. N. Moreira, J. M. S. Lobo, & H. Almeida (Eds.), *Current Applications of Pharmaceutical Biotechnology* (pp. 1-22). Springer International Publishing. https://doi.org/10.1007/10_2019_120

Schumann, W. (2016, Nov). Regulation of bacterial heat shock stimulons. *Cell Stress Chaperones, 21*(6), 959-968. https://doi.org/10.1007/s12192-016-0727-z

Selas Castineiras, T., Williams, S. G., Hitchcock, A. G., & Smith, D. C. (2018, Aug 1). E. coli strain engineering for the production of advanced biopharmaceutical products. *FEMS Microbiol Lett, 365*(15). https://doi.org/10.1093/femsle/fny162

Seo, J. H., & Bailey, J. E. (1985, Dec). Effects of recombinant plasmid content on growth properties and cloned gene product formation in Escherichia coli. *Biotechnol Bioeng, 27*(12), 1668-1674. https://doi.org/10.1002/bit.260271207

Shaner, N. C., Lin, M. Z., McKeown, M. R., Steinbach, P. A., Hazelwood, K. L., Davidson, M. W., & Tsien, R. Y. (2008, Jun). Improving the photostability of bright monomeric orange and red fluorescent proteins. *Nat Methods, 5*(6), 545-551. https://doi.org/10.1038/nmeth.1209

Shaner, N. C., Patterson, G. H., & Davidson, M. W. (2007, Dec 15). Advances in fluorescent protein technology. *J Cell Sci, 120*(Pt 24), 4247-4260. https://doi.org/10.1242/jcs.005801

Shiloach, J., & Fass, R. (2005, Jul). Growing E. coli to high cell density--a historical perspective on method development. *Biotechnol Adv, 23*(5), 345-357. https://doi.org/10.1016/j.biotechadv.2005.04.004

Silva, F., Queiroz, J. A., & Domingues, F. C. (2012, May-Jun). Evaluating metabolic stress and plasmid stability in plasmid DNA production by Escherichia coli. *Biotechnol Adv, 30*(3), 691-708. https://doi.org/10.1016/j.biotechadv.2011.12.005

Sletta, H., Nedal, A., Aune, T. E., Hellebust, H., Hakvag, S., Aune, R., Ellingsen, T. E., Valla, S., & Brautaset, T. (2004, Dec). Broad-host-range plasmid pJB658 can be used for industrial-level production of a secreted host-toxic single-chain antibody fragment in Escherichia coli. *Appl Environ Microbiol, 70*(12), 7033-7039. https://doi.org/10.1128/AEM.70.12.7033-7039.2004

Sletta, H., Tondervik, A., Hakvag, S., Aune, T. E., Nedal, A., Aune, R., Evensen, G., Valla, S., Ellingsen, T. E., & Brautaset, T. (2007, Feb). The presence of N-terminal secretion signal sequences leads to strong stimulation of the total expression levels of three tested medically important proteins during high-cell-density cultivations of Escherichia coli. *Appl Environ Microbiol, 73*(3), 906-912. https://doi.org/10.1128/AEM.01804-06

Stafsnes, M. H., Rost, L. M., & Bruheim, P. (2018, Apr 15). Improved phosphometabolome profiling applying isotope dilution strategy and capillary ion chromatography-tandem mass spectrometry. *J Chromatogr B Analyt Technol Biomed Life Sci, 1083*, 278-283. https://doi.org/10.1016/j.jchromb.2018.02.004

Summers, D. (1998, Sep). Timing, self-control and a sense of direction are the secrets of multicopy plasmid stability. *Mol Microbiol, 29*(5), 1137-1145. https://doi.org/10.1046/j.1365-2958.1998.01012.x

Summers, D. K. (1991, Aug). The kinetics of plasmid loss. *Trends Biotechnol, 9*(8), 273-278. https://doi.org/10.1016/0167-7799(91)90089-z

Teixeira de Mattos, M. J., & Neijssel, O. M. (1997, Dec 17). Bioenergetic consequences of microbial adaptation to low-nutrient environments. *J Biotechnol, 59*(1-2), 117-126. https://doi.org/10.1016/s0168-1656(97)00174-0

Tenaillon, O., Skurnik, D., Picard, B., & Denamur, E. (2010, Mar). The population genetics of commensal Escherichia coli. *Nat Rev Microbiol, 8*(3), 207-217. https://doi.org/10.1038/nrmicro2298

Terpe, K. (2006, Sep). Overview of bacterial expression systems for heterologous protein production: from molecular and biochemical fundamentals to commercial systems. *Appl Microbiol Biotechnol, 72*(2), 211-222. https://doi.org/10.1007/s00253-006-0465-8

Thomas, C. M., Cross, M. A., Hussain, A. A., & Smith, C. A. (1984, Jan). Analysis of copy number control elements in the region of the vegetative replication origin of the broad host range plasmid RK2. *EMBO J, 3*(1), 57-63. https://doi.org/10.1002/j.1460-2075.1984.tb01761.x

Thorfinnsdottir, L. B., Garcia-Calvo, L., Bo, G. H., Bruheim, P., & Rost, L. M. (2023, Jan 18). Optimized Fast Filtration-Based Sampling and Extraction Enables Precise and Absolute Quantification of the Escherichia coli Central Carbon Metabolome. *Metabolites, 13*(2). https://doi.org/10.3390/metabo13020150

Toukdarian, A. E., & Helinski, D. R. (1998, Nov 26). TrfA dimers play a role in copy-number control of RK2 replication. *Gene, 223*(1-2), 205-211. https://doi.org/10.1016/s0378-1119(98)00370-9

Traxler, M. F., Summers, S. M., Nguyen, H. T., Zacharia, V. M., Hightower, G. A., Smith, J. T., & Conway, T. (2008, Jun). The global, ppGpp-mediated stringent response to amino acid starvation in Escherichia coli. *Mol Microbiol, 68*(5), 1128-1148. https://doi.org/10.1111/j.1365-2958.2008.06229.x

Tripathi, N. K., Sathyaseelan, K., Jana, A. M., & Rao, P. V. L. (2009, Mar). High Yield Production of Heterologous Proteins with Escherichia coli. *Defence Science Journal, 59*(2), 137-146. https://doi.org/DOI 10.14429/dsj.59.1501

Unden, G., & Bongaerts, J. (1997, Jul 4). Alternative respiratory pathways of Escherichia coli: energetics and transcriptional regulation in response to electron acceptors. *Biochim Biophys Acta, 1320*(3), 217-234. https://doi.org/10.1016/s0005-2728(97)00034-0

Valdez-Cruz, N. A., Ramirez, O. T., & Trujillo-Roldan, M. A. (2011, Mar-Apr). Molecular responses of Escherichia coli caused by heat stress and recombinant protein production during temperature induction. *Bioeng Bugs, 2*(2), 105-110. https://doi.org/10.4161/bbug.2.2.14316

Valenzuela, M. S., Ikpeazu, E. V., & Siddiqui, K. A. (1996, Feb 27). E. coli growth inhibition by a high copy number derivative of plasmid pBR322. *Biochem Biophys Res Commun, 219*(3), 876-883. https://doi.org/10.1006/bbrc.1996.0339

Valgepea, K., Adamberg, K., & Vilu, R. (2011, Jul 5). Decrease of energy spilling in Escherichia coli continuous cultures with rising specific growth rate and carbon wasting. *BMC Syst Biol, 5*(1), 106. https://doi.org/10.1186/1752-0509-5-106

Vee Aune, T. E., Bakke, I., Drablos, F., Lale, R., Brautaset, T., & Valla, S. (2010, Jan). Directed evolution of the transcription factor XylS for development of improved expression systems. *Microb Biotechnol, 3*(1), 38-47. https://doi.org/10.1111/j.1751-7915.2009.00126.x

Vemuri, G. N., Altman, E., Sangurdekar, D. P., Khodursky, A. B., & Eiteman, M. A. (2006, May). Overflow metabolism in Escherichia coli during steady-state growth: transcriptional regulation and effect of the redox ratio. *Appl Environ Microbiol, 72*(5), 3653-3661. https://doi.org/10.1128/AEM.72.5.3653-3661.2006

Vemuri, G. N., Eiteman, M. A., & Altman, E. (2006, Jun 20). Increased recombinant protein production in Escherichia coli strains with overexpressed water-forming NADH oxidase and a deleted ArcA regulatory protein. *Biotechnol Bioeng, 94*(3), 538-542. https://doi.org/10.1002/bit.20853

Waegeman, H., & Soetaert, W. (2011, Dec). Increasing recombinant protein production in Escherichia coli through metabolic and genetic engineering. *J Ind Microbiol Biotechnol, 38*(12), 1891-1910. https://doi.org/10.1007/s10295-011-1034-4

Walsh, G. (2018, Dec 6). Biopharmaceutical benchmarks 2018. *Nat Biotechnol, 36*(12), 1136-1145. https://doi.org/10.1038/nbt.4305

Wang, Z., Jin, L., Yuan, Z., Wegrzyn, G., & Wegrzyn, A. (2009, Jan). Classification of plasmid vectors using replication origin, selection marker and promoter as criteria. *Plasmid, 61*(1), 47-51. https://doi.org/10.1016/j.plasmid.2008.09.003

Wang, Z., Xiang, L., Shao, J., Wegrzyn, A., & Wegrzyn, G. (2006, Nov 17). Effects of the presence of ColE1 plasmid DNA in Escherichia coli on the host cell metabolism. *Microb Cell Fact, 5*(1), 34. https://doi.org/10.1186/1475-2859-5-34

Ward, O. P. (2012, Sep-Oct). Production of recombinant proteins by filamentous fungi. *Biotechnol Adv, 30*(5), 1119-1139. https://doi.org/10.1016/j.biotechadv.2011.09.012

Wendrich, T. M., Blaha, G., Wilson, D. N., Marahiel, M. A., & Nierhaus, K. H. (2002, Oct). Dissection of the mechanism for the stringent factor RelA. *Mol Cell, 10*(4), 779-788. https://doi.org/10.1016/s1097-2765(02)00656-1

Wilke, M. S., Lovering, A. L., & Strynadka, N. C. (2005, Oct). Beta-lactam antibiotic resistance: a current structural perspective. *Curr Opin Microbiol, 8*(5), 525-533. https://doi.org/10.1016/j.mib.2005.08.016

Wilson, D. N., & Nierhaus, K. H. (2007, May-Jun). The weird and wonderful world of bacterial ribosome regulation. *Crit Rev Biochem Mol Biol, 42*(3), 187-219. https://doi.org/10.1080/10409230701360843

Wimpenny, J. W., & Firth, A. (1972, Jul). Levels of nicotinamide adenine dinucleotide and reduced nicotinamide adenine dinucleotide in facultative bacteria and the effect of oxygen. *J Bacteriol, 111*(1), 24-32. https://doi.org/10.1128/jb.111.1.24-32.1972

Winther-Larsen, H. C., Josefsen, K. D., Brautaset, T., & Valla, S. (2000, Apr). Parameters affecting gene expression from the Pm promoter in gram-negative bacteria. *Metab Eng, 2*(2), 79-91. https://doi.org/10.1006/mben.1999.0142

Womack, J. E., & Odonovan, G. A. (1978). Orotic-Acid Excretion in Some Wild-Type Strains of Escherichia-Coli K-12. *Journal of bacteriology, 136*(2), 825-828. https://doi.org/Doi 10.1128/Jb.136.2.825-827.1978

Wood, K. V. (1995, Feb). Marker proteins for gene expression. *Curr Opin Biotechnol, 6*(1), 50-58. https://doi.org/10.1016/0958-1669(95)80009-3

Wurm, F. M. (2004, Nov). Production of recombinant protein therapeutics in cultivated mammalian cells. *Nat Biotechnol, 22*(11), 1393-1398. https://doi.org/10.1038/nbt1026

Xu, B., Jahic, M., Blomsten, G., & Enfors, S. O. (1999, May). Glucose overflow metabolism and mixed-acid fermentation in aerobic large-scale fed-batch processes with Escherichia coli. *Appl Microbiol Biotechnol, 51*(5), 564-571. https://doi.org/10.1007/s002530051433

Xu, X., Niu, Y., Liang, K., Wang, J., Li, X., & Yang, Y. (2015, Apr 3). Heat shock transcription factor delta(3)(2) is targeted for degradation via an ubiquitin-like protein ThiS in Escherichia coli. *Biochem Biophys Res Commun, 459*(2), 240-245. https://doi.org/10.1016/j.bbrc.2015.02.087

Yates, R. A., & Pardee, A. B. (1956). Control of Pyrimidine Biosynthesis in Escherichia-Coli by a Feed-Back Mechanism. *Journal of Biological Chemistry, 221*(2), 757-770. <Go to ISI>://WOS:A1956WA45300020

Yoon, S. H., Han, M. J., Jeong, H., Lee, C. H., Xia, X. X., Lee, D. H., Shim, J. H., Lee, S. Y., Oh, T. K., & Kim, J. F. (2012, May 25). Comparative multi-omics systems analysis of Escherichia coli strains B and K-12. *Genome Biol, 13*(5), R37. https://doi.org/10.1186/gb-2012-13-5-r37

Yoon, S. H., Jeong, H., Kwon, S.-K., & Kim, J. F. (2009). Genomics, biological features, and biotechnological applications of Escherichia coli B:"Is B for better?!". *Systems biology and biotechnology of Escherichia coli*, 1-17.

Yoshida, A., Nishimura, T., Kawaguchi, H., Inui, M., & Yukawa, H. (2005, Nov). Enhanced hydrogen production from formic acid by formate hydrogen lyase-overexpressing Escherichia coli strains. *Appl Environ Microbiol, 71*(11), 6762-6768. https://doi.org/10.1128/AEM.71.11.6762-6768.2005

Zhang, J., ten Pierick, A., van Rossum, H. M., Seifar, R. M., Ras, C., Daran, J. M., Heijnen, J. J., & Wahl, S. A. (2015, Aug 5). Determination of the Cytosolic NADPH/NADP Ratio in Saccharomyces cerevisiae using Shikimate Dehydrogenase as Sensor Reaction. *Sci Rep, 5*(1), 12846. https://doi.org/10.1038/srep12846

Appendix

A Calibration curves

A.1 CDW calibration curves

The CDW acquired from the OD_{600} measurements was performed on *E. coli* BL21 WT and A2mCh as described in subsection 2.4.2. The average CDW was plotted against the corresponding average OD_{600}. Thereafter, linear regression was performed to get a relationship between the OD_{600} measurements and the CDW. The optical density and the weight of the medium was corrected for by measuring the CDW and OD_{600} of blanks. The linear regression was performed using Excel. The results for the two different strains are given in Table A.1.

Table A.1: CDW as a function of OD_{600} for the *E. coli* BL21 strains WT and A2mCh, with the R^2 value for the given function. y represents the CDW and x the OD_{600}.

Strain	CDW as a function of OD_{600}	R^2 value
WT	$y = 0.406x + 0.056$	0.9969
A2mCh	$y = 0.4016x + 0.0483$	0.9961

A.2 mCherry calibration curve

A.2.1 From fluorescence

The mCherry concentration acquired from the fluorescence measurement was performed on commercial mCherry as described in subsection 2.4.5.3. Known concentrations of mCherry were plotted against average fluorescence. The autofluorescence of the dilution medium was corrected for by measuring the fluorescence of a blank. Thereafter, power regression was performed using Excel, with an R^2 value of 0.9946. mCherry concentration (ng/µL) as a function of fluorescence is given in Equation A-1,

$$y = 0.159x^{0.6697} \qquad \text{Equation A-1}$$

where y represents the mCherry concentration and x the fluorescence.

The relationship between the fluorescence of whole cells and lysed cells was also acquired. Linear regression through origo was performed in Excel, giving an R^2 value of 0.9997. Fluorescence of lysed cells as a function of fluorescence of whole cells is given in Equation A-2,

$$y = 1.1182x \qquad \text{Equation A-2}$$

where y represents the fluorescence of lysed cells and x the fluorescence of whole cells.

Both equations were acquired from master students in the last year's MetaboProt group (Everson, 2022; Humlebrekk, 2022; Mathiassen, 2022).

A.2.1.1 Quantification of mCherry in cultivations

The concentration of mCherry in the cultivation broth of each cultivation was quantified by measuring the fluorescence. The concentration at each time point is given in Table A.2.

Table A.2: Concentration of mCherry produced by *E. coli* BL21 A2mCh at different conditions at different time points in the cultivation. The concentration was quantified from the fluorescence of the cultivation broth in technical triplicates.

	mCherry [mg/L]				
	At induction	T1	T2	T3	T4
Limited II	2.02 ± 0.02	27.64 ± 0.16	37.74 ± 0.12	36.10 ± 0.11	35.08 ± 0.18
Limited III	2.03 ± 0.02	27.71 ± 0.15	36.67 ± 0.05	35.71 ± 0.18	35.17 ± 0.17
Non-limited I	2.02 ± 0.02	23.44 ± 0.06	38.11 ± 0.15	53.97 ± 0.41	76.98 ± 0.48
Non-limited II	2.04 ± 0.02	24.2 ± 0.07	40.88 ± 0.15	55.10 ± 0.15	78.76 ± 0.14
Non-limited III	2.07 ± 0.00	27.73 ± 0.04	47.67 ± 0.2	62.68 ± 0.01	76.44 ± 0.03

A.2.2 From western blot

The mCherry amount acquired from the western blot was performed on commercial mCherry as described in subsection 2.4.5.4. Known amounts of mCherry were plotted against the band intensity using Software Image Lab 6.0.1, giving a standard curve. The standard curve differed between western blots. Therefore, one example of a standard curve is given in Equation A-3, with a R^2-value of 0.808017,

$$y = 7.34 * 10^{-6}x - 17 \qquad \text{Equation A-3}$$

where y represents the amount of mCherry (ng) and x is the band intensity.

Thereafter, the concentration of mCherry in the sample was possible to quantify with the known volume of loaded sample and extracted volume from the bioreactors.

A.2.3 Comparison of fluorescent and western blot

Looking at the concentration of mCherry, it was seen discrepancies between the amount quantified from the fluorescence and the western blot. Figure A.1 shows the concentration of mCherry, given as mg/L, plotted against the time points it was sampled for. The figure shows both the control cultivation and limited cultivation for both fluorescence and western blot.

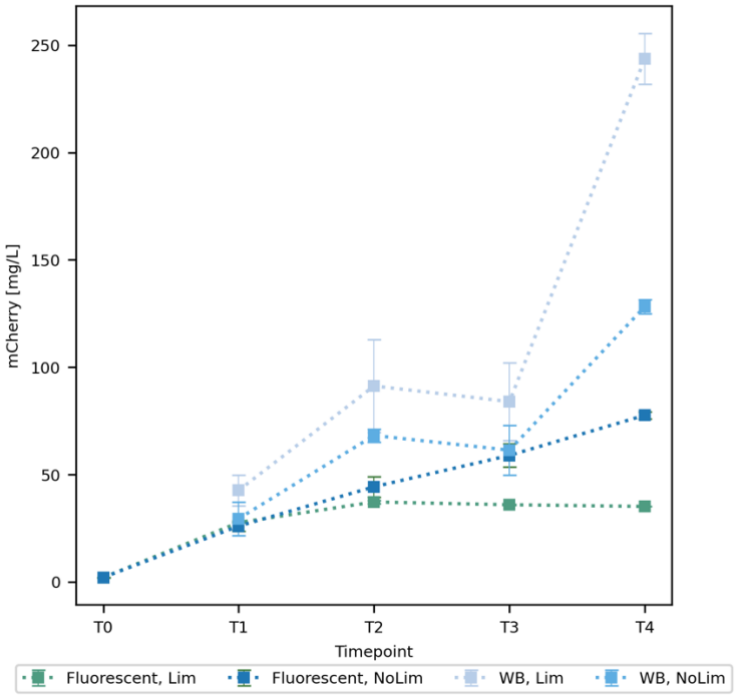

Figure A.1: Concentration of mCherry plotted against the time point it was sampled at. T0 represents the amount prior to induction of mCherry production. Concentration quantified from fluorescence was sampled in technical triplicates and biological duplicates or triplicates, dependent upon if the samples are from the oxygen-limited or the non-limited cultivation, respectively. The concentration interpolated from the western blot (WB) was measured in technical duplicates.

A.3 Determination of growth rate

To determine the growth rate in exponential growth phases, the OD_{600} values were plotted against time in a semi-log plot. The growth rate was determined from the equation of the straight line on the exponential form $y = Ae^{bx}$, where b represents the growth rate. Figure A.2 shows an example of the OD_{600} plotted against time on a semi-log scale in the exponential growth phase. The exponential function of the line is shown, including the R^2-value, where the growth rate is 0.3296 h^{-1}.

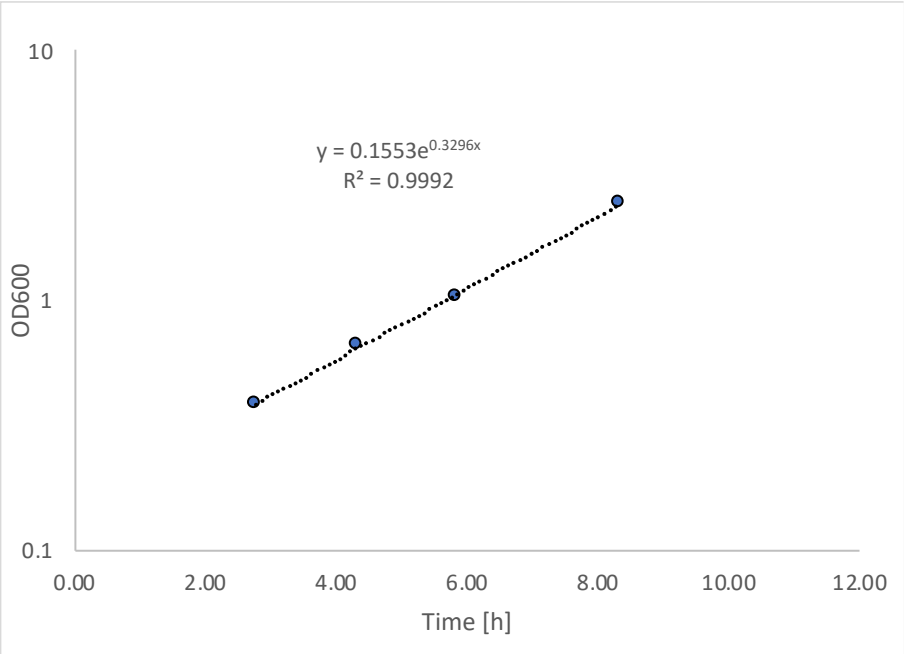

Figure A.2: A semi-log plot of OD_{600} plotted against time as an example of how to find the growth rate in the exponential growth phase of *E. coli*. The linear graph gives an exponential function on the form $y = Ae^{bx}$, where b represents the growth rate.

B Optimisation of media and preliminary cultivations

To figure out what media to use, both M9-MtPr media 1 and 2 were tested under different conditions. Both media were tested at 30 and 37 °C with one biological replicate when cultivating *E. coli* BL21 WT and A2mCh. Afterwards, M9-MtPr media 2 was tested at 37 °C with and without EDTA, to prevent precipitation, with biological duplicates when cultivating *E. coli* BL21 WT. The cultivation plots are shown in Figure B.1.

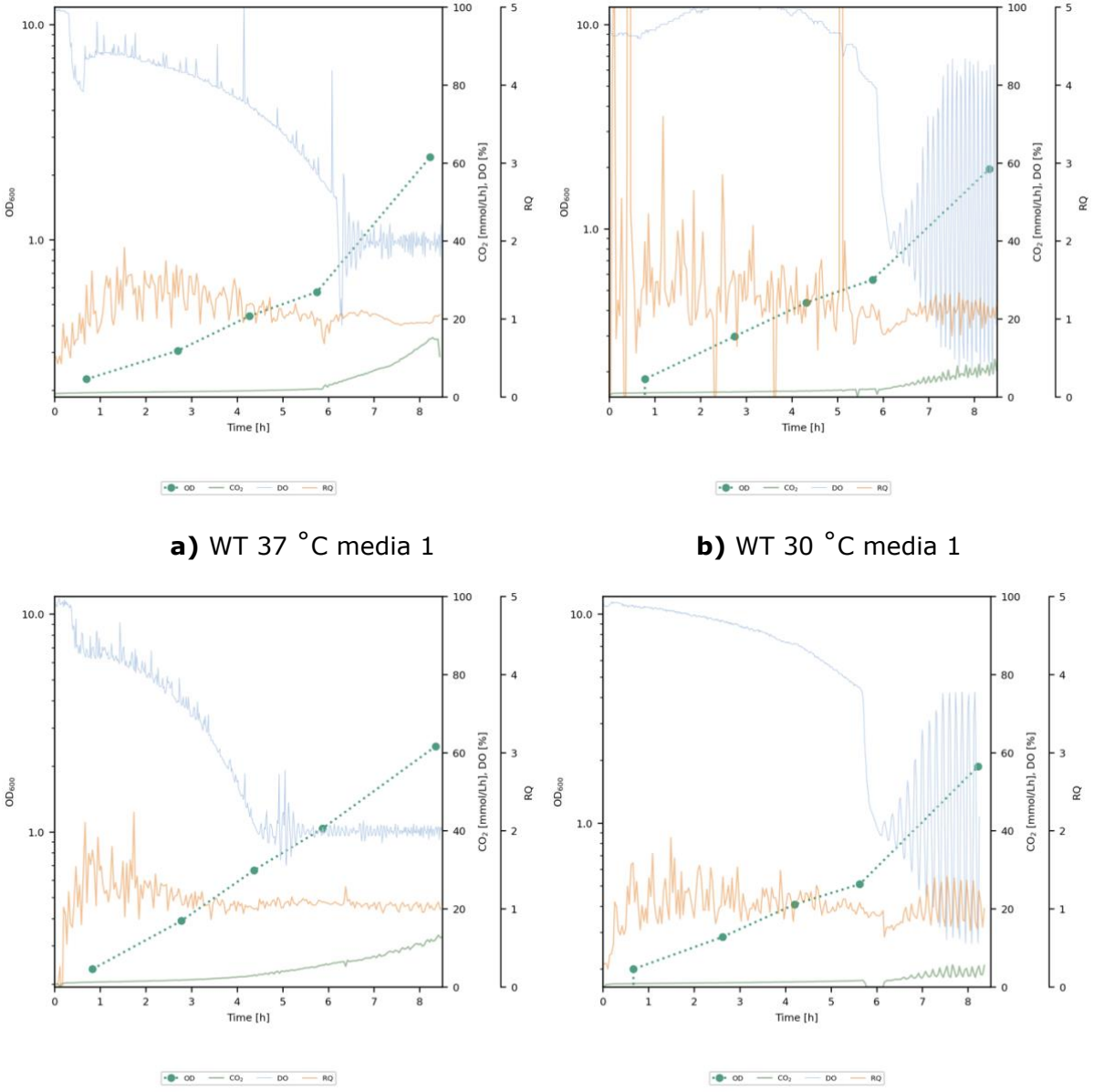

a) WT 37 °C media 1

b) WT 30 °C media 1

c) A2mCh 37 °C media 1

d) A2mCh 30 °C media 1

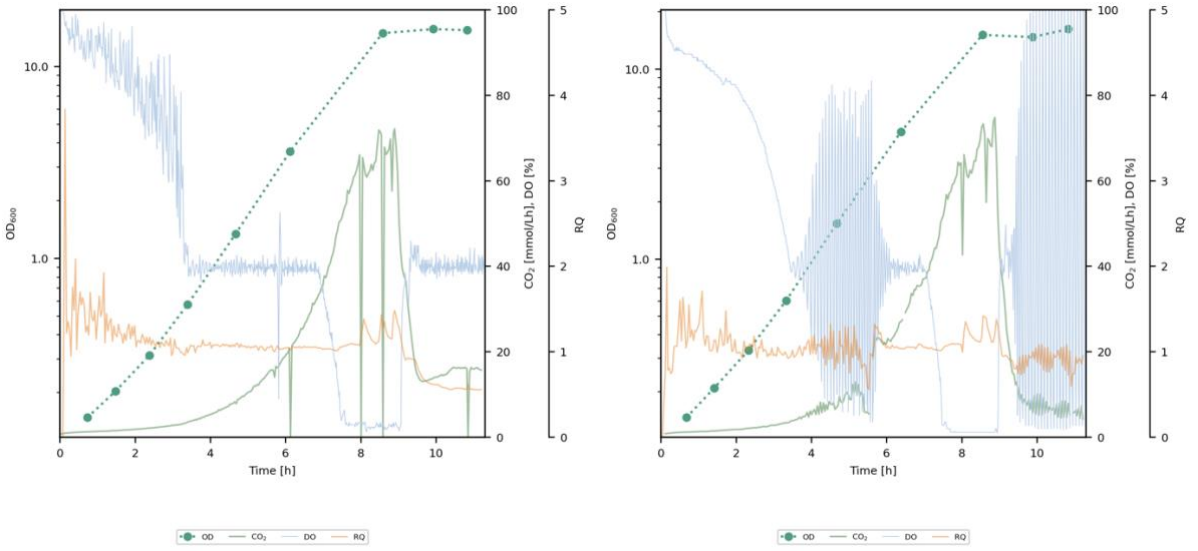

e) WT-I 37 °C media 2 **f)** WT-II 37 °C media 2

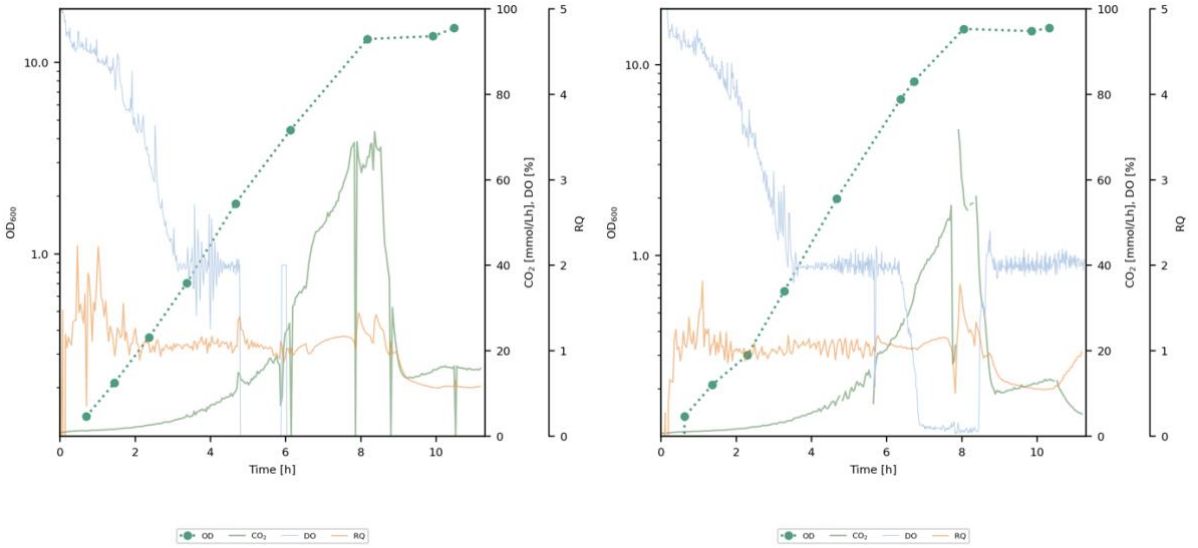

g) WT-I 37 °C EDTA media 2 **h)** WT-II 37 °C EDTA media 2

Figure B.1: Cultivation plots for E. coli BL21 WT (a, b) and A2mCh (c, d) using M9-MtPr media 1 at 37 °C (a, c) and 30 °C (b, d), and for E.coli BL21 WT at 37 °C using M9-MtPr media 2 with (f, h) and without (e, g) the addition of EDTA to prevent precipitation. The dissolved oxygen (DO, light blue line), CO2 off-gas (green line) and respiratory quotient (RQ, yellow line) were measured online. Optical density (OD_{600}, green dotted line) was measured at regular intervals. The cultivations were performed using 1 L bench-top bioreactors. The pH was constantly adjusted to 7.00. The dissolved oxygen was kept above 40 %. Roman numerals indicate biological replicate.

In addition to optimizing the media, when to induce the production of mCherry and when to limit the oxygen availability for *E. coli* BL21 A2mCh was also investigated. The cultivation plots are shown in Figure B.2.

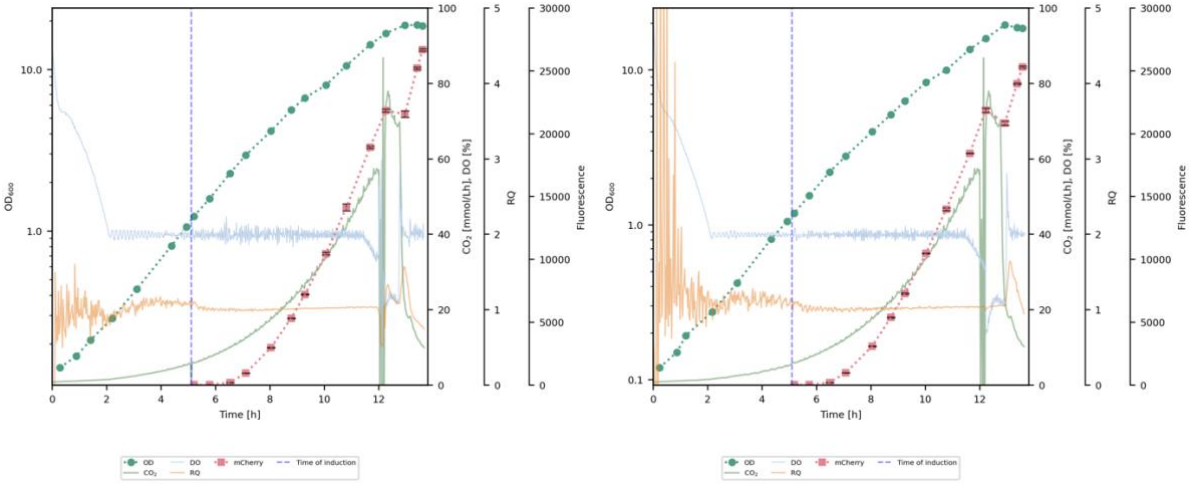

a) Induced at 1

b) Induced at 1

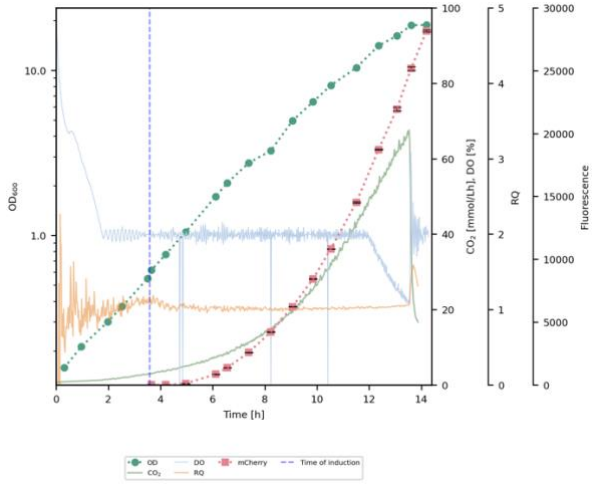

c) induced at 0.5

Figure B.2: Cultivation plots for *E. coli* BL21 A2mCh using M9-MtPr media 2 at 30 °C. The production of mCherry was induced at OD_{600} ~ 1.0 (a, b) or 0.5 (c). The dissolved oxygen (DO, light blue line), CO2 off-gas (green line) and respiratory quotient (RQ, yellow line) were measured online. Optical density (OD_{600}, green dotted line) and the fluorescence of mCherry (red dotted line) were measured at regular intervals. The cultivations were performed using 1 L bench-top bioreactors. The pH was constantly adjusted to 7.00. The dissolved oxygen was kept above 40 %.

The growth characteristics of *E. coli* BL21 WT and A2mCh were investigated under oxygen limitation. An example of the cultivation plot for each strain is shown in Figure B.3

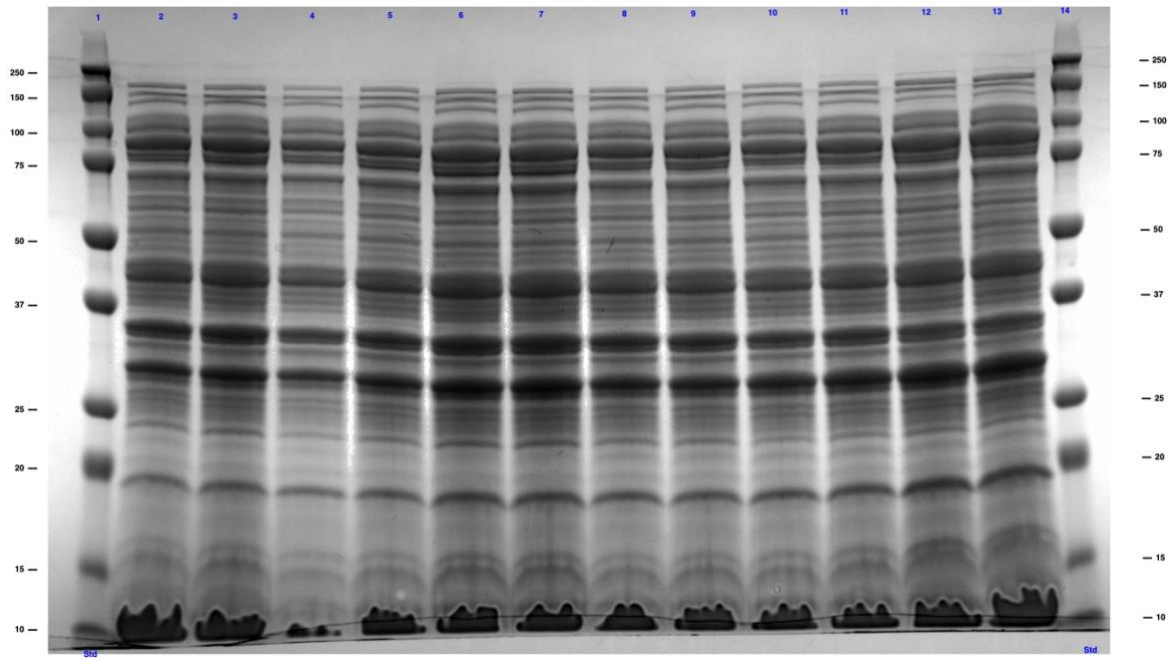

Figure D.1: SDS-PAGE performed on samples from the soluble fraction of proteins extracted from *E. coli* BL21 A2mCh and prepared according to subsection 2.4.5.2. Samples were taken at four different time points, but T3 was omitted from the SDS-PAGE. Lanes 1 and 14 corresponds to the molecular weight ladder. Lanes 2-7 is from the control cultivation of A2mCh, while lanes 8-13 is from the oxygen-limited cultivation of A2mCh. Even numbered lanes are from technical replicates E, odd numbered lanes are from technical replicates F. The time points were analysed chronologically. The protein analysed for, mCherry, is the band corresponding to a molecular weight of 26.7 kDa.

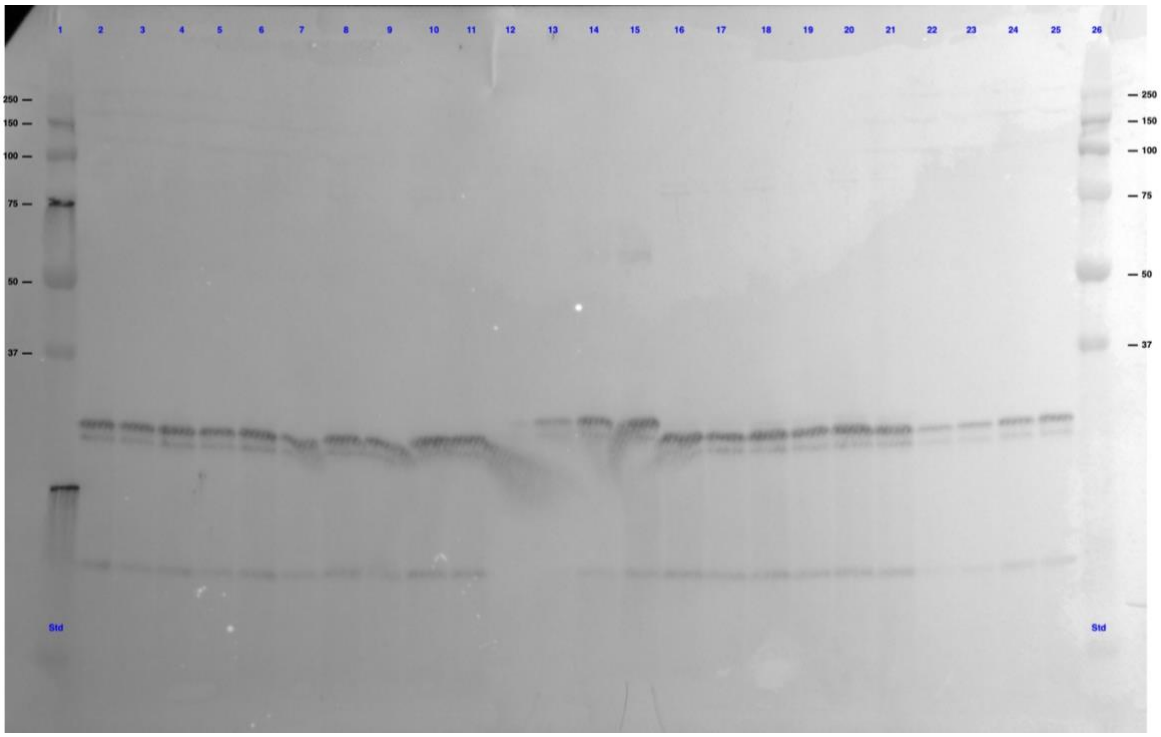

Figure D.2: Western blot performed on samples extracted from one of the oxygen-limited cultivations of *E. coli* BL21 A2mCh prepared according to subsection 2.4.5.2. Samples were taken at four different time points. Lanes 1 and 26 corresponds to the molecular weight ladder. Lanes 12-15 contain pure mCherry used to make a standard curve for the quantification of the amount of mCherry

in the samples from the band strength. Lanes 2-11 and 16-21 contain samples from the soluble fraction of the proteins, while lanes 22-25 contain samples from the insoluble fractions. Two technical replicates from each time point are loaded, with each being diluted either 500 or 1000 times.

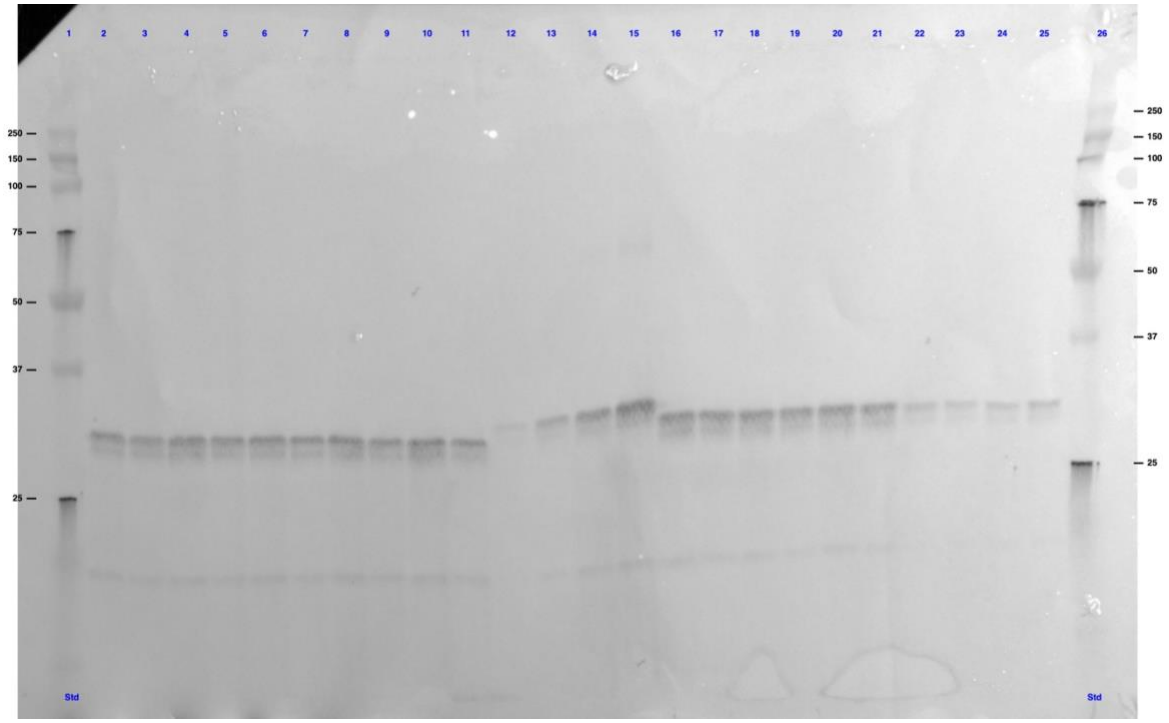

Figure D.3: Western blot performed on samples extracted from one of the control cultivations of *E. coli* BL21 A2mCh prepared according to subsection 2.4.5.2. Samples were taken at four different. Lanes 1 and 26 corresponds to the molecular weight ladder. Lanes 12-15 contain pure mCherry used to make a standard curve for the quantification of the amount of mCherry in the samples from the band strength. Lanes 2-11 and 16-21 contain samples from the soluble fraction of the proteins, while lanes 22-25 contain samples from the insoluble fractions. Two technical replicates from each time point are loaded, with each being diluted either 500 or 1000 times.

.

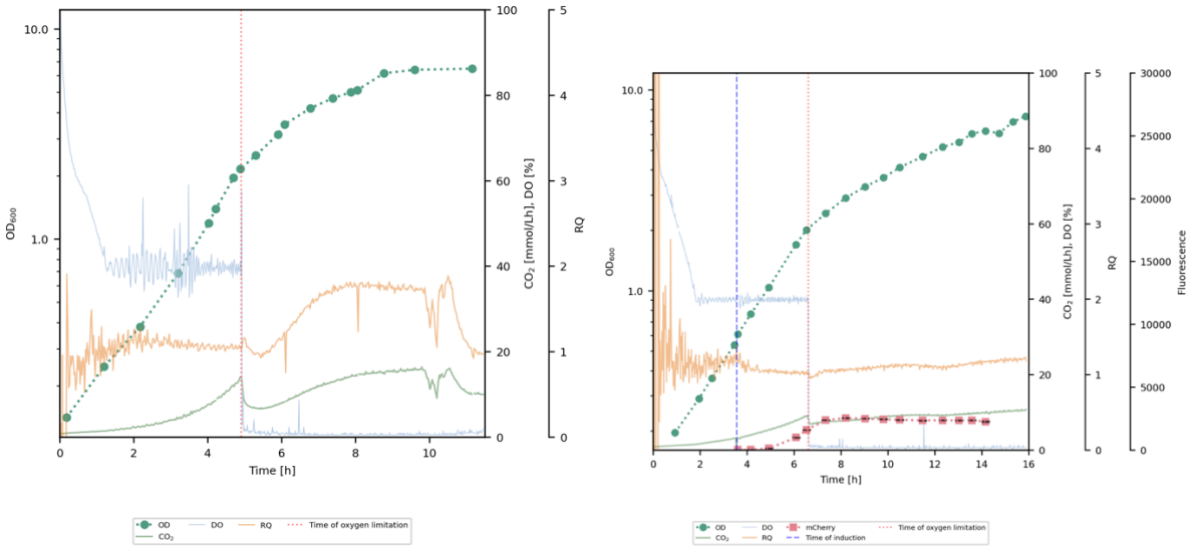

a) WT **b)** A2mCh

Figure B.3: Cultivation plots for *E. coli* BL21 WT (a) and A2mCh (b) using M9-MtPr media 2 at 37 °C and 30 °C, respectively. Oxygen limitation was induced at OD_{600} ~ 2.0, by setting the agitation to 400 rpm. The production of mCherry was induced at OD_{600} ~ 0.5. The dissolved oxygen (DO, light blue line), CO_2 off-gas (green line) and respiratory quotient (RQ, yellow line) were measured online. Optical density (OD_{600}, green dotted line) and the fluorescent of mCherry (red dotted line) were measured at regular intervals. The cultivations were performed using 1 L bench-top bioreactors. The pH was constantly adjusted to 7. The dissolved oxygen was kept above 40 % before oxygen limitation was induced.

C Additional batch cultivation plots

C.1 *E. coli* BL21 WT

As only one representative cultivation plot of each condition (control or oxygen limitation) of *E. coli* BL21 WT was shown in subsection 3.2.1, the remaining plots are shown in Figure C.1.

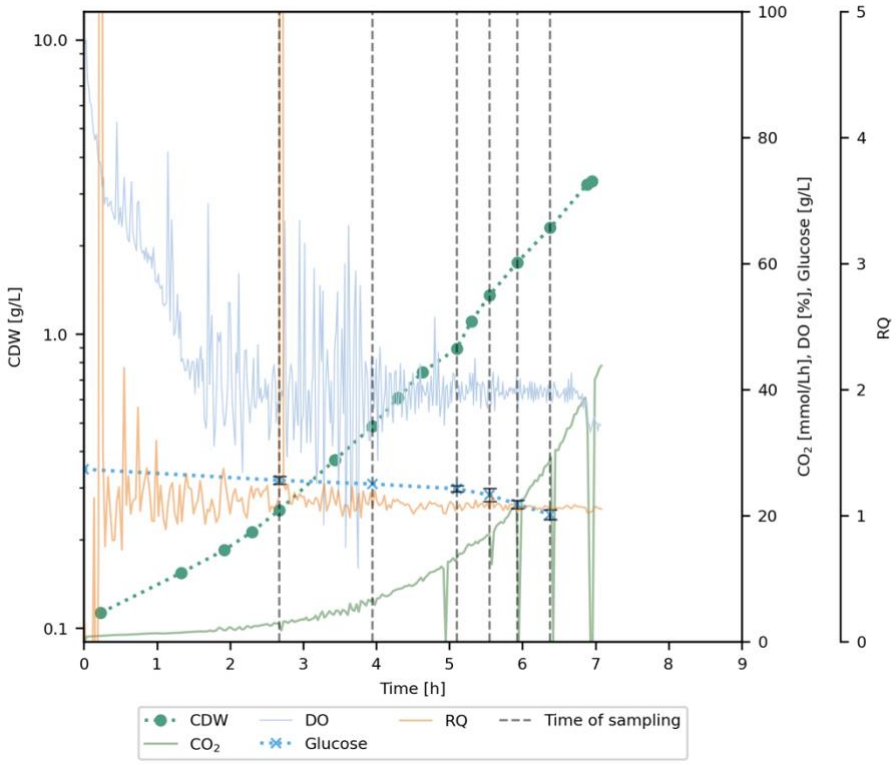

a) *E. coli* BL21 WT-II, no oxygen limitation.

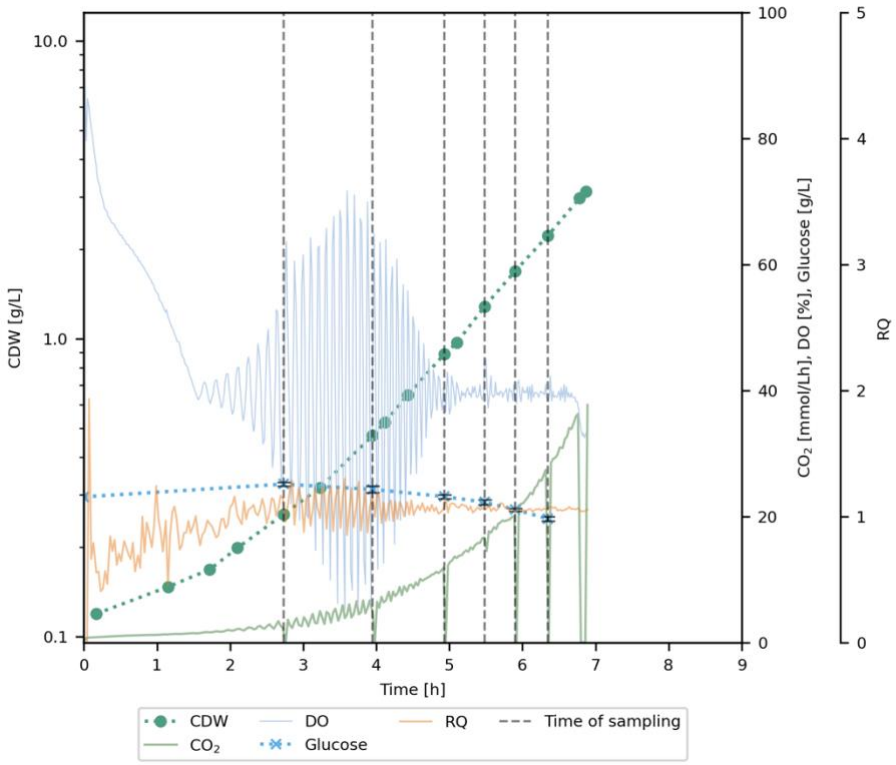

b) *E. coli* BL21 WT-III, no oxygen limitation.

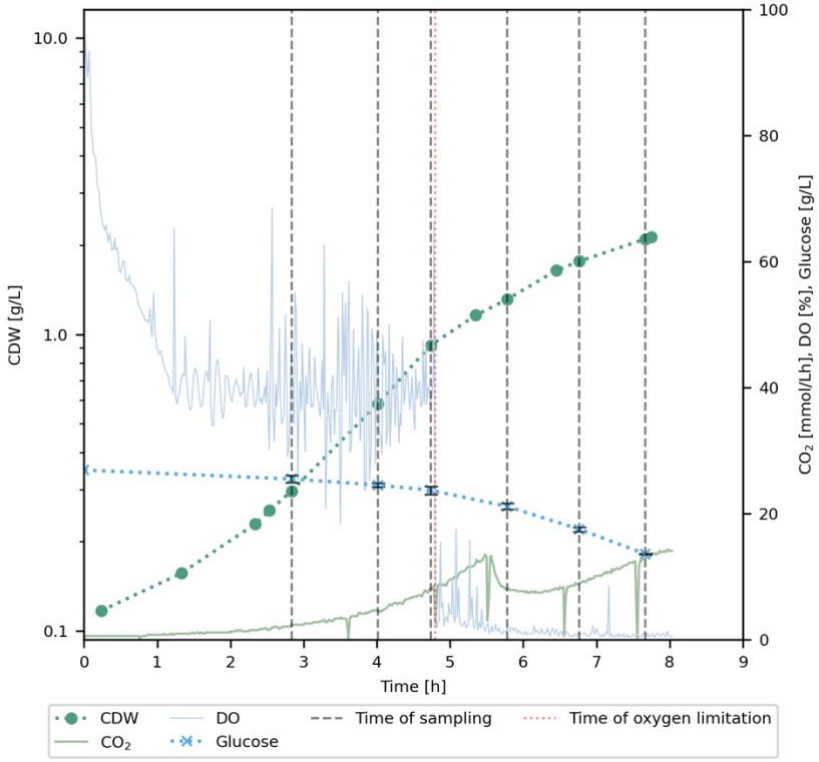

c) *E. coli* BL21 WT-II, oxygen limitation.

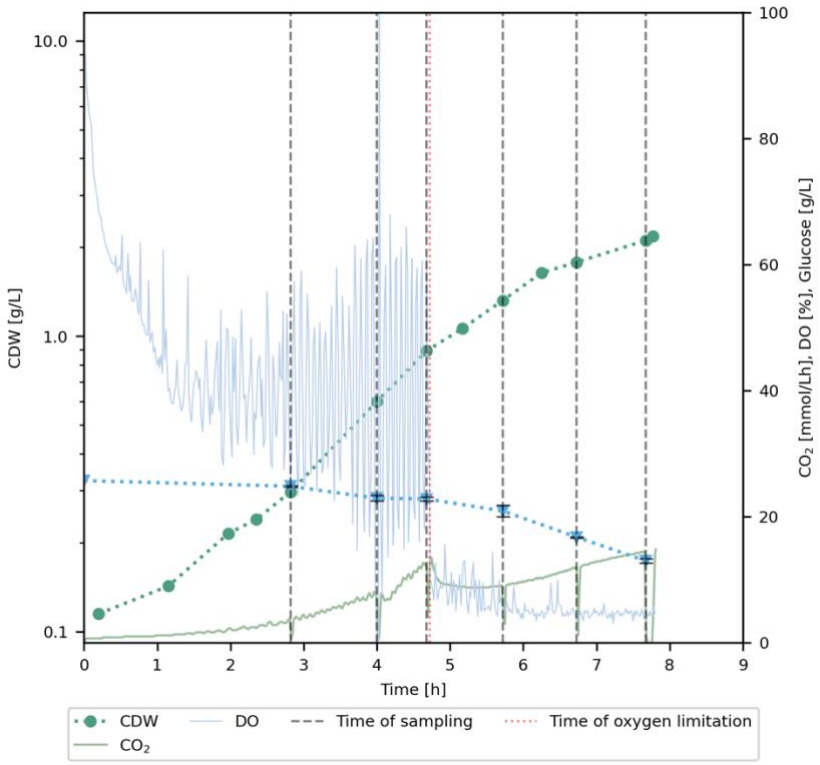

d) *E. coli* BL21 WT-III, oxygen limitation.

Figure C.1: Remaining cultivation plots for *E. coli* BL21 WT of the biological triplicates grown under no oxygen limitation (a-b) and oxygen limitation (c-d). The dissolved oxygen (DO, light blue line), CO_2 off-gas (green line) and respiratory quotient (RQ, yellow line) were measured online (RQ not measured for (a) due to instrument malware). Cell dry weight (CDW, green dotted line) was calculated from the measured OD_{600} (see Appendix A.1 for how to calculate CDW from OD_{600}). Glucose (blue dotted line) was sampled for, along with other exometabolites and pyridine nucleotides, as indicated by the vertical, black dashed lines, and were sampled in technical quadruplicates. The cultivations were performed using 1 L bench-top bioreactor with M9-MtPr medium 2 (Table **2.10**) at 37 °C. The pH was constantly adjusted to 7.00. For (c) and (d) the oxygen cascade was turned off and agitation set to 400 rpm, to simulate oxygen limitation, when the CDW was at 0.868 g/L (OD_{600} ~ 2.0), while for (a) and (b) the dissolved oxygen was kept above 40 %. The induction of oxygen limitation is indicated by the vertical, red dashed line. Roman numerals indicate the biological replicate.

C.2 *E. coli* BL21 A2mCh

As only one representative cultivation plot of each condition (control or oxygen limitation) of *E. coli* BL21 A2mCh was shown in subsection 3.2.2, the remaining plots are shown in Figure C.2.

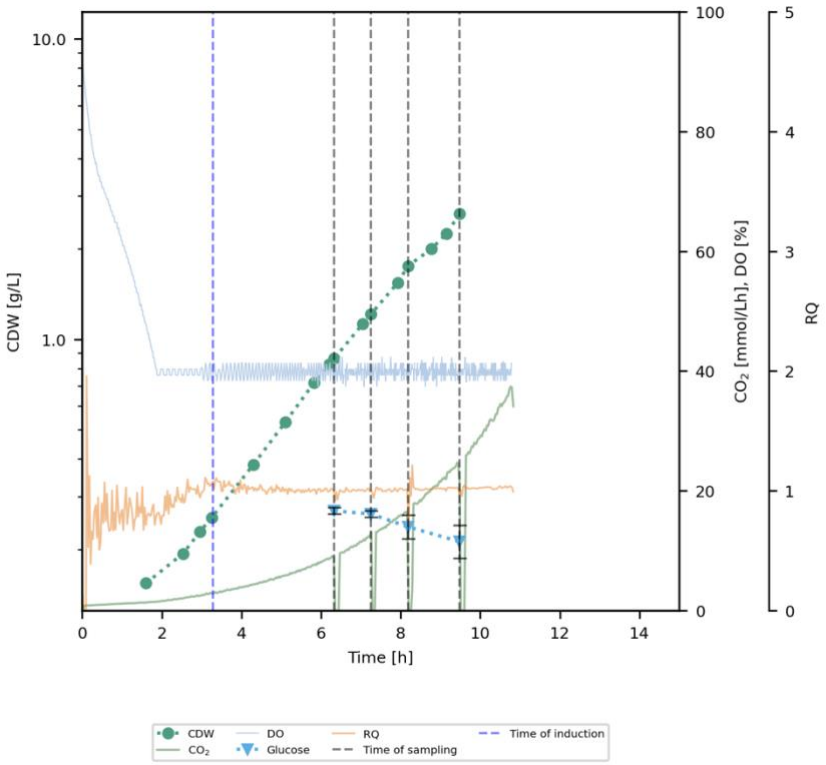

a) E. coli BL21 A2mCh-I, no oxygen limitation.

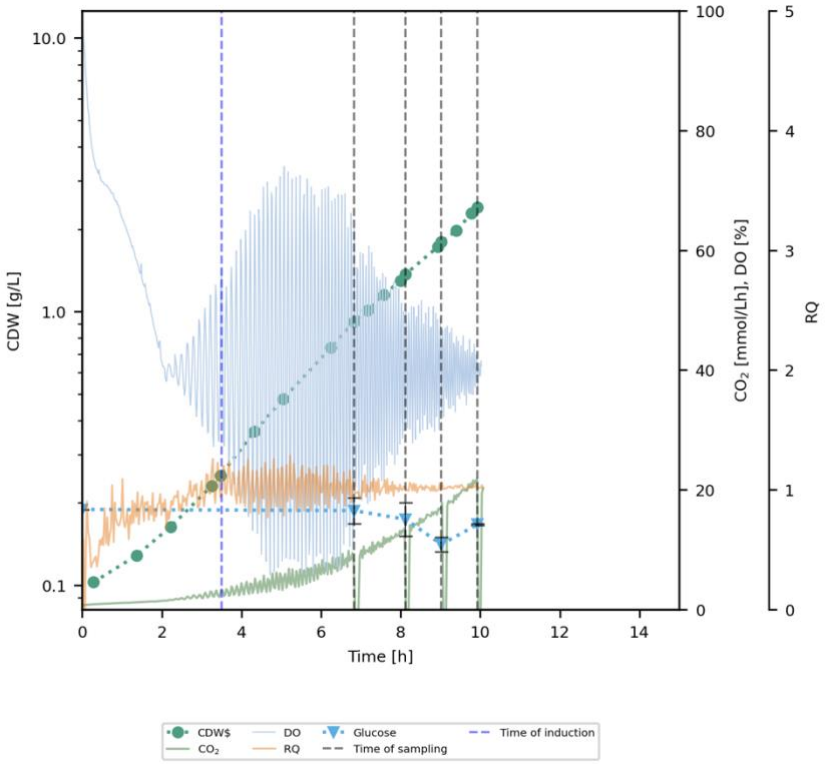

b) *E. coli* BL21 A2mCh-III, no oxygen limitation.

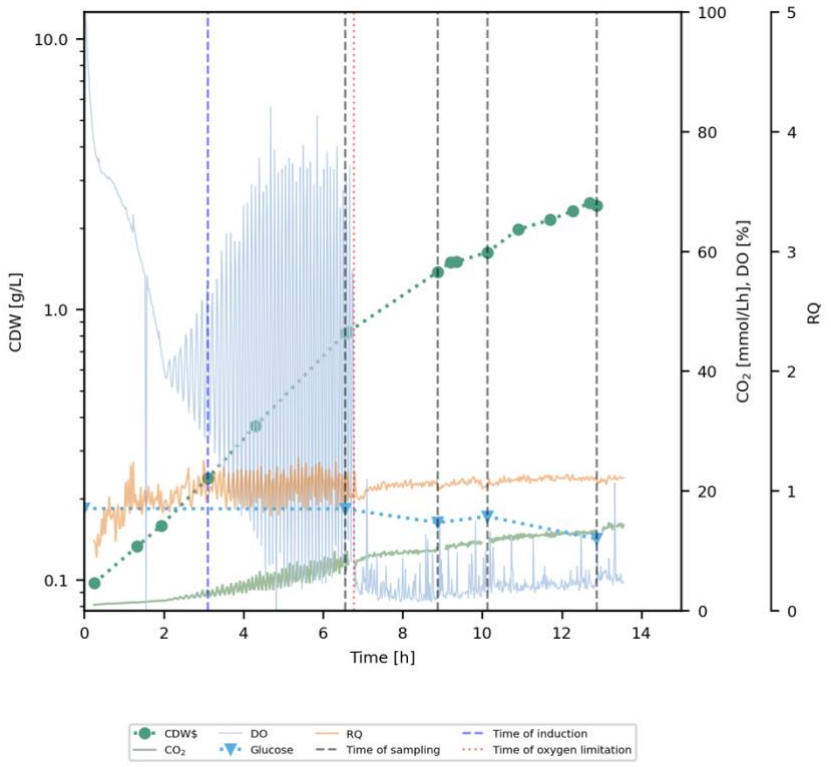

c) *E. coli* BL21 A2mCh-II, oxygen limitation.

Figure C.2: Remaining cultivation plots for *E. coli* BL21 A2mCh of the biological duplicates and triplicates under no oxygen limitation (a-b) and oxygen limitation (c), respectively. The dissolved oxygen (DO, light blue line), CO_2 off-gas (green line) and respiratory quotient (RQ, yellow line) was measured online. Cell dry weight (CDW, green dotted line) was calculated from the measured OD_{600} (see Appendix A.1 for how to calculate CDW from OD_{600}). Glucose (blue dotted line) was sampled for, along with other exometabolites, pyridine nucleotides and central carbon metabolites, as indicated by the vertical, black dashed lines, and were sampled in technical quadruplicates. The concentration of mCherry (salmon pink dotted line) was measured in technical duplicates for only WT-II and A2mCh-II, using western blot. The cultivations were performed using 1 L bench-top bioreactors with M9-MtPr medium 2 (Table 2.10) at 30 °C. The pH was constantly adjusted to 7.00. For (c) the oxygen cascade was turned off and agitation set to 400 rpm, to simulate oxygen limitation, when the CDW was at 0.8515 g/L (OD_{600} ~ 2.0), while for (a) and (b) the dissolved oxygen was kept above 40 %. The induction of oxygen limitation is indicated by the vertical, red dashed line. The production of mCherry was induced when the CDW was at 0.2491 g/L (OD_{600} ~0.5), indicated by the vertical, blue dashed line. Roman numerals indicate the biological replicate.

C.3 Additional yields and carbon recoveries

The yield and the carbon recovery of each strain and condition was calculated between each sampling point. This is given in Table C.1.

Table C.1: The biomass yield ($Y_{biomass/s}$), overflow metabolite yield ($Y_{acid/s}$) and % carbon recovery between sampling points observed for *E. coli* BL21 WT and A2mCh under oxygen limitation and no oxygen limitation. For the yield, all strains and conditions had three biological replicates except for A2mCh under oxygen limitation, which had two biological replicates. Where no standard deviation is stated, samples were not included due to negative values for glucose consumption in the given phase. Ethanol is not included in the organic acid yield for A2mCh..

Strain	Condition	Phase	$Y_{biomass/s}$ [g CDW/g Glc]	$Y_{acid/s}$ [g/g Glc]	% Carbon recovery
WT	No O_2-lim	T0-T1	0.13	0.064	21
		T1-T2	0.68 ± 0.54	0.23 ± 0.18	95
		T2-T3	0.45 ± 0.05	0.040 ± 0.006	80
		T3-T4	0.49 ± 0.07	0.039	82
		T4-T5	0.37 ± 0.06	0.0051 ± 0.0018	58
		T5-T6	0.44 ± 0.08	0.019 ± 0.009	72
WT	O_2-lim	T0-T1	0.31 ± 0.13	-0.038 ± 0.020	40
		T1-T2	0.28 ± 0.08	0.089 ± 0.035	47
		T2-T3	0.55 ± 0.12	0.59 ± 0.67	124
		T3-T4	0.19 ± 0.06	0.41 ± 0.03	68
		T4-T5	0.15 ± 0.02	0.46 ± 0.09	68
		T5-T6	0.093 ± 0.01	0.43 ± 0.05	61
A2mCh	NO_2-lim	T0-T1	0.66	0.25	265
		T1-T2	0.41 ± 0.25	0.14 ± 0.10	71
		T2-T3	0.15 ± 0.02	0.076	30
		T3-T4	0.37 ± 0.19	0.11 ± 0.01	60
A2mCh	O_2-lim	T0-T1	0.32	0.14	133
		T1-T2	0.25 ± 0.04	0.22 ± 0.05	74
		T2-T3	0.69	0.76	220
		T3-T4	0.20 ± 0.02	0.19 ± 0.01	67

D SDS-PAGE and western blot

To quantify the amount of mCherry that was produced by *E. coli* BL21 A2mCh, western blot was performed. Prior to this, the presence of mCherry was validated by use of SDS-PAGE. Both of these were performed as according to subsection 2.4.5.2.2. The results of the SDS-PAGE are shown in Figure D.1, where the mCherry is at roughly 27.5 kDa. The results of the western blot are shown in Figure D.2 and Figure D.3.

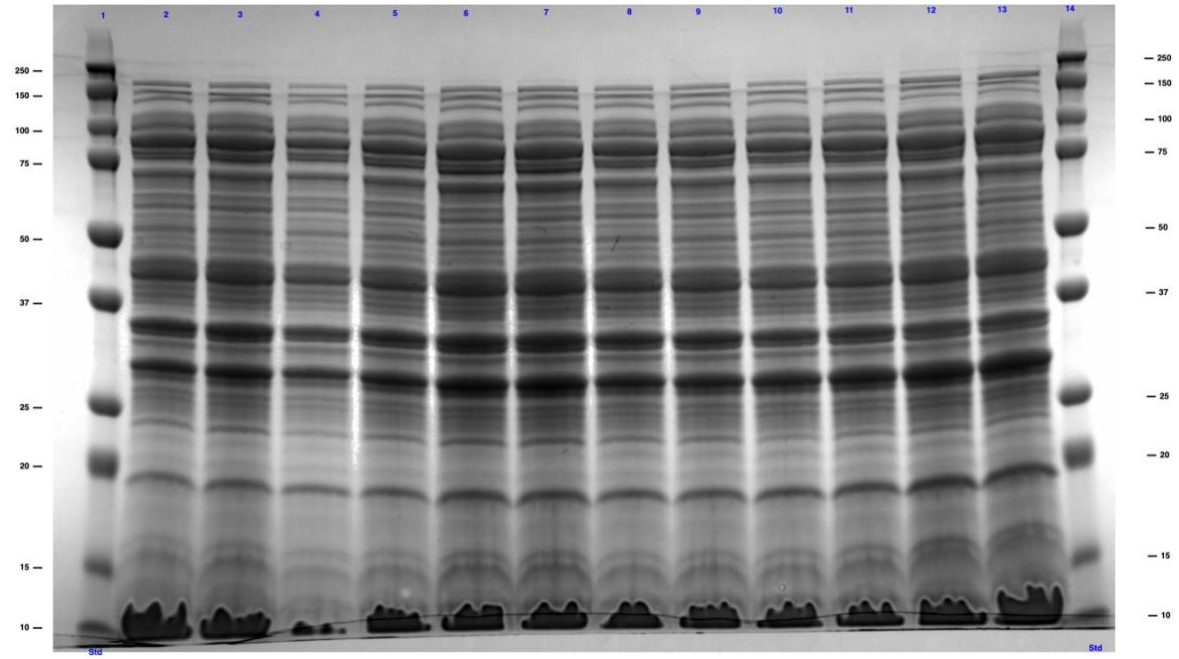

Figure D.1: SDS-PAGE performed on samples from the soluble fraction of proteins extracted from *E. coli* BL21 A2mCh and prepared according to subsection 2.4.5.2. Samples were taken at four different time points, but T3 was omitted from the SDS-PAGE. Lanes 1 and 14 corresponds to the molecular weight ladder. Lanes 2-7 is from the control cultivation of A2mCh, while lanes 8-13 is from the oxygen-limited cultivation of A2mCh. Even numbered lanes are from technical replicates E, odd numbered lanes are from technical replicates F. The time points were analysed chronologically. The protein analysed for, mCherry, is the band corresponding to a molecular weight of 26.7 kDa.

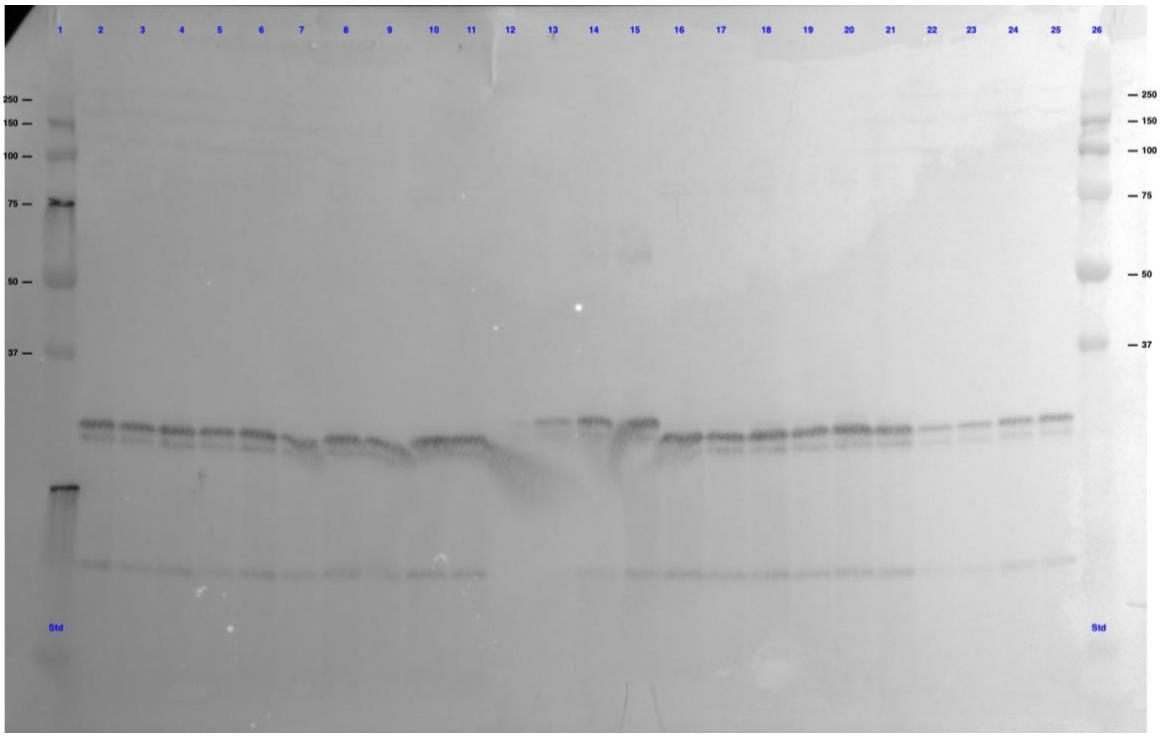

Figure D.2: Western blot performed on samples extracted from one of the oxygen-limited cultivations of *E. coli* BL21 A2mCh prepared according to subsection 2.4.5.2. Samples were taken at four different time points. Lanes 1 and 26 corresponds to the molecular weight ladder. Lanes 12-15 contain pure mCherry used to make a standard curve for the quantification of the amount of mCherry in the samples from the band strength. Lanes 2-11 and 16-21 contain samples from the soluble fraction of the proteins, while lanes 22-25 contain samples from the insoluble fractions. Two technical replicates from each time point are loaded, with each being diluted either 500 or 1000 times.

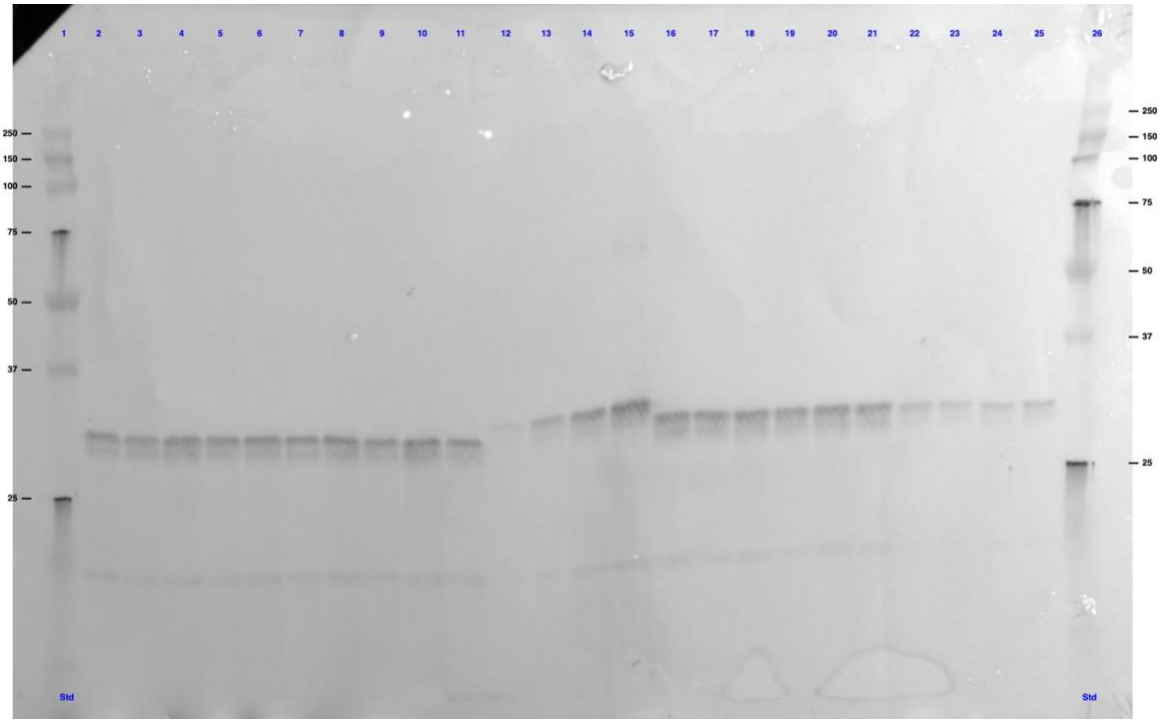

Figure D.3: Western blot performed on samples extracted from one of the control cultivations of *E. coli* BL21 A2mCh prepared according to subsection 2.4.5.2. Samples were taken at four different. Lanes 1 and 26 corresponds to the molecular weight ladder. Lanes 12-15 contain pure mCherry used

to make a standard curve for the quantification of the amount of mCherry in the samples from the band strength. Lanes 2-11 and 16-21 contain samples from the soluble fraction of the proteins, while lanes 22-25 contain samples from the insoluble fractions. Two technical replicates from each time point are loaded, with each being diluted either 500 or 1000 times.

E Statistical tests

E.1 Dixon's Q-test

Dixon's Q-test is a statistical method to identify and exclude outliers from a dataset with few observations (Dean & Dixon, 1951). The test assumes the data set has a Gaussian distribution of error, and can only be applied once per data set (Efstathiou, 2006). Dixon's Q-test finds outliers by calculating the gap between the possible outlier and the closest value and divides it by the range of the data set. For a data set arranged increasingly, the equation to find the Q_{exp} is as shown in Equation E-1,

$$Q_{exp} = \frac{gap}{range} = \frac{x_1 - x_2}{x_{\max} - x_{min}} \qquad \text{Equation E-1}$$

where x_1 represents the possible outlier, x_2 is the closest value to the possible outlier, x_{max} is the highest value in the data set and x_{min} is the lowest value in the data set.

For the potential outlier to be rejected, Q_{exp} must be lower than the critical value, Q_{crit}, for a data set with a given confidence interval and sample size. The relevant values of Q_{crit} for our dataset, with a 95% confidence, is given in Table E.1

Table E.1: The critical values, Q_{crit}, for a data set with the given sample sizes, with 95% confidence, for Dixon's Q-test (Rorabacher, 1991).

Sample size, N	Critical value, Q_{crit}
3	0.970
4	0.829

F Principal component analysis

PCA was performed on the data from the pyridine nucleotide analysis (subsection 3.3) to find differences in the observed phenotype of *E. coli* BL21 WT and A2mCh under oxygen limitation and the control. To do this, 2D score plots were produced. These are shown in Figure F.1. Figure F.1a shows the biological triplicates of the WT at the two last time points under both oxygen limitation and the control to highlight the separation seen as an effect of the oxygen limitation. 93.4 % of the variance is explained by the PCA, 69.3 % by PC1 and 24.1 % by PC2. Figure F.1b shows the biological triplicates of A2mCh at all time points under both oxygen limitation and the control to highlight the separation seen as an effect of the time the samples are taken at. 95.9 % of the variance is explained by the PCA, 83.4 % by PC1 and 12.5 % by PC2. Figure F.1c shows the biological triplicates of A2mCh at the two last time points to highlight the separation seen as an effect of the oxygen limitation. 93.6 % of the variance is explained by the PCA, 77.8 % by PC1 and 15.8 % by PC2.

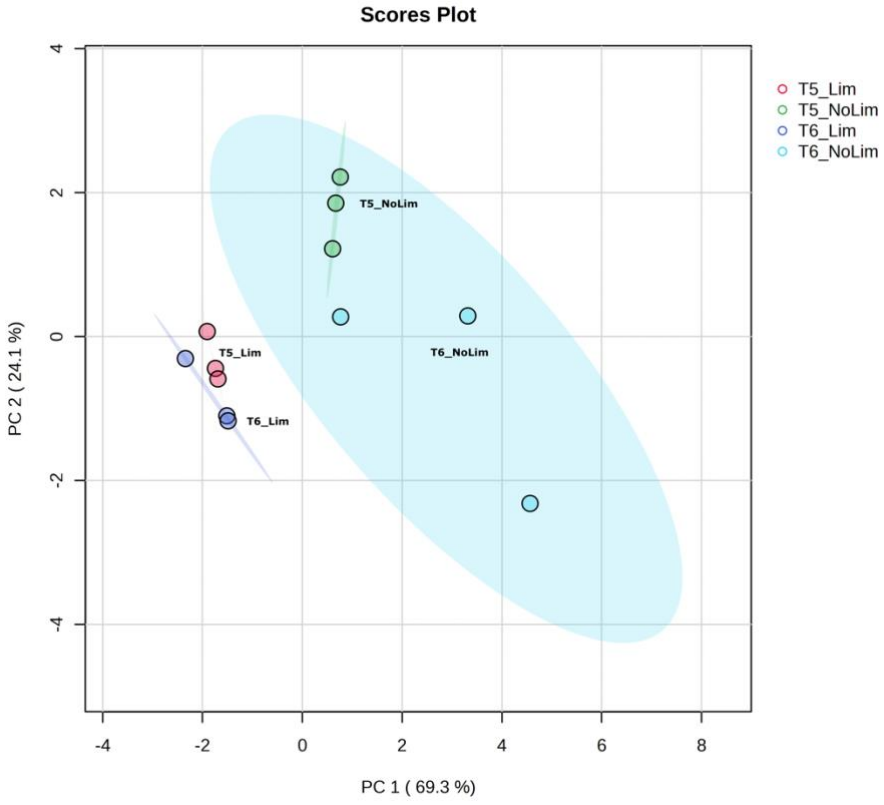

a) Biological replicates of WT at the two last time points.

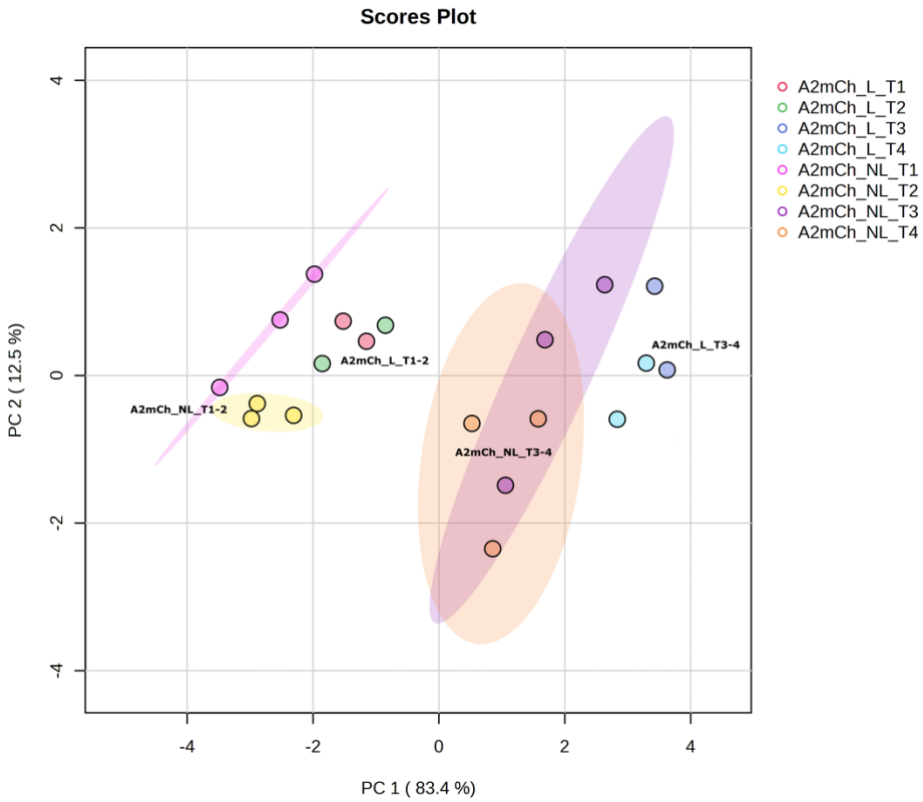

b) Biological replicates of A2mCh.

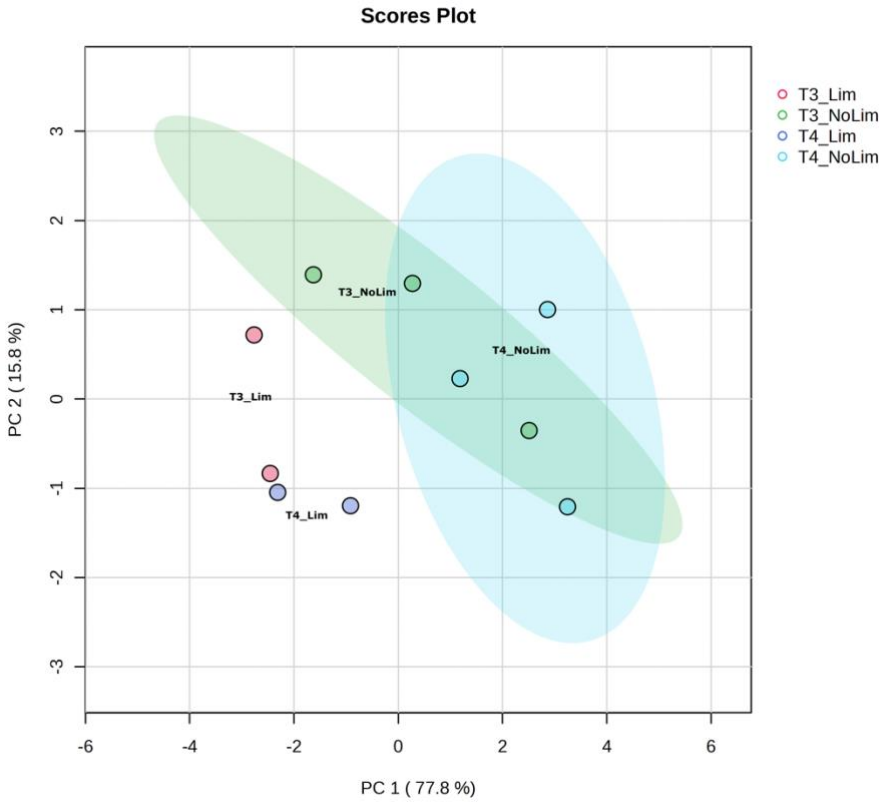

c) Biological replicates of A2mCh at the two last time points.

Figure F.1: 2D score plots from PCA of the metabolite concentrations in the pyridine nucleotide samples taken during cultivation of *E. coli* BL21 WT and A2mCh under oxygen limitation and the controls. a) Biological replicates of the WT at the two last time points. b) Biological replicates of A2mCh at all time points. c) Biological replicates of A2mCh at the two last time points. All strains were cultivated as biological triplicates, except A2mCh under oxygen limitation which was cultivated as biological duplicates. All sampling was done as technical quadruplicates. The metabolites were quantified by zwitterionic HILIC-MS/MS and processed as described in subsection 2.4.4.3. The PCA was performed on autoscaled data, using MetaboAnalyst 5.0 (Pang et al., 2021).

G Plasmid map

The plasmid map of the A2mCh expression vector is shown in Figure G.1. The expression vector is based on the RK2 plasmid, with a XylS/*Pm* expression system, a *bla* gene conferring ampicillin resistance, a mutated *trfA* gene controlling the PCN, and a *mCherry* gene encoding the fluorescent protein mCherry.

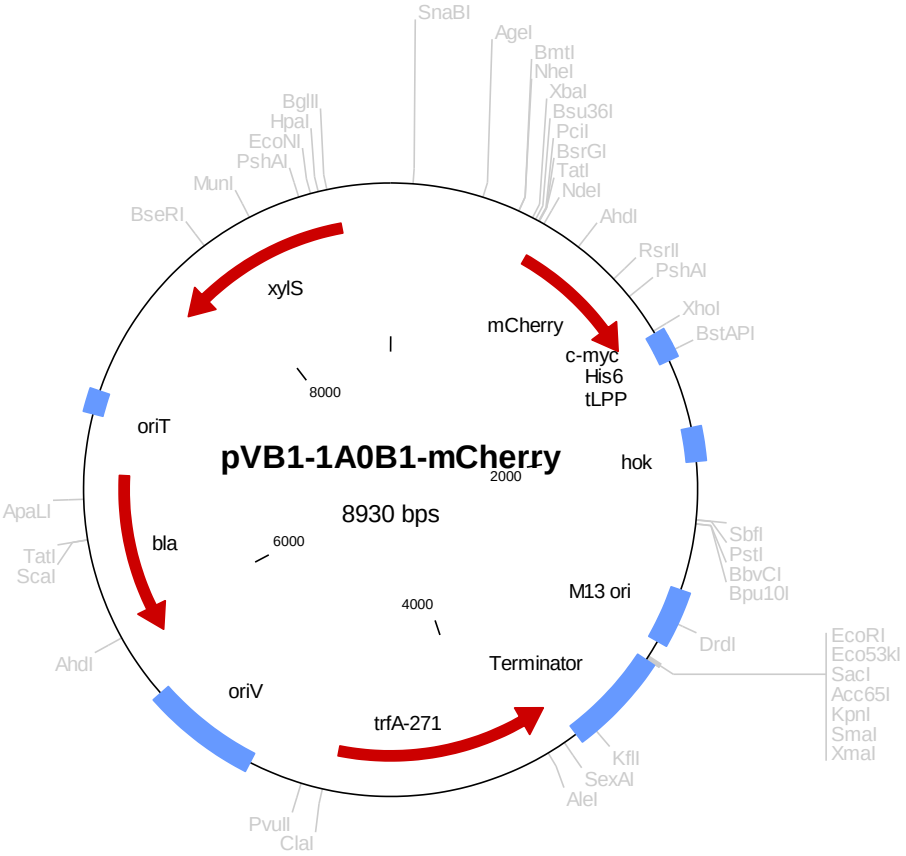

Figure G.1: Plasmid map for the expression vector of *E. coli* BL21 A2mCh. The expression vector contains the ampicillin resistance encoding *bla* gene, the transcription regulator XylS encoding *xylS* gene and the mutated *trfA* gene which controls the PCN to be 20. In addition, the mCherry encoding gene *mCherry* is also present, all in red.

H mCherry sequence

H.1 Nucleotide sequence

ATGGTTTCTAAAGGTGAAGAAGACAACATGGCTATCATCAAAGAATTTATGCGTTTCAAAGTTCAC
ATGGAAGGTTCTGTGAACGGTCACGAATTTGAAATCGAAGGTGAAGGTGAAGGTCGTCCGTATG
AAGGCACCCAGACCGCTAAACTGAAAGTTACCAAAGGTGGTCCGCTGCCGTTCGCTTGGGACAT
CCTGTCTCCGCAGTTCATGTACGGTTCTAAAGCGTATGTTAAACACCCGGCTGACATCCCGGACT
ACCTGAAACTGTCTTTCCCGGAAGGTTTCAAATGGGAACGTGTTATGAACTTTGAAGACGGTGGT
GTTGTTACCGTTACCCAGGACTCTTCTCTGCAAGACGGTGAATTTATCTACAAAGTTAAACTGCGT
GGCACCAACTTCCCGTCTGACGGTCCGGTTATGCAGAAAAAAACGATGGGTTGGGAAGCGTCTT
CTGAACGTATGTACCCGGAAGACGGTGCTCTGAAAGGTGAAATCAAACAGCGTCTGAAACTGAA
AGACGGTGGTCACTACGACGCTGAAGTTAAAACCACCTACAAAGCTAAAAAGCCGGTTCAACTGC
CGGGTGCTTACAACGTGAACATCAAACTGGACATCACCTCTCACAACGAAGACTACACCATCGTT
GAACAGTACGAACGTGCTGAAGGTCGTCACTCTACCGGCGGTATGGACGAACTGTATAAATGA

H.2 Amino acid sequence

MVSKGEEDNMAIIKEFMRFKVHMEGSVNGHEFEIEGEGEGRPYEGTQTAKLKVTKGGPLPFAWDILS
PQFMYGSKAYVKHPADIPDYLKLSFPEGFKWERVMNFEDGGVVTVTQDSSLQDGEFIYKVKLRGTNF
PSDGPVMQKKTMGWEASSERMYPEDGALKGEIKQRLKLKDGGHYDAEVKTTYKAKKPVQLPGAYN
VNIKLDITSHNEDYTIVEQYERAEGRHSTGGMDELYK

The amino acid composition of mCherry is given in Table H.1.

Table H.1: Amino acid composition of mCherry.

Amino acid	One letter code	Number of residues	Percentage [%]
Alanine	A	11	4.66
Arginine	R	8	3.39
Asparagine	N	7	2.97
Aspartic acid	D	14	5.93
Cysteine	C	0	0.00
Glutamine	Q	8	3.39
Glutamic acid	E	24	10.17
Glycine	G	25	10.59
Histidine	H	6	2.54
Isoleucine	I	10	4.24
Leucine	L	13	5.51
Lysine	K	24	10.17
Methinione	M	10	4.24
Phenylalanine	F	10	4.24
Proline	P	12	5.08
Serine	S	12	5.08
Threonine	T	12	5.08
Tryptophan	W	3	1.27
Tyrosine	Y	12	5.08
Valine	V	15	6.36

NTNU

Norwegian University of
Science and Technology